Holistic complex systems modelling approaches for cell signalling networks - Mammalian cell cycle control system

A thesis

submitted in partial fulfilment

of the requirements for the Degree of

Doctor of Philosophy in Computer Science

at

Lincoln University

by

Ali Abroudi

Lincoln University

2019

Abstract of a thesis submitted in partial fulfilment of the
requirements for the Degree of Doctor of Philosophy in Computer Science.

Holistic complex systems modelling approaches for cell signalling networks - Mammalian cell cycle control system

by

Ali Abroudi

Cell cycle is a precisely regulated process in which cells of living organisms go through a sophisticated growth and division cycle that eventually leads to production of two daughter cells (Morgan, 2007; Satyanarayana & Kaldis, 2009). The progression of cell cycle is monitored through different checkpoints to guarantee the genome integrity (Kastan & Bartek, 2004; Novák et al., 2001; Nyberg et al., 2002; Walworth, 2000). Understanding the underlying mechanism and behaviour of these checkpoints is one of the most important topics in biology. In this study, Ordinary Differential Equation (ODE) and Petri Net (PN) modelling techniques and numerical analyses have been used to gain deeper insights into (i) the efficiency of checkpoints in detecting damaged/healthy cells, (ii) identifying the most significant parts of the system on G1-S and G2-M transitions, (iii) and the behaviour of the whole mammalian cell cycle control system (not just a part of it) from a systems perspective where all the crucial cell cycle sub-systems interact with each other to control cell cycle progression.

This research begins with identifying the current gaps in the field of mammalian cell cycle modelling. The findings led us to developing a comprehensive mathematical model with all the missing essential components to integrate the important cell cycle sub-systems (Growth Factor, G1-S checkpoint, G2-M checkpoint and DNA damage signalling sub-systems) and their constituent modules (i.e., modules of G2-M sub-system are: Cdk1_Related, Tyrosine Phosphatase, Tyrosine Kinase, APC-Related and Plk1-Related modules). This arrangement maintains the functionality of the cell cycle control system while giving a better understanding of the underlying interactions by lessening the complexity of the system as a whole. The proposed comprehensive mathematical model was evaluated and further analysed in order to investigate the behaviour of mammalian cell cycle system and DNA damage response as well as to verify the role of the newly added components in cell cycle.

The next part of this research is devoted to system behaviour analysis using parameters of the comprehensive mathematical model presented in the first section of the thesis. Therefore, we

developed an analytical model (named SOMCCA) based on Self-Organizing Map (SOM) and Correlation Coefficient Analysis (CCA) to perform Global Sensitivity Analysis (GSA) on model parameters. Through this analysis, the most significant parameters, modules and sub-systems on G1-S and G2-M transitions were identified. The results of the SOMCCA model revealed that two sub-systems (the Growth Factor signalling and G1-S checkpoint) and seven parameters in the modules within them are significant on G1-S and G2-M transitions.

The third part of this research investigates the efficacy of cell cycle checkpoints in correctly detecting damaged and healthy cells under DNA damage condition as there is biological evidence that G2-M checkpoint is relatively more efficient in detecting damaged/healthy cells in comparison to G1-S checkpoint. To do this analysis, we developed a model called Checkpoint Efficiency Evaluation (CEE) model based on statistical Type II error and Probability Density Function (PDF) of Peak Times (PTs) of G1-S and G2-M indicators (CycE_Cdk2 and CycB_Cdk1, respectively). The CEE model was applied to the comprehensive mathematical model presented in the first part of the thesis and the results were in good agreement with biological findings.

Having developed a comprehensive mathematical model in the first part of this thesis, the main focus of the last part of the thesis is to perform a model abstraction in order to develop an abstract minimised model where the main characteristics of the model (such as dynamics of cell cycle core components, G1-S and G2-M transitions and response to DNA damage) remain qualitatively the same. First step towards model abstraction was to determine the key components that should be present in the abstract model. This was done based on the most significant parameters of the comprehensive model identified in the second part of the thesis. The next step was to determine the most suitable modelling approach. The presence of different time scales (from quick activations to slow synthesis processes) as well as presentation at different levels (from sub-systems down to modules and proteins) led us to choose Petri Net (PN) modelling for model abstraction because PN can be developed as a hybrid model and it is also an intuitive graphical approach that has the ability to present complex systems at different levels of abstraction. Therefore, we developed a hybrid PN-based model called Multi-Level Hybrid Petri Net (MLHPN). The MLHPN model has just four equations while the comprehensive model has 61 equations. In order to scrutinize the efficiency of G1-S and G2-M checkpoints in correctly detecting damaged and healthy cells, the CEE model was applied to the MLHPN model, and similar to the analysis results for the comprehensive model, the results for the MLHPN model showed that G2-M is more efficient than G1-S.

In conclusion, this study showed the value of computational modelling (Ordinary Differential Equations (ODE) and Petri Net (PN)-based models) and Artificial Neural Networks/statistical methods (Self Organising Maps and Correlation Coefficient Analysis (SOMCCA) and Checkpoint Efficiency

Evaluation (CEE) models) in comprehending complex signalling networks and obtaining deeper insights into the underlying mechanisms of the mammalian cell cycle control system from a systems point of view integrating all the essential cell cycle sub-systems including G1-S and G2-M checkpoints, the Growth Factor signalling and the DNA damage signalling pathway. Furthermore, the thesis showed the importance of newly added components and modules along with the Artificial Neural Networks and statistics based numerical investigation to identify the most significant parts of the system on system response. The demonstration of the value of the comprehensive mathematical model and the MLHPN model in investigating the efficiency of G1-S and G2-M checkpoints and verifying the greater efficiency of G2-M checkpoint in correctly detecting damaged/healthy cells is an important contribution of this research. Finally, this research demonstrated the value of model abstraction from a comprehensive model with 61 equations down to a hybrid PN-based model with just four equations while the system characteristics remained the same.

Keywords: Mammalian cell cycle, Growth Factor signalling, G1-S checkpoint, G2-M checkpoint, DNA damage signalling pathway, Petri Net, Ordinary Differential Equation, Artificial Neural Networks, Self Organising Maps, Correlation Coefficient, Global Sensitivity Analysis

List of Publications

Publications from this thesis:

- Abroudi, A., Samarasinghe, S., & Kulasiri, D. (2017). A comprehensive complex systems approach to the study and analysis of mammalian cell cycle control system in the presence of DNA damage stress. *Journal of Theoretical Biology (JTB)*, *429*, 204-228.

- Abroudi, A., Samarasinghe, S., & Kulasiri, D. (2015). *A Review of Computational Models of Mammalian Cell Cycle*. Paper presented at the meeting of the 21st International Congress on Modelling and Simulation (MODSIM), Australia.

- Abroudi, A., Samarasinghe, S. (2015). *System Modelling of Mammalian Cell Cycle Regulation Using Multi-Level Hybrid Petri Nets*. Paper presented at the meeting of the 21st International Congress on Modelling and Simulation (MODSIM), Australia.

Abstract presentations from this thesis:

- Abroudi, A. (2014). *System Modelling in Biology – Mammalian Cell Cycle.* Abstract presented at the Lincoln University Postgraduate Conference, Lincoln, New Zealand.

- Abroudi, A. (2015). *Multi-Level Modelling of Cell Cycle System - A Petri Net Approach.* Abstract presented at the Lincoln University Postgraduate Conference, Lincoln, New Zealand.

Submitted to Journal of Theoretical Biology (JTB) - 2019:

- Abroudi, A., Samarasinghe, S., & Kulasiri, D. Towards Abstraction of Computational Modelling of Mammalian Cell Cycle: A Petri Net Approach.

Acknowledgements

I would like to express my sincere gratitude to my supervisors Prof. Sandhya Samarasinghe and Prof. Don Kulasiri for the continuous support of my Ph.D, for thier patience, motivation, and immense knowledge. Their guidance helped me during all the time of research and writing of this thesis. I could not have imagined having a better supervisors and mentors for my research.

I greatly appreciate Lincoln University for granting me the Lincoln University Doctoral Scholarship which gave me the opportunity to undertake this research and I have always been proud of holding this prestigious scholarship. I also greatly thank Lincoln university for supporting me to attend conferences and meet so many interesting people. I take this opportunity to thank the administrative staff of the Faculty of Environment, Society and Design: Douglas Broughton, Tracey Shields, and Michelle Collings for their friendly and professional support. My gratitude goes out to the Library, Teaching and Learning of Lincoln University for holding helpful academic workshops.

Last but not least, I would like to thank my parents for their great support, although they were thousands miles away, they listened to me and my challenges everyday. I also want to greatly thank my lovely wife, Zohreh, for supporting me. Without her encouragement, I would have never been able to finish this long journey.

Table of Contents

List of Tables

List of Figures

Chapter 1

Introduction

1.1 Overview

An important process in the growth of any biological organism is its ability to proliferate, a tightly controlled process called the cell cycle in which a cell divides into two daughter cells (Morgan, 2007; Satyanarayana & Kaldis, 2009). Although the dependent sequence of cell cycle events has been identified for decades, the underlying regulatory basis was not completely clear until the introduction of checkpoint concept by Hartwell and Weinert (1989). They demonstrated that there are some checkpoints which arrest the cell cycle progression in the case of an uncompleted event or DNA damage. This arrest can provide enough time for a repairing process so that fidelity of genome is maintained (Kastan & Bartek, 2004; Novák et al., 2001; Nyberg et al., 2002; Walworth, 2000). Upon discovery of underlying elements of the cell cycle control system, and thanks to fast technical improvements, a lot of knowledge about involved biochemical interactions has been produced for all kinds of species. Therefore, it is obvious now that the complex behaviour of cell cycle and its response to different types of internal and external signals are due to chemical interactions between a large variety of proteins (Berridge, 2014; Morgan, 2007; Novák et al., 2001; Nurse, 2000; Tyers, 2004; Tyson et al., 2001; Tyson et al., 2003; Vermeulen et al., 2003).

The complex system of cell cycle can be presented through computational models which have the ability to reproduce the system dynamics and they generally belong to a rather new framework called Systems Biology. Based on this framework, an entity is considered as a part of a system which has interaction with other elements in the system rather than being an individual unit. In fact, systems biology is an inter-disciplinary area that concentrates on system-level understanding of complex biological systems (Alon, 2006; Kitano, 2002a; Klipp et al., 2008; Noble, 2008). The initial attempts to model the cell cycle using mathematical methods date back to more than fifty years ago (Koch & Schaechter, 1962; Shields, 1977; Smith & Martin, 1973). Due to the availability of more detailed data from the last decade of the twentieth century, there has been an explosion in the field of computational modelling of cell cycle (Goldbeter, 1991; Norel & Agur, 1991; Nurse, 1990; Thron, 1991; Tyson, 1991). Over the past years, systems biology has led to creation of more comprehensive models (Aderem, 2005; Csikász-Nagy, 2009; Ideker et al., 2001; Kitano, 2002a, 2002b; Klipp et al., 2016; Palsson & Palsson, 2015). In this chapter, we briefly present the current gaps in mammalian cell cycle modelling which lead us to motivations for our study. We also provide our research objectives together with some challenging questions that can be answered through this study.

1.2 Research Motivation

In this study, our focus is on *mammalian* cell cycle because there is a lack of proper modelling for this most complicated cell cycle system in the current literature. Having reviewed literature in the field of mammalian cell cycle modelling, we have recognized some gaps in the field. Most models have utilized the mathematical formulation for representing the dynamical behaviour of the cell cycle with different number of equations, ranging from a few to tens of equations. Small-scale models suffer the problem of comprehensiveness and they cannot be considered as a complete representation of the whole cell cycle system. For instance, some of them just consider the effect of cyclins. On the other hand, more complicated models, which have tens of different equations, lack a deep understanding of biological processes in cell cycle. Investigators mostly investigate the dynamics of some biomarkers in their large-scale models but rarely study the interconnected and purposeful cause and effect mechanisms in cell cycle, especially from systems point of view. Therefore, there is a need to characterise all the major and supporting components as well as their inter-relationships in order to draw a clear picture of underlying mechanism, particularly for a well-organized system like mammalian cell cycle.

In current models, G1-S and G2-M checkpoint signalling pathways have not been properly incorporated from systems perspective and also there are some missing elements whose existence can shed more light on the function of key players of cell cycle control system. Therefore, there is a need for proper incorporation of these checkpoints together with missing elements. Another gap is related to investigation of DNA damage and its impact on cell cycle system. There exist many articles dedicated to modelling DNA damage but they do not give a complete picture of the two different DNA damage pathways, namely rapid and delayed pathways. Thus, it is important to cover the two different DNA damage pathways in order to understand the reason why there should exist rapid and delayed pathways. It will definitely help us grasp biological meaning of these pathways and their essential effects on cell cycle progression. There is also a gap in incorporating Growth Factor signalling pathway into mammalian cell cycle models as Growth Factor has been modelled through a constant on-off signal in current models.

Therefore, in our study, the important sub-systems of mammalian cell cycle, which are Growth Factor signalling, G1-S and G2-M checkpoints, and DNA damage pathways, will be included to achieve a better understanding of behaviour of this complex system. We divide the system into its constituent sub-systems and further divide the sub-systems into their constituent modules, which interact with each other to fulfil the function of the corresponding sub-system. As a case in point, G1-S checkpoint signalling sub-system has the following modules: (1) Cdk4-Related module (receives the signal from Growth Factor sub-system to initiate the cell cycle); (2) E2F-pRb module (receives the

signal from Cdk4-Related module and induces the production of some critical cell cycle proteins through transcription factor, E2F); (3) Cdk2-Related module (talks to other internal and external modules and sub-systems to prepare the cell for entering into S phase); and (4) Tyrosine Phosphatase module (stimulates the activation of Cyc_Cdk2 complexes which are crucial for G1-S transition).

Our intention is to create an inherently easy to understand yet comprehensive model which can help readers (modellers, biologists, etc.) grasp concepts of mammalian cell cycle control system. In this study, we aim to apply and advance methods for developing and implementing a comprehensive systemic mathematical model with sub-systems and modules as well as an abstract Petri Net (PN)-based model for the whole cell cycle at different levels of abstraction. These systemic approaches incorporating all known aspects of cell cycle allow us to (i) study, through dynamic simulation of an ODE model, comprehensive details of cell cycle dynamics under normal and DNA damage conditions revealing the role and value of the added new modules and elements (presented in Chapter 3), (ii) assess, through a Global Sensitivity Analysis (GSA), the most influential sub-systems, modules and parameters on system response, such as G1-S and G2-M transitions (presented in Chapter 4), (iii) probe deeply into the relationship between DNA damage and cell cycle progression and test the biological evidence that G1-S checkpoint is relatively inefficient in arresting damaged cells compared to G2-M (presented in Chapter 5), and (iv) perform a model abstraction through developing an intuitive multi-level PN-based model for cell cycle based on the comprehensive mathematical model presented in Chapter 3 to gain deeper insights into how the abstract model can coordinate such an intricate system of interactions in a robust and timely manner (presented in Chapter 6). Thus, this study shows the efficacy of the proposed systems approaches to gain a better understanding of different aspects of mammalian cell cycle system separately and as an integrated system that will also be useful in investigating targeted therapy in future cancer treatments.

1.3 Research Objectives

The first objective of this research is to mathematically present the whole mammalian cell cycle control system together with its constituent sub-systems. Therefore, we need to determine the sub-systems and the underlying mechanism for their elegant cooperation. We further identify the constituent functional modules of each sub-system.

To achieve the first objective, we update an existing mathematical model of mammalian cell cycle (Iwamoto et al., 2011) and therefore develop a new ODE model with the most recent knowledge of mammalian cell cycle (Abroudi et al., 2017). In our comprehensive model, some important elements missing in existing models have been added. Furthermore, key inter-connecting sub-systems are identified where each sub-system is demonstrated separately with its corresponding wiring diagram.

In order to better understand the function of sub-systems, each sub-system is decomposed into its constituent modules. Hence, based on this objective, the following critical questions can be asked:

1. *What are the newly added elements in our model and what is the rationale for adding each of them?*

Past models have considered Growth Factor to be a binary signal - on or off (Iwamoto et al., 2011; Iwamoto et al., 2008). The reality is that following the presence of Growth Factor, a transcription factor (c-Myc) through a particular signalling cascade (MAPK signalling) is responsible for triggering cell cycle machinery. It stimulates the synthesis of Cyclin D, one of the most critical controllers in early-mid G1 phase of mammalian cell cycle (Adhikary & Eilers, 2005; Alberts et al., 2014; de Alboran et al., 2001; Morgan, 2007; Schmidt, 1999). We believe that addition of c-Myc has value in the model because of its biological significance to the cell cycle system. Further, as an extension to the cell cycle model, it gives a more complete description of the cell cycle. In our model, the relationship (continuous dynamic) between c-Myc and Cyclin D is realistically represented. Also, with c-Myc in the system, we now have the transcription factors of all cyclins of cell cycle in one model. Furthermore, our numerical analysis shows that c-Myc is the most significant element in the whole system from a systems perspective and adding it is beneficial. Therefore, we add transcription factor c-Myc in our model (see Chapter 3 for details).

Polo-like kinase-1 (Plk1) is another newly added element which is one of the most important proteins in mitotic entry. In Iwamoto model, there were two versions of CycB_Cdk1: nucleus and cytoplasmic versions; but there was no explanation for the translocation of the cytoplasmic into nucleus, which marks the mitotic entry (Iwamoto et al., 2011). Our model provides this explanation through Plk1. Plk1 has multiple functions including activation of Cdc25C phosphatase and APC_Cdc20 (degrader of Cyclin A & Cyclin B), inactivation of Wee1 kinase, and translocation of CycB_Cdk1 from cytoplasm to nucleus (Golan et al., 2002; Lindqvist et al., 2009; Van De Weerdt & Medema, 2006; van Vugt & Medema, 2005; Zitouni et al., 2014). Plk1 modifies the peak time (PT) and concentration of the two versions of CycB_Cdk1 (i.e., PT of CycB_Cdk1_Nuc with Plk1 is 3208 and without Plk1 is 3238; PT difference is 30 simulation time units). Importantly, the model now incorporates correctly a process that explains an important cell cycle stage transition- mitotic entry. The full details can be found in Chapter 3.

Protein Phosphatase 1 (PP1) is another newly added protein. It should be noted that Iwamoto model is not cyclic because PP1 is missing in that model. It has been biologically proven that at the end of cell cycle (mid-late M phase), Retinoblastoma protein (pRb) becomes dephosphorylated by a crucial phosphatase called Protein Phosphatase 1 (PP1) (Berndt, 2002; Ludlow et al., 1993; Nelson et al., 1997; Trinkle-Mulcahy et al., 2003). Through our numerical analysis, we found out that the

parameter associated with dephosphorylation of pRb by PP1 is one of the most significant parameters in the system which shows the importance of this addition. By adding this element to correct the situation, we have made the model cyclic (Chapter 3).

SCF is another newly added element that is a ubiquitin ligase whose function is to degrade a number of core components in the cell cycle control system. The reason for adding SCF to our model is that there is biological evidence that Cyclin E, which is the key player of cell cycle during G1 phase, is degraded by SCF (Ang & Harper, 2004; Cardozo & Pagano, 2004; Nakayama & Nakayama, 2005). In Iwamoto model (Iwamoto et al., 2011), the process of Cyclin E degradation is not complete and we believe that adding SCF to the model makes it more accurate. Specifically, in Iwamoto model, biologically relevant Cyclin E degradation details are not incorporated as in our model and therefore, CycE_Cdk2 degradation happens over a longer time. With SCF, CycE_Cdk2 peaks slightly sooner and degrades quicker. Peak time of aCycE_Cdk2 (which indicates G1-S transition) with SCF is 1095 and without SCF is 1133 (peak time difference is 38). Therefore, we can assume that Cyclin E degrades more realistically in our model (see Chapter 3 for details).

The DNA damage part in Iwamoto model has p53 as a transcription factor that induces synthesis of a number of proteins. One of them was 14-3-3σ that affects (inactivates) B-type Cyclin_Cdk complex (the main controller of cell cycle during M phase) to arrest cell cycle in the case of DNA damage. However, that does not represent the complete picture of impact of p53 on CycB_Cdk1. To make that picture more complete, we found another product of p53, Gadd45α, that also inactivates CycB_Cdk1 (Jin et al., 2002; Zhan, 2005). Furthermore, biological evidence shows that the way that 14-3-3σ and Gadd45α act upon CycB_Cdk1 inactivation is different. The first factor (14-3-3σ) inhibits Cdc25C (which is the CycB_Cdk1 activator), while the second (Gadd45α) physically interacts with Cdk1 in order to stimulate CyclinB_Cdk1 unbinding (Jin et al., 2002; Zhan, 2005). Therefore, Gadd45α is added to the model to present a more complete picture of G2-M checkpoint. Gadd45α is produced throughout the period of activity of p53 (see Chapter 3 for details).

Newly added elements provide an opportunity for biologists to set up new hypothesis to experiment in their lab for targeted cancer therapies. For example, PP1 can be used for cancer therapy as its knocking out can halt the cell proliferation by stopping the system from cycling.

2. *Why is it important to have sub-systems in our model and what are the model sub-systems and corresponding modules?*

The model with sub-systems enables us to seamlessly and realistically study the function of sub-systems as well as the influence of sub-systems on each other where the Growth Factor sub-system senses the Growth Factor signals and triggers the activation of subsequent sub-systems. This

presentation also retains the functionality of the system and provides a clearer interpretation of the processes within it while reducing the complexity in comprehending these processes.

The Growth Factor signalling is a sub-system that has not been properly incorporated into mammalian cell cycle modelling yet and existing models have assumed just a constant signal as Growth Factor. We present it as a continuous signal and now the relationship between c-Myc and Cyclin D is realistically represented. The function of Growth Factor signal is to activate c-Myc that in essence initiates the cell cycle by triggering the synthesis of Cyclin D. Therefore, this sub-system is added to our model to give a better understanding of the interplay between Growth Factor signalling and cell cycle initiation. G1-S and G2-M checkpoints play an important role in controlling cell cycle progression, particularly in the presence of DNA damage, and their response mechanisms and corresponding inter-relationships should be properly investigated to understand DNA damage response in cell cycle more comprehensively. G1-S checkpoint sub-system is abstracted into four interconnected modules (Cdk4-Related, E2F-pRb, Cdk2-Related and Tyrosine phosphatase where the latter is a novel addition to this sub-system and E2F-pRb module is expanded and modified to make the model cyclic); G2-M is abstracted into five modules (Cdk1-Related, Tyrosine phosphatase, Tyrosine kinase, Plk1-Related and APC-Related where the latter four are novel additions and contained new components). To provide a complete picture of DNA damage signalling and its impact on cell cycle progression, we incorporate both rapid and delayed pathways into one sub-system. Therefore, DNA damage sub-system is abstracted into two modules including Chk-Related (rapid) and newly added elements in p53-Related (delayed) modules. The details of the abovementioned four sub-systems and the corresponding mathematical equations are given in Chapter 3.

3. *Are the results of our comprehensive model consistent with biological findings?*

The simulation results are in good agreement with biological findings about the dynamics of the newly added elements as well as the key players of the cell cycle system (Chapter 3). The results associated with this study objective have been published in Journal of Theoretical Biology (JTB) with the title of “A comprehensive complex systems approach to the study and analysis of mammalian cell cycle control system in the presence of DNA damage stress” (Abroudi et al., 2017).

The second objective corresponds to identifying the parts (sub-systems, modules, and parameters) of the mammalian cell cycle system which have the most significant effect on system response with and without DNA damage. The system response is either G1-S or G2-M transition.

Regarding the second objective, the following questions can be asked:

4. *What are the biological indicators associated with G1-S and G2-M transitions?*

Peak times (PTs) of aCycE_Cdk2 and aCycB_Cdk1 are considered as indicators of G1-S and G2-M, respectively.

5. *How is it possible to investigate and characterise the most influential parts of the system from systems point of view?*

Using the comprehensive mathematical model developed in Chapter 3, we propose an analytical approach through Global Sensitivity Analysis (GSA), which focuses on global impact of parameters. A model based on Artificial Neural Networks (ANNs) and statistical analysis called Self-Organizing Map with Correlation Coefficient Analysis (SOMCCA) is developed to perform GSA which shows that Growth Factor and G1-S checkpoint sub-systems and seven parameters in the modules within them are significant towards both G1-S and G2-M transitions (see details in Chapter 4).

The third objective is about exploring the relationship between DNA damage and cell cycle progression since there is biological evidence that G1-S checkpoint is relatively inefficient in arresting damaged cells compared to G2-M.

According to the third objective, the following questions can be asked:

6. *Is it possible to define and formulate the efficiency of checkpoints using our comprehensive mathematical model to recapitulate the corresponding biological findings?*

To study the relative efficiency of DNA damage checkpoints, a Checkpoint Efficiency Evaluation (CEE) model is developed based on perturbation studies and statistical Type II error using the comprehensive model presented in Chapter 3. This is based on the number of damaged cells passing checkpoints as normal cells. For this analysis, Probability Density Functions (PDFs) of PT for normal and damaged cells for both G1-S and G2-M checkpoints are developed. From these two tests, we first assess the number of damaged cells that escape the two checkpoints. Then, the damaged cells that escape G2-M checkpoint are compared with those passing G1-S to determine the proportion of the latter that also escapes G2-M. G2-M checkpoint is capable of identifying and arresting a greater percentage of damaged cells than G1-S. For example, under ±5% perturbation, 543 out of 2000 damaged cells pass G1-S checkpoint as healthy cells and then only 78 out of these 543 damaged cells are not caught at G2-M checkpoint. Therefore, the efficiency of G1-S is $\frac{2000-543}{2000} = 72.8\%$, while the efficiency of G2-M is $\frac{543-78}{543} = 85.6\%$ (the efficiency of G2-M is higher than that of G1-S). The rate at which damage cells pass the combined checkpoint system as healthy cells is 3.9% (78/2000) (False Negative rate) making the whole system efficiency $\frac{2000-78}{2000} = 96.1\%$. The full details of the CEE model are presented in Chapter 5.

7. *Although it is more important for damaged cells to be stopped, it is not beneficial for the cell to sacrifice many healthy cells. Therefore, what is the statistic for healthy cells to become arrested?*

We also conduct the checkpoint efficiency analysis for incorrectly sacrificing healthy cells. Results show that both checkpoints are highly efficient and near perfect in recognising healthy cells (99.15% for G1-S and 99.49% for G2-M). As the perturbation level increases, both checkpoints drop in efficiency but G2-M not only remains more efficient but also is more robust against sacrificing healthy cells. Results are shown in Chapter 5.

8. *What is the benefit of having a model that can represent the efficiency of checkpoints?*

Biological findings have shown that cancer cells relay more on G2-M checkpoint in order to repair their excess DNA damage and avoid Apoptosis as their G1-S checkpoint is usually deficient which causes accumulation of mutations (Bucher & Britten, 2008; Chen et al., 2012). Therefore, having a model that can represent the behaviour of checkpoints is beneficial for targeted cancer therapies. New hypotheses can be formulated by scientists to test in their lab, such as knocking out G2-M proteins in order to push cancer cells into unscheduled M-phase which leads to Apoptosis through mitotic catastrophe.

The forth objective of this research involves how Petri Nets (PNs) modelling approach can be applied towards model abstraction.

This objective leads us to a number of challenging questions:

9. *Why PN-based modelling is selected as a suitable approach for model abstraction?*

Mammalian cell cycle is a sophisticated system comprising specified phases which occur in a purposeful and timely way. There exist a huge number of chemical reactions that make accurate modelling of this system a challenging issue. In Chapters 3, we propose a comprehensive mathematical model of mammalian cell cycle control system and published a journal article (as mentioned before) based on that (Abroudi et al., 2017) and now, it is of interest to develop an abstract/minimised model of mammalian cell cycle in a way that the main system characteristics (such as dynamics of key players) and system response (such as G1-S and G2-M transitions as well as response to DNA damage) are qualitatively similar. Petri Nets are well suited to represent biological systems, especially complex systems like mammalian cell cycle, which comprises different timescales. In PN modelling, biological entities, such as genes and proteins, can be presented as Places; different kinds of interactions can be denoted by Transitions. This one to one mapping of molecules-reactions to places-transitions permits a powerful intuitive structure for such a computational modelling

approach (Gilbert & Heiner, 2006; Hardy & Robillard, 2004; Herajy et al., 2013; Koch et al., 2010; Matsuno et al., 2003). Furthermore, it provides an appropriate platform for combining continuous and discrete processes at different levels of abstraction. Therefore, Multi-Level Hybrid Petri Net (MLHPN), a graphical Petri Net-based modelling method, is proposed to model the mammalian cell cycle regulation system. It involves incorporation of Cyc_Cdks (as the most essential controllers of mammalian cell cycle) and regulators of Cyc_Cdks at different levels of abstraction to develop a minimal yet comprehensive model. For example, CycB_Cdk1 is the key player of G2-M transition, which controls the progression of cell cycle through Mitosis (presented at high-level of abstraction); there are some regulatory elements which regulate CycB_Cdk1 complex in either positive or negative way (presented at low-level of abstraction). Cdc25C is one of the positive regulators and APC_Cdc20 is a negative one (Bollen & Beullens, 2002; Boutros et al., 2007; Goulev & Charvin, 2011; Mateo et al., 2009; Perry & Kornbluth, 2007). This way, with the MLHPN model, we minimise the comprehensive mathematical model with 61 ODEs and 148 parameters down to just four equations and 31 parameters. The study related to this part is given in Chapter 6.

10. *How do we select the components of the abstract model?*

In order to perform model abstraction, we identify the core components of the comprehensive mathematical model presented in Chapter 3 with the highest significance on system response (G1-S and G2-M transitions). The most effective parameters are identified using the "Self-Organizing Map with Correlation Coefficient Analysis" (SOMCCA) model. Full details are presented in Chapter 6.

11. *Is it possible to evaluate the efficiency of checkpoints using the abstract MLHPN model and if so, are the results consistent with the results from the comprehensive model?*

We conduct the Checkpoint Efficiency Evaluation (CEE) analysis on the MLHPN model and the results confirm that G2-M checkpoint performs better than G1-S in detecting damaged cells under DNA damage. Furthermore, the trend of efficiencies for G1-S and G2-M checkpoints (and combined checkpoint efficiency) is the same for both models on either detecting damaged cells passing checkpoints as healthy or healthy cells getting arrested as damaged cells. However, the MLHPN is more sensitive to system perturbation which is expected because of the smaller number of elements and parameters in this model.

12. *How close the PN abstract model results are to those of the comprehensive model?*

The trends of Cyc_Cdks are qualitatively similar between the two models. In order to compare the results of the two models, we convert the results of the comprehensive model to the scale of the MLHPN model (or vice versa) as each cell cycle of the MLHPN model is 20.57 simulation time units

while the corresponding value for the comprehensive model is approximately 3700 simulation time units (they can easily be converted to each other as well as to hours as shown in the corresponding simulation figures). The results show that G1-S and G2-M transitions in the MLHPN model (6.0756 and 17.2901 for G1-S and G2-M transitions, respectively) happen almost at the same time points as those of the comprehensive mathematical model (6.0876 and 17.8347 for G1-S and G2-M transitions, respectively – converted to the simulation time unit of the MLHPN). Furthermore, the simulation results show that following the DNA damage, the G1-S transition time shifts from 6.0756 (no damage) to 6.2232 (damage condition). Moreover, the corresponding shift for the G2-M transition is from 17.2901 (no damage) to 17.9438 (damage condition). Thus, the G1-S and G2-M arrest durations are 26.5 and 117.5, respectively (converted to the simulation time unit of the comprehensive model), which are close to the corresponding arrest durations for the comprehensive model (30 and 122, respectively). Therefore, similar to the comprehensive model, the MLHPN model can qualitatively present the cell cycle arrest under a DNA damage condition. In conclusion, the proposed abstract model provides an intuitive approach to represent the complex system of mammalian cell cycle from different levels of abstraction where the sub-systems and their constituent elements (different places and transitions) interact with each other in the most intuitive way (see Chapter 6 for details).

Chapter 2

Literature Review

This chapter provides a literature review on mammalian cell cycle and an overview of the chapter is provided in the first section (Section 2.1). Then, the literature review is presented from two different aspects. The first is the biological point of view where a comprehensive background of mammalian cell cycle control system is presented (Section 2.2). The second aspect is related to the computational modelling of mammalian cell cycle (Section 2.3). A summary of the chapter is presented in Section 2.4.

2.1 Overview

The cell cycle refers to a number of phases that happen in a proliferating cell which eventually leads to production of two daughter cells (Morgan, 2007; Satyanarayana & Kaldis, 2009). This happens within a dynamic environment, where a cell responds to various internal and external signals through a well-ordered sequence of events called cell cycle. Any defect in the function of cell cycle control system may lead to a variety of diseases, such as cancer (Hartwell & Kastan, 1994; Park & Lee, 2003; Stein & Pardee, 2004). In eukaryotic cells, cell cycles have more or less similar sequence of events (Novák et al., 2001; Novak et al., 2007). First, cell grows to an appropriate size to be eligible for DNA duplication. Then, it goes through a process of division (Ferrell et al., 2011). There are some DNA damage checkpoints in order to monitor the progression of cell cycle in the case of any DNA damage (Kastan & Bartek, 2004; Novák et al., 2001; Nyberg et al., 2002; Walworth, 2000).

This complex system can be represented by computational models which have the ability to reproduce the dynamics of the corresponding system. Most computational models have studied the behaviour of yeast cell cycle system and there have been fewer models on mammalian cell cycle, which is the most complicated amongst different species. Therefore, our focus in this chapter is mainly on reviewing mammalian cell cycle regulation system, its response to DNA damage, and corresponding computational modelling approaches. This can be useful for understanding and gaining deeper insights into cell cycle control system as well as potential ways to treatment of cell cycle related diseases, like cancer. Furthermore, integrating all the available information, this chapter attempts to provide the most complete yet succinct functional overview of mammalian cell cycle from a holistic perspective.

2.2 Mammalian Cell Cycle Regulation

Generally, there are two different types of cell: Prokaryotic and Eukaryotic. A prokaryotic cell (such as bacteria) doesn't have a nucleus while the latter has a nucleus (Nelson et al., 2008; Stein & Pardee, 2004). A cell can duplicate itself by the process of growth and division which eventually leads to production of two cells (daughter cells) with identical genetic information (Morgan, 2007). Mammalian cells are in the category of eukaryotic cells which have four phases in each cell cycle. Typically, these phases refer to DNA duplication (S) and DNA segregation (M) separated by two gaps (G1 & G2 phases). There is a cell cycle control mechanism whose function is to ensure the correct ordering and timing of the cell cycle events and its malfunction may result in many diseases, such as cancer (Hartwell & Kastan, 1994; Park & Lee, 2003; Stein & Pardee, 2004). A schematic of cell cycle phases together with checkpoints is shown in Figure 2.1 and described in the following sections.

Figure 2.1 **A schematic of Cell Cycle and its corresponding phases/events and sub-phases. Cell cycle comprises four main phases (G1, S, G2, and M): during G1 a cell grows following the presence of Growth Factor, then in S its DNA is replicated, and following further growth in G2 the mother cell divides into two daughter cells during M. These phases are controlled by four different Cyclins (Cyclin D, Cyclin E, Cyclin A, and Cyclin B) in complex with corresponding Cdks. There are also two important DNA damage checkpoints (G1-S and G2-M) to guarantee genome integrity.**

2.2.1 Cell Cycle Events

The first cell cycle phase is G1 in which a cell grows and becomes ready for DNA replication in S phase. G1 is the most studied phase due to the existence of the Restriction Point (R) in this phase. The R is considered as a point of no return because it is here that a cell is committed to either keep continuing cell cycle or exit from it (Berridge, 2014). Cells may go into a stationary state called G0 (during early G1) if the environmental conditions are not favourable or the cell growth is not enough, but the cell exits from G0 following the presence of Growth Factors (Figure 2.1). If the cell commits to cell cycle and passes beyond R, it proceeds to S phase, where DNA is replicated. In S phase, DNA strands become separated and each strand helps the production of a new DNA strand by functioning as a template (Nelson et al., 2008). At the end of DNA synthesis process, two identical DNA molecules, which have one strand from the original DNA and a new one from the replication process, are produced. The replicated chromosomes are called sister chromatids (Morgan, 2007; Seeley et al., 2007).

In the second gap phase (G2), the DNA replication accuracy, environmental condition, and the volume of the cell are checked. Typically, the gap phases characterise crucial regulatory events associated with transition in which some extracellular or intracellular signals control the cell cycle progression to the next phase. Part of this transition process is preparation for cell division, which happens in M phase. A cell cycle can also be divided into two distinct stages: Interphase and M phase. Interphase includes the G1, S, and G2 phases in which a cell prepares to divide. Generally, the time duration of the interphase is more than ninety percent of a typical cell cycle time (Morgan, 2007).

M phase (cell division) is composed of two main parts: Mitosis and Cytokinesis (Cyt). At the beginning of Mitosis, the cell has a set of condensed pairs of chromosomes (sister chromatids) which are first segregated and then distributed into separate regions of the cell. Mitosis usually has five main sub-phases: Prophase (Pro), ProMetaphase (ProM), Metaphase (Meta), Anaphase (Ana), Telophase (Telo) as demonstrated in Figure 2.1.

During Prophase, Chromatin condensation, centrosome separation, and nuclear envelope breakdown (NEB) are initiated. Next, the spindle assembly is carried out in ProMetaphase right before the chromosome alignment on the spindle plate that happens during Metaphase. Completion of spindle alignment is a signal to start the next sub-phase, Anaphase. All chromosomes are separated and moved toward the opposite spindle poles during Anaphase. Eventually, in Telophase, the chromosomes become decondensed and two nuclei appear. Division into two distinct daughter cells is carried out in Cytokinesis phase. At the end of M phase, each of the new daughter cells has

one of the newly created nuclei and its function is similar to that of the parent cell (Berridge, 2014; Cooper, 2000; Morgan, 2007).

2.2.2 Key Cell Cycle Regulators

Cyclin-Dependent Kinases (Cdks) are the core components of the cell cycle control system and regulate the coordination and timing of the cell cycle events. Mammalian cells have at least ten different kinds of Cdks. Cdk 1, 2, 4, and 6 are the kinases that appear in the mammalian cell cycle (Malumbres & Barbacid, 2005). There is another Cdk (Cdk7) which phosphorylates and activates other Cdks and it is usually known as Cdk-Activating Kinase (CAK) (Harper & Elledge, 1998). It is important to note that the Cdk4 and Cdk6 (also known as starter kinases) have the crucial duty in ensuring a cell's entering cell cycle following the presence of Growth Factor signals. On the other hand, Cdk1 and Cdk2 control the M phase and S phase of the mammalian cell cycle, respectively.

During cell cycle, the levels of Cdks oscillate and these oscillations lead to phase transitions. Activation of the Cdks during cell cycle is mainly due to the binding of cyclins. Four different kinds of cyclins (see Figure 2.1) have crucial effects on mammalian cell cycle system (Cyclin D, Cyclin E, Cyclin A, Cyclin B). These cyclins, which bind to and activate Cdks, stimulate particular cell cycle events. For example, CycE_Cdk2 complex leads to the phosphorylation of some proteins that begin the DNA Replication in S phase. As shown below, there are three regulatory mechanisms that control Cdk activities (Berridge, 2014; Morgan, 1997; Ruddon, 2007; Satyanarayana & Kaldis, 2009). These three processes are also shown in Figure 2.2.

- Cyclins synthesis and degradation (activates and deactivates Cdks) (bottom part of Figure 2.2)
- Presence of Cdk inhibitors, CKIs (inhibits Cdks) (top left-hand side of Figure 2.2)
- Addition/removal of inhibitory phosphate groups by Tyrosine kinases/phosphatases (inhibition/activation of Cdks) (top right-hand side of Figure 2.2)

It is important to note that levels of different Cdks are always high during cell cycle and therefore their gene expressions have little effect on Cdk activities. The levels of cyclins and CKIs are low and high, respectively, during stationary state (G0), but following the presence of Growth Factor, cyclin levels increase and lead to the formation of more Cyc_Cdk complexes. The required elements for each process are clearly illustrated in Figure 2.2. As shown in this figure, cyclins and CKIs affect Cdks through binding processes while the corresponding impact of Tyrosine kinases and phosphatases on Cdks is through dephosphorylation and phosphorylation processes, respectively. As the above-mentioned regulators (CKIs and Tyrosine kinases and phosphatases) can regulate Cyc_Cdk activity,

active Cyc_Cdk can also regulate those regulators via phosphorylation reactions. This process comprises regulation of transcription factors of CKIs and cyclins as well as phosphorylation of ubiquitin ligases, CKIs, and Tyrosine kinases/phosphatases through feedback processes (not shown here).

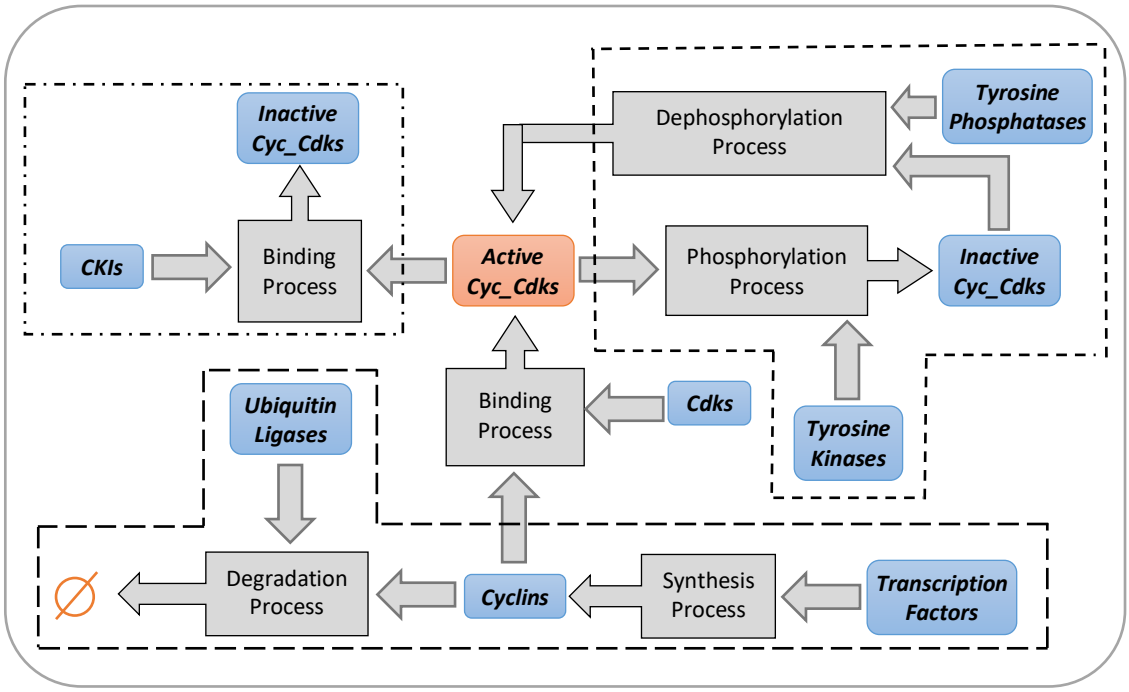

Figure 2.2 Three main regulatory mechanisms of Cdk activity: Synthesis and Degradation of Cyclins (Bottom), Activation and Inactivation of Cyc_Cdk complexes through Tyrosine Phosphatases and Kinases (top right), and Inhibition of Cyc_Cdks through CKIs (top left).

These three Cdk regulatory processes are described in detail in the following sections.

Cyclins

Cyclins act as triggers or switches (activating Cdks) in cell cycle (Figure 2.2, bottom part). The cyclin protein concentrations keep changing during cell cycle due to their regulated expression and degradation. The gene expression depends on transcription factor which binds to the promoter of a gene to induce the expression of that particular gene (Chen & Rajewsky, 2007; Latchman, 1997; Levine & Tjian, 2003). For instance, E2F is a transcription factor that induces the production of Cyclin A and Cyclin E (Trimarchi & Lees, 2002) (bottom right part of Figure 2.2).

The degradation of cyclins is mainly carried out by the process of ubiquitination (tagging for destruction) via ubiquitin ligases, such as “Skp_Cullin_F-box containing complex” (SCF) and “Anaphase-Promoting Complex” (APC) which become activated after binding to two different sub-

units, Cdc20 and Cdh1. Following ubiquitination, protease complexes named Proteasomes recognize tagged cyclins and destroy them (Cardozo & Pagano, 2004; Nakayama & Nakayama, 2006; Vodermaier, 2004) (Figure 2.2, bottom left part).

The first cyclin which has a major influence on start of a new cell cycle in mammalian cells is Cyclin D. The D-type cyclin which is also called G1 Cyclin has the key role in synchronization of cell growth and cell cycle initiation. The level of Cyclin D starts to increase after sensing the Growth Factor signals by the cell's receptors. The level of Cyclin D can be a biomarker for Restriction point (R) transition in G1 phase. Cyclin E (G1-S Cyclin) is another cyclin whose major function is to help transition from G1 to S that eventually leads to the initiation of DNA synthesis process. Cyclin E does this job in two ways: first, it triggers the destruction of a Cdk Inhibitor, p27. The main function of p27 is to maintain the cell in stationary state by binding to and inhibiting Cyc_Cdk complexes. In fact, following the presence of Growth Factors, first, Cyclin D and subsequently, Cyclin E are produced. Afterwards, some of CycE_Cdk complexes, which are not suppressed by p27, induce release of p27 from inactive CycE_Cdks and thereby, stimulate their activation. The second function of Cyclin E is to inactivate APC_Cdh1. This ubiquitin ligase degrades some proteins, such as Cdc25A, Cyclin A, and Cyclin B. CycE_Cdk2 complex causes phosphorylation of APC_Cdh1 and therefore, dissociation of Cdh1 sub-unit from APC leading to inactivation of APC_Cdh1 (Murray, 2004). It is important to note that Cyclin E is degraded by another ubiquitin ligase (SCF) at the end of G1 phase (Cardozo & Pagano, 2004).

Cyclin A (S Cyclin) has a key function in the process of DNA replication. Its level starts to increase at the end of G1 phase with a gradually increasing trend from early S phase to early M phase, where it triggers the activation of the next cyclin (Cyclin B) in the cell cycle. Cyclin A is destroyed by APC_Cdc20 through the ubiquitination process which occurs after nuclear envelope breakdown in early M phase (Prometaphase). Cyclin B (M Cyclin) concentration begins to increase from the end of S phase and it helps the spindle assembly and chromosomes alignment at Metaphase. During Anaphase, the concentration level of Cyclin B falls due to the ubiquitination process that is started by APC_Cdc20 and finished by APC_Cdh1 (Morgan, 2007; Vodermaier, 2004). It is this destruction mechanism that leads to the M phase exit at the end of cell cycle.

Cyclin-Dependent Kinase Inhibitors (CKIs)

When a cell is not in cell cycle, its Cdks must be regulated to keep them in check. One of the most important categories of Cdk regulators is the family of Cdk inhibitors or CKIs, which bind to and supress the activity of Cyc_Cdk complexes (see Figure 2.2, top left part). Some important CKIs are p21 and p27, which have different functions toward different Cyc_Cdk complexes (Besson et al., 2008; Malumbres & Barbacid, 2005).

Passing through G1-S and entering a new cell cycle require the rise of CycE_Cdk2 levels which is kept suppressed by p27. Therefore, p27 should be destroyed by the end of G1 phase. This removal of p27 from CycE_Cdk2 is carried out via two mechanisms: first one is related to CycD_Cdk4 complexes. Since p27 is required for the activation of CycD_Cdk4 complex, after sensing the Growth Factor during G1 phase, more complexes of CycD_Cdk4s bind to p27 leaving less free p27 proteins for binding and suppressing CycE_Cdk2s. Secondly, in the mid to late G1, Growth Factors and mitogens cause the phosphorylation of p27 on Ser10 and Thr157 residues and their destruction. This process leads to the activation of a small number of CycE_Cdk2 complexes in late G1. These active complexes, in turn, trigger the destruction of remaining p27 inhibitors via phosphorylation on Thr187. This results in full activation of CycE_Cdk2 complexes at the G1-S transition. In either case, the phosphorylation of p27 leads to SCF-dependent ubiquitination and degradation of p27 (Hao et al., 2005; Kamura et al., 2004; Morgan, 2007; Sherr & Roberts, 1999). CKI p21 has also a crucial function in mammalian cell cycle in that it leads to cell cycle arrest in the presence of DNA damage. The corresponding impact of p21 on G1-S transition is that it binds to CycE_Cdk2 and CycA_Cdk2 and inactivates them. Likewise, it binds to and inactivates CycB_Cdk1 therefore supresses the G2_M transition. On the other hand, p21 activates CycD_Cdk4 by mediating assembly of this complex in cytoplasm (Cazzalini et al., 2010; Karimian et al., 2016; Yoon et al., 2012). Table 2.1 shows the most important mammalian Cdk Inhibitors and the corresponding functions.

Table 2.1 The most important Cyclin-Dependent Kinase Inhibitors in mammalian cells.

CKI Name	Function
p21, p27	Suppresses CycE_Cdk2, CycA_Cdk2, and CycB_Cdk1. Activates CycD_Cdk4,6

Tyrosine Kinases and Tyrosine Phosphatases

The phosphorylation of Thr14 and Tyr15 residues in mammalian Cdks inhibits the activity of Cyc_Cdk complexes. In particular, the phosphorylation state of these sites is important in Cdk1 at the initiation of M phase. The phosphorylation of Cdks is regulated by Tyrosine kinases and phosphatases. The most important Tyrosine kinase and phosphatase in the mammalian cell cycle are Wee1 and Cdc25 family, respectively (Boutros et al., 2006; Morgan, 2007; Perry & Kornbluth, 2007). There is also another kinase (Myt1) which phosphorylates both Tyr15 and Thr14 residues in vertebrates. The family of Cdc25 includes three different Cdc25 proteins whose functions, together with those of Wee1 and Myt1, are summarized in Table 2.2. Phosphorylation of Cdk1 on the aforementioned residues, which leads to CycB_Cdk1 inactivation, can be neutralized by dephosphorylation via Cdc25 phosphatases (Figure 2.2, top right part). These interactions trigger a process that leads to the activation of Cdk1 and the onset of M phase.

Table 2.2 Tyrosine kinases and phosphatases

Tyrosine Kinases (phosphorylate Cdks)		
Name	**Function**	**Corresponding Cdks**
Wee1	Tyr 15 Phosphorylation	Cdk1 & Cdk2
Myt1	Tyr 15 and Thr14 Phosphorylation	Cdk1 & Cdk2
Tyrosine Phosphatases (dephosphorylate Cdks)		
Name	**Function Point**	**Corresponding Cdks**
Cdc25A	Important at transition from G1 to S	Cdk2
Cdc25B	Important at transition from G2 to M	Cdk1
Cdc25C	Important at transition from G2 to M	Cdk1

In the following section, the important effect of Cyc_Cdk complexes on cell cycle progression and DNA damage checkpoints will be described.

2.2.3 Cell Cycle Progression

The progression of the cell cycle is tightly controlled by a set of interactions characterized by synthesis/degradation and activation/inactivation of some regulators. Furthermore, there are some checkpoints whose function is to check the fidelity of the genome and to arrest the cell cycle progression in the presence of unfavourable conditions such as DNA damage (Nyberg et al., 2002; Zhou & Elledge, 2000). The existence of Growth Factor signal (or mitogen) can either make a cell in G0 state enter G1 phase (initiate cell cycle) or allow a newly synthesized cell to go directly from M to G1 phase. Likewise, if the Growth Factor signal is removed, it lets the cell return to the stationary state G0, provided that this removal happens before the Restriction point (R). The Restriction point, which is in the late G1 phase, is the point from which the cell cycle progression will be independent of Growth Factors. A cell which passes the Restriction point is committed to finishing the current cycle. After the Restriction point, different types of cyclins, which have a key role in the cell cycle signalling system, operate at particular points in order to control cell cycle progression.

It has been proven that Growth Factor signals induce the synthesis of Cyclin D via a Ras-mediated pathway (Alberts et al., 2014; Morgan, 2007). The Growth Factor signalling is shown in Figure 2.3. The activated Growth Factor receptors cause binding of the guanine-nucleotide exchange factor Sos to GDP-bound Ras via interaction with an SH2-containing protein named Grb2. This binding stimulates the activation of Ras by turning it in the form of GTP-bound Ras. Thereafter, a cascade of protein kinase activation is initiated which finally leads to the phosphorylation and activation of MAP

Kinase (MAPK). This kinase is translocated to the nucleus and eventually causes the synthesis of Cyclin D through a number of gene regulation processes. The corresponding gene regulations start with the transcription of immediate early genes. Serum-Response Factor (SRF) is one of the gene regulatory proteins which stimulates the transcription of immediate early genes. The proteins that are the products of the aforementioned process (such as c-Fos and c-Myc) induce the expression of a second series of genes called delayed response genes (Adhikary & Eilers, 2005; Alberts et al., 2014; Morgan, 2007). Cyclin D is a product of these genes.

Image removed for copyright compliance

Figure 2.3 Growth Factor signalling pathway (Morgan, 2007).

The story begins when a cell receives the Growth Factor signals which eventually lead to production of Cyclin D through activation of a transcription factor called c-Myc. Once produced, Cyclin D binds to Cdk4,6 to form CycD_Cdk4,6 complex, which triggers activation of transcription factor E2F. This Transcription factor, in turn, induces the expression of two key cyclins (Cyclin A and Cyclin E) as well as Cdc25A, B-Myb and E2F itself. There are two important inhibitory regulators (p27 and APC_Cdh1) during the G1 phase that inhibit Cyclin E and Cyclin A. The function of these regulators is to make sure that no new cell cycle starts unless the environmental conditions favour the proliferation process. B-Myb is another transcription factor (which is produced and activated by E2F and CycA_Cdk2, respectively) that triggers the production of Cyclin A (Fung & Poon, 2005; Joaquin & Watson, 2003; Zhu et al., 2004). However, Transcription factor NFY, which also becomes activated by CycA_Cdk2, stimulates the production of both Cyclin A and Cyclin B (Chae et al., 2004; Chae & Shin, 2011; Fung & Poon, 2005; Yun et al., 2003). Cdc25A is a phosphatase that induces activation of CycE_Cdk2 and active CycE_Cdk2 promotes degradation of p27 and APC_Cdh1. This results in higher expression of proteins needed for DNA synthesis, such as Cyclin A. In mammalian cells, Cyclin E typically increases transiently at late G1 phase. But, Cyclin A starts to rise from the beginning of S phase and is degraded during prometaphase, after nuclear envelope breakdown (Berridge, 2014; Morgan, 2007).

Cyclin B is synthesised through transcription factor NFY and then binds to Cdk1 to create CycB_Cdk1 complex. The activity of this complex is low during G2 phase due to inhibitory phosphorylation by Tyrosine kinase, Wee1. Dephosphorylation of CycB_Cdk1 by Tyrosine phosphatases (Cdc25 proteins) triggers the activation of this complex. It is important to note that CycA_Cdk2 complex stimulates activation of Cdc25 phosphatases. In late Prometaphase, free APC is phosphorylated and activated by CycB_Cdk1 complex and binds to APC20. But this type of active APC_Cdc20 (partially active form) just functions toward Cyclin A (by ubiquitination and degradation of Cyclin A) till the end of Metaphase. Upon the deactivation of spindle assembly checkpoint during Metaphase, APC_Cdc20 attains its full activity and trigger the destruction Cyclin B. Cyclin B is degraded during Anaphase and this leads to dephosphorylation of Cdh1 which results in formation of APC_Cdh1. Active APC_Cdh1, in turn, stimulates the degradation of Cdc20 and drives the final steps of M phase that leads to ending a cell cycle (Morgan, 2007).

There are two main checkpoints in cell cycle (G1-S and G2-M) which control the progression through cell cycle stages (Hartwell & Weinert, 1989). Various proteins and complexes, such as cyclins, CKIs, Tyrosine kinases and phosphatases, ubiquitin ligases, etc. are the players which regulate the cell cycle events at G1-S and G2-M checkpoints. These checkpoints are related to DNA damage checking. Mutation in one or more of these regulators can cause diseases like different types of cancer (Kastan & Bartek, 2004). It should be noted that there is another checkpoint called Mitotic Spindle or Spindle

Assembly Checkpoint (SAC), which takes place during M phase. This checkpoint monitors the assembly of all sister chromatids' kinetochores to microtubules on the mitotic plate to make sure that all of them are correctly connected and it happens at Metaphase to Anaphase transition.

The cell cycle can be considered as an engine with some brakes and accelerators which monitor the cell cycle system to ensure the correct order of events. Furthermore, this robust surveillance mechanism can block an event if any problem occurs. Therefore, entering into the next phase is delayed until the problem is resolved or the previous phase is finished. As mentioned before, the components of the cell cycle control system exert their regulatory effects on progression of cycle in different stages. The appropriate conditions (like sufficient cell size or enough nutrients) can accelerate the cell cycle engine while the inhibitory signals (such as DNA damage or unreplicated DNA) lead to a brake in cell cycle progression (Novák et al., 2001; Nyberg et al., 2002). Therefore, the DNA damage checkpoints and their core elements are explained in the following section as a lot of existing computational models of mammalian cell cycle have investigated these checkpoints.

2.2.4 DNA Damage Checkpoints

There are some sensing mechanisms which detect DNA damage and send negative signals to cell cycle control system that can lead to cell cycle arrest at particular places. After sensing DNA damage by special sensor proteins, the damage signal is transduced by a cascade of protein kinases that eventually phosphorylate and activate some effector proteins. Some of these effector proteins stimulate the expression of some enzymes that repair the DNA damage. Some other effectors are responsible for cell cycle arrest. Usually, cell cycle can be resumed after the repair process is done if the damage is not severe (Fry et al., 2005; Morgan, 2007; Nyberg et al., 2002; Rouse & Jackson, 2002). In the case of severe damage, cell goes through Apoptosis or programmed cell death (Elmore, 2007). Figure 2.4 shows a holistic picture of DNA damage response.

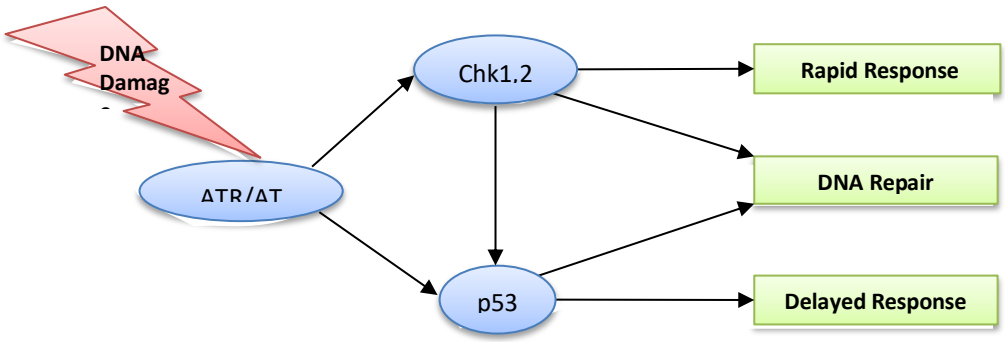

Figure 2.4 A holistic picture of DNA damage response.

Two protein kinases (ATM & ATR) are at the centre of DNA damage signalling pathway. ATM is related to Double-Strand Breaks (DSBs) and ATR is responsible for other kinds of DNA damage, like stalled replication fork and Single-Strand Breaks (SSB) (Nyberg et al., 2002). There are two types of DNA damage responses: rapid response and delayed (or maintenance) response. Rapid response pathway, which is transcription-independent, gets activated within a few minutes. It acts through the activation of two effector kinases called Chk1 and Chk2 which inhibit some cell cycle regulators, such as Cdc25 phosphatases. These kinases trigger a signalling pathway which leads to quick blocking of cell cycle as well as production of some DNA repair enzymes (Figure 2.4) (Bartek & Lukas, 2001; Morgan, 2007; Sancar et al., 2004).

The delayed signalling pathway, which is transcription-dependent and is based on a protein called p53 (ATR and ATM activate p53), is activated following the activation of rapid pathway and leads to prolonged cell cycle arrest (Figure 2.4). Transcription factor p53 stimulates higher production of various target proteins related to DNA repair and temporary and permanent cell cycle arrest. Activation of p53 results in expression of a CKI protein called p21 which inactivates some key components of cell cycle progression, such as CycE_Cdk2, CycA_Cdk2, and CycB_Cdk1. It (p53) is also responsible for programmed cell death or Apoptosis if the damage is irreparable (Abraham, 2001; Bartek & Lukas, 2003; Liu et al., 2006; Zhou & Elledge, 2000).

G1-S Checkpoint

The first checkpoint in the eukaryotic cell cycle is called G1-S checkpoint and it occurs after the Restriction point. This checkpoint can block the cell cycle system from entering into S phase in the presence of different DNA damages. In fact, DNA damage can trigger some signalling pathways which lead to cell cycle arrest that stops the onset of DNA duplication process. The purpose of this arrest is to provide enough time for the cell cycle control system to assess the damage and either repair the DNA damage before allowing the cell to enter S phase or eliminate/kill the cell (apoptosis) if damage is irreparable.

It is important to note that the Restriction point and G1-S checkpoint are two distinct points in the cell cycle. For instance, in the presence of favourable environmental conditions, a cell with or without DNA damage can pass through Restriction point but not G1-S checkpoint (Bartek & Lukas, 2001; Pardee, 2002). Following DNA damage, either ATR or ATM is auto-phosphorylated and activated and therefore it can phosphorylate some target proteins such as Chk1/Chk2 and p53 as shown in Figure 2.4. As mentioned before, the phosphorylation of these proteins triggers two different signalling pathways; one for initiating and another for maintaining the G1-S blockage (Bartek & Lukas, 2001). G1-S checkpoint details with these two response pathways are shown in Figure 2.5. Regardless of DNA damage type, activated Chk1/Chk2 causes phosphorylation and

inactivation of Cdc25A phosphatase (Figure 2.5). As a result, there are no active phosphatases to remove the inhibitory phosphate group from Cyc_Cdks and therefore cell cycle is halted at G1-S checkpoint (Bartek et al., 2001; Molinari et al., 2000).

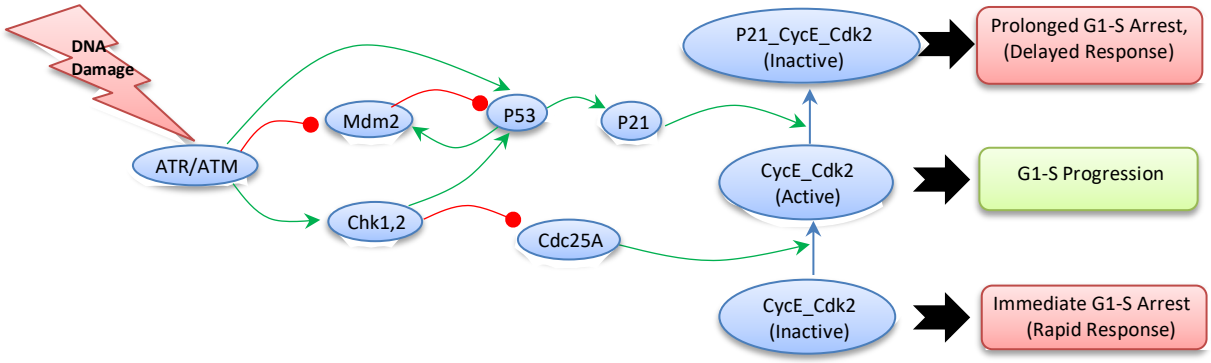

Figure 2.5 **G1-S checkpoint with rapid and delayed DNA damage response pathways. Red round-ended arrows indicate negative effects (i.e., inhibition, inactivation, etc.); green arrows denote positive effects (i.e., activation, synthesis, etc.); blue arrows correspond to biochemical reactions (i.e., binding of two proteins, etc.) and thick black arrows show the results of formation of a particular complex (i.e., formation of active CycE_Cdk2 leads to G1-S progression, etc.).**

The rapid response which is mediated by Chk1/Chk2 is followed by the delayed response. The latter comes into the picture after the rapid response (Bartek & Lukas, 2001). In the delayed stage, Ser15 and Ser20 residues of p53 are phosphorylated by ATR/ATM and Chk1/Chk2, respectively (Banin et al., 1998; Chehab et al., 1999; Kastan & Lim, 2000; Ryan et al., 2001). There is an important ubiquitin ligase named Mdm2 which has an inhibitory effect on p53 under no DNA damage condition. Mdm2 causes instability and nuclear export of p53 but Mdm2 is inactivated by ATR-/ATM-mediated phosphorylation at Ser395 following the presence of DNA damage signal (Meek, 2004; Nyberg et al., 2002; Zhang & Xiong, 2001).

Activated p53 acts as a transcription factor for inducing the synthesis of p21 which is a Cyclin-Dependent Kinase inhibitor that inhibits the activity of CycE_Cdk2 complexes needed for G1-S transition. The whole point in inhibiting CycE_Cdk2 is to stop preparing the conditions for G1-S transition, such as preparation of Cyclin A. As discussed before, there is a protein called Retinoblastoma protein (pRb) which inhibits the activity of transcription factor E2F by binding to it. The phosphorylation of pRb (via active Cyc_Cdk2 complexes) leads to the release of E2F which stimulates the expression of G1-S cyclins. Therefore, inactive Cyc_Cdk2 complexes, which become inactive by the DNA damage response, suppress the production of proteins (such as E2F) which are required for preparing Cyclin E and Cyclin A for G1-S transition.

G2-M Checkpoint

When DNA damage happens, G2 cells (cells that are in G2 phase) are prevented from entry into M phase. This checkpoint controls the transition from G2 to M phase by regulating CycB_Cdk1 complex as shown in Figure 2.6. Following the DNA damage in G2 phase, either ATR→Chk1→Cdc25 or ATM→Chk2→Cdc25 pathway is stimulated to block the cell cycle progression (rapid response) (Brown & Baltimore, 2003; Xu et al., 2002; Zhao & Piwnica-Worms, 2001). As demonstrated in Figure 2.6, Chk1/Chk2 (shown as Chk1,2 in the figure) inhibits the activity of Cdc25 phosphatases (by phosphorylating their different sites).

The delayed response, which is mediated by ATM/ATR→p53 pathway, induces the expression of some genes that encode inhibitor regulators such as p21, 14-3-3σ, and Gadd45α. The first one (p21) is a CKI which binds to and inhibits the activity of CycB_Cdk1 complex. The second one (14-3-3σ) is a phosphoserine binding protein that following phosphorylation of Cdc25 proteins by Chk1/Chk2 binds to these phosphatases to further suppress their activity (Chan et al., 2000). Another crucial protein synthesised after DNA damage is "Growth Arrest and DNA Damage-Inducible" (Gadd) protein, Gadd45α. Although both Cdc25-Related pathway and Gadd45α inactivate CycB_Cdk1 complex, the way they do this inactivation is different. The former uses dephosphorylation of Cdk1, but the latter (Gadd45α) establishes a physical interaction with Cdk1 and triggers an unbinding reaction between Cyclin B and Cdk1. This way, Gadd45α stimulates cell cycle arrest at G2-M transition (Jin et al., 2002; Zhan, 2005).

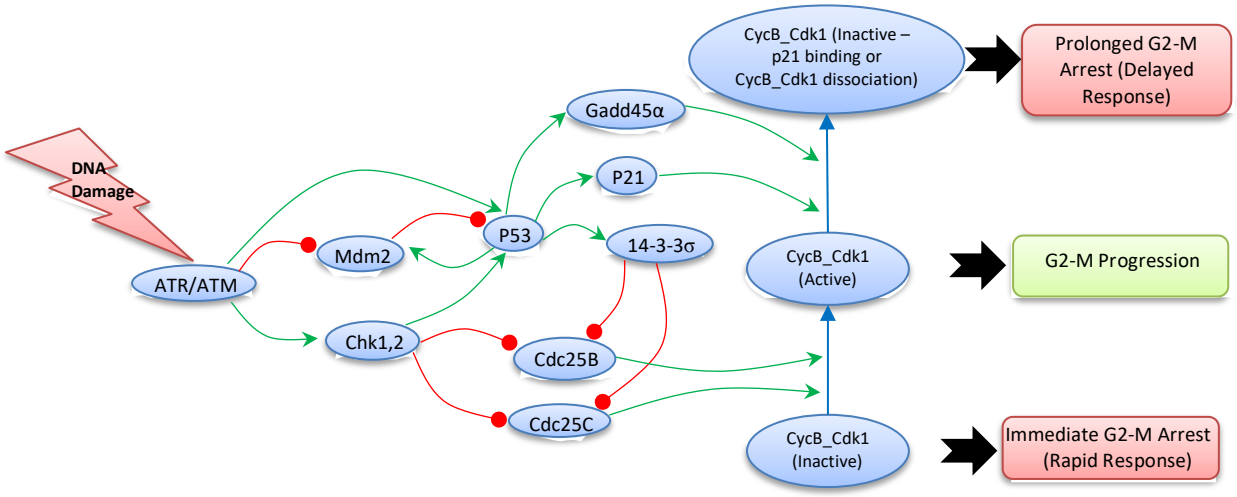

Figure 2.6 **Cell cycle arrest at G2-M checkpoint. Red round-ended arrows indicate negative effects (i.e., inhibition, inactivation, etc.); green arrows denote positive effects (i.e., activation, synthesis, etc.); blue arrows correspond to biochemical reactions (i.e., binding of two proteins, etc.) and thick black arrows show the results of formation of a particular complex (i.e., formation of active CycB_Cdk1 leads to G2-M progression, etc.).**

Following the increase in cell cycle-Related experimental data in the last two decades, a variety of computational models aimed at understanding the behaviour of this complex system have been developed (Csikász-Nagy, 2009). Majority of these models have focused on yeast cell cycle. Mammalian cell cycle has been less investigated and modelled in comparison to that of other eukaryotes due to its higher complexity. Furthermore, most mammalian cell cycle models have been concentrated just on a part of cell cycle, such as G1-S checkpoint. In the next section, we describe modelling approaches to mammalian cell cycle and also provide a list of computational models in each category.

2.3 Computational Models of Mammalian Cell Cycle

There are five main approaches for modelling biological systems: Discrete, Continuous Deterministic, Stochastic, Hybrid, and Petri Net-based. A summary of all mammalian cell cycle models including the corresponding reference and modelling type is presented at the end of this section in Table 2.4.

The first category is the group of discrete/logical models that qualitatively describe the system behaviour, and mostly correspond to Boolean networks. They provide a high degree of abstraction as well as a fundamental understanding of dynamical behaviour of system under different conditions. Such models are not only flexible but also easy to fit into cell cycle system. These models introduce the states of species in the form of active/inactive (present/absent) and construct causal relationships between them. These models do not have the problem of parameter estimation that ODE models have and they in particular are useful for large scale networks. A main disadvantage of Boolean modelling is that it cannot describe intermediate states such as slow or small state changes and it can easily generate spurious results (Albert & Wang, 2009). Most Boolean models of cell cycle were developed for yeast and not many for mammalian cell cycle. In one of the most referenced Boolean models of mammalian cell cycle, Fauré et al. (2006) constructed a discrete version of an ODE model in synchronous as well as asynchronous updating schemes. They assessed the corresponding merits and limitations of these two schemes in determining the regulatory network behaviour. A logical simulation software named “GINsim” was also developed by this group. However, this model does not take the important effect of some cell cycle regulatory proteins such as Cdc25, Wee1, etc. into consideration.

For construction of a discrete model, three main steps should be followed: (1) constructing network graph; (2) determining logical nodes; (3) defining rules. Logical operators, such as AND, OR, and NOT, are used to define the rules that update the state of the nodes. An example of a discrete graph for a small part of mammalian cell cycle, which shows the regulation of Cyclin B controlled by two ubiquitin ligases (APC_Cdc20 & APC_Cdh1), is illustrated in Figure 2.7 (Morgan, 2007). The logical rule for updating the activity of Cyclin B is illustrated in Table 2.3. According to Figure 2.7 and Table 2.3,

CycB node becomes active (state = 1) if both APC_Cdc20 AND APC_Cdh1 are absent or inactive. These ubiquitin ligases may have some effects on other elements of cell cycle, but just the effect on CycB has been highlighted here to illustrate the Boolean concept.

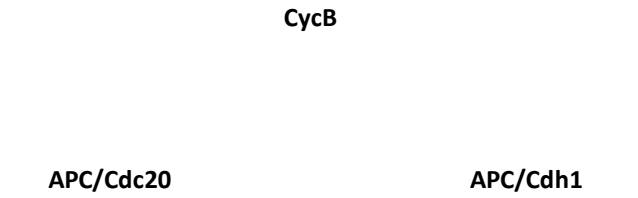

Figure 2.7 An example of a discrete Boolean graph for CycB (Cyclin B) regulation. Green arrows and red round-ended arrows indicate activation and inhibition, respectively.

Table 2.3 Updating rule for CycB activation

Updating rule for CycB	Rationale
CycB: $NOT(APC\_Cdc20)\ AND\ NOT(APC\_Cdh1)$	To become active, CycB needs absence of two ubiquitin ligases, APC_Cdc20 AND APC_Cdh1 (Morgan, 2007).

As discrete models are only able to present system variables discretely, continuous models have become more popular in the field of cell cycle modelling. The main approach here has been mathematical models based on Ordinary Differential Equations (ODEs) that deterministically track the exact concentration of species via continuous representation of system dynamics using a set of ODEs (Fuβ et al., 2005). The rate of chemical reaction m in a dynamic system is expressed as a function (g_m) of species $y_1, y_2, \ldots$, and y_k that effect m and can be presented as r_m:

$$r_m = g_m(y_1, y_2, \ldots, y_k) \tag{2-1}$$

Different kinetic laws are used to mathematically formulate r_m. Mass Action law and Michaelis-Menten are two common kinetic laws used in mathematical models (Sauro, 2012). Mass Action Kinetic is utilized for elementary reactions with single transition step (Eq. (2-2)) and describes the rate of reaction as in Eq. (2-3); therefore, change in concentration of reactants and product can be calculated by Eq. (2-4)

$$dD + eE \xrightarrow{k} pP \tag{2-2}$$

$$r = k \times [D]^d \times [E]^e \tag{2-3}$$

$$\frac{d[D]}{dt} = -d \times r, \quad \frac{d[E]}{dt} = -e \times r, \quad \frac{d[P]}{dt} = p \times r \tag{2-4}$$

where D and E are reactants and P is product; d, e, and p are stoichiometric coefficients; and k is rate constant (Sauro, 2012). On the other hand, Michaelis-Menten law is used when the reaction is enzymatic. The typical reaction of this type can be shown as follows:

$$S + E \underset{k_b}{\overset{k_a}{\rightleftharpoons}} ES \overset{k_c}{\rightarrow} P + E \tag{2-5}$$

where S, E, ES, and P are substrate, enzyme, enzyme-substrate compound, and product, respectively. k_a, k_b, and k_c are rate constants. There are two assumptions to write the Michaelis-Menten kinetic: ES concentration is almost constant; and the total concentration of enzyme (bounded and unbounded) (Etotal) is constant. Therefore, Michaelis-Menten equation formulates the rate of enzymatic reaction or change in concentration of P as hyperbolic with respect to S, as follows:

$$\frac{d[P]}{dt} = r_{max} \frac{[S]}{K_M + [S]} \tag{2-6}$$

where $r_{max} = k_c \times [E_{total}]$ is the maximum reaction rate and $K_M = \frac{k_b + k_c}{k_a}$ is Michaelis-Menten constant. The detailed description of other kinetic laws (such as Hill Function) can be found in (Sauro, 2012). Due to data availability, the last decade of the 20th century has seen a much growth in computational modelling of cell cycle. The first mathematical model of cell cycle was “Modelling the cell division cycle: cdc2 and cyclin interactions” (Tyson, 1991). Comprising six species, this model could qualitatively represent cell division. Tyson characterized “M phase Promoting Factor” (MPF) as the most crucial regulatory element in the cell cycle (MPF corresponds to CycB_Cdk1) which can be regulated by synthesis and degradation of cyclins, dephosphorylated by phosphatase Cdc25, and phosphorylated by kinase Wee1. Also, Novak and Tyson (Novak & Tyson, 1993) showed that “Hysteresis” exists in the MPF–Cyclin relationship which was confirmed experimentally ten years later (Sha et al., 2003), demonstrating the value of computational modelling in biological discovery. In 2004, Novak and Tyson developed a mathematical model for the Restriction point control (Novak & Tyson, 2004) where they investigated the mutations in some key elements of mammalian cell cycle, like Cyclin E and Retinoblastoma protein (pRb). They also considered the important effect of Growth Factor on passage through the Restriction point by exploring the interactions between Growth Factors and cell cycle core components, such as Cyclin_Cdks, and made a good comparison between mammalian and yeast cell cycle dynamics. But their model lacked a strategy to investigate the mechanism of coordination between cell growth and division.

In 1999, Aguda and Tang published a detailed mathematical model to investigate the kinetic origin of the Restriction point in mammalian cell cycle (Aguda & Tang, 1999). In the same year, Aguda explored the effect of DNA damage on G2-M checkpoint (Aguda, 1999a). Iwamoto et al. who partly utilized Aguda's models, developed more complex models of mammalian cell cycle checkpoints and investigated the effect of DNA damage (following UV-irradiation) on G1-S transition in mammalian cell cycle (Iwamoto et al., 2008). This study inspired Ling et al. to investigate the robustness of G1-S checkpoint in depth. Using Type II Error, they introduced a novel approach to quantify the percentage of damaged cells passing G1-S checkpoint under different system perturbations (Ling et al., 2010).

In 2011, Iwamoto et al. added G2-M checkpoint to their previous model in order to make it more comprehensive and meaningful as it then covered almost the whole cell cycle (Iwamoto et al., 2011). This model was insightful in that it could determine cell fate based on DNA damage strength. One of the most complete models of mammalian cell cycle was constructed by Gauthier and Pohl (2011). It included both molecular and cellular systems from nucleotides and amino acids to proteins (33 cell cycle proteins) and consisted 387 equations and around 1100 rates represented in elementary mass action kinetics. The authors presented a table to describe the corresponding location, ubiquitinator, inducer, activator, inactivator and function of each cell cycle protein. This model presented some predictions on both molecular and system levels including the effect of cell growth (Gauthier & Pohl, 2011). The drawback of deterministic models such as ODE is that model complexity increases with the number of chemical reactions. Furthermore, it is hard to estimate kinetic parameters with the limited available data and it becomes even harder for large scale systems.

The third category of models is based on the fact that the functionality of cell cycle regulatory network is often influenced by noise. Unlike deterministic models, stochastic models consider the random variations in concentration of biological species. They are suitable for cases where concentration levels of species are lower than what are applicable for deterministic ones (of the order of many hundreds or above). Thus, as concentrations become lower, the variability of concentration becomes higher and therefore the random element in chemical interactions becomes significant (Donnet & Robert, 2012). In a model, stochasticity can be presented by Gillespie Stochastic Simulation Algorithm (GSSA) (Kar et al., 2009) or Stochastic Langevin Equations (SLA) (Steuer, 2004). The mathematical details of these algorithms can be found in the three aforementioned references. As stochastic models take the number of molecules into account (instead of concentrations), they suffer from the problem of computational complexity.

The next category of models is hybrid type. They integrate strengths of other methods, such as discrete models for rapid changes, continuous models for slow changes, deterministic and stochastic

models for predictable and unpredictable behaviours, respectively (Kiehl et al., 2004). Majority of hybrid models have aimed to overcome the limitations of ODE-based models. Some of these constraints are: (1) problem of passing from the number of molecules to concentration levels; (2) difficulty in combining discrete state transitions and continuous dynamics which is particularly needed throughout cell cycle; (3) limited available experimental data for reaction rates, parameters, and real protein concentrations. In recent years, hybrid modelling has become popular and a few cell cycle models, but not many for mammals, have been proposed and proved to be successful due to incorporation of the best features of individual models as well as the capability to represent different timescales. Singhania et al. (2011) developed a simplified hybrid model emphasizing the vital effect of cyclins on mammalian cell cycle regulation. The authors combined discrete (Boolean), deterministic (ODEs), and stochastic approaches, just three different cyclins (Cyclin E, A, and B) and continuous tracking of cell mass. Here, cyclins were considered as continuous variables but regulators of cyclins as discrete variables which followed Boolean logic with some time delays. However, this model is not completely autonomous and the Boolean part could not update itself based on the current system state. Noel et al. (2013) developed a hybrid model for mammalian cell cycle by combining discrete and continuous methods. They transformed an ODE model developed by Csikász-Nagy et al. (2006) into a piecewise smooth hybrid model with simplified reaction rates using an approximate hybridization scheme.

Petri Nets (PNs) are the last category of models which have emerged as a strong graphical method for modelling biological systems. Following its introduction in the 60's by Carl Adam Petri, PN has been expanded with many extensions, such as Discrete, Continuous, Time-Delayed, Stochastic and Hybrid, which make it possible to incorporate different modular elements into a single model (Baldan et al., 2010; Chaouiya, 2007; Koch et al., 2010; Murata, 1989; Peleg et al., 2005; Pinney et al., 2003; Silva, 2013). Furthermore, it provides a graphical representation of the corresponding network, so that the whole framework can be easily understood by readers (especially those with less mathematical background). All PN models, more or less, share some common features: first, entities and interactions are defined by groups of Places and Transitions, respectively. Second, a number of Tokens which is also called Marking can be assigned to each place to describe the PN state at any given time. Third, a transition can be fired if all the corresponding pre-places have enough tokens to overcome some thresholds. These thresholds are represented by the corresponding values (weights) of the edges which connect the transitions (places) to the places (transitions). As a result of firing, some tokens are subtracted from pre places of the corresponding transition and added to its post places, leading to a change in the state of the PN (Koch et al., 2010; Peleg et al., 2005).

Over the recent years, PN-based modelling started to be implemented for modelling biological networks and cell cycle, but unfortunately there are not many Petri Net models for mammalian cell cycle at the moment (Fujita et al., 2004; Gilbert & Heiner, 2006; Grunwald et al., 2008; Hardy & Robillard, 2004; Herajy & Heiner, 2012; Herajy et al., 2013; Matsui et al., 2004; Matsuno et al., 2003; Mura & Csikász-Nagy, 2008; Windhager & Zimmer, 2008). More models of this type are expected to be developed in near future and the reason is that PNs are intuitive (due to their graphical representation) and they also have different extensions that can be combined to attain better results. Figure 2.8 shows an E2F-dependent production of Cyclin E through a hybrid PN, which includes both discrete and continuous parts. The box on the right side of Figure 2.8 illustrates some comments. In this model, transcription factor E2F is modelled as a discrete variable that can be switched on or off according to some conditions (i.e., inactive EF2 becomes activated through discrete transition T1) and after activation, it leads to initiation of Cyclin E synthesis continuously (continuous transition T3 represents the synthesis of Cyclin E).

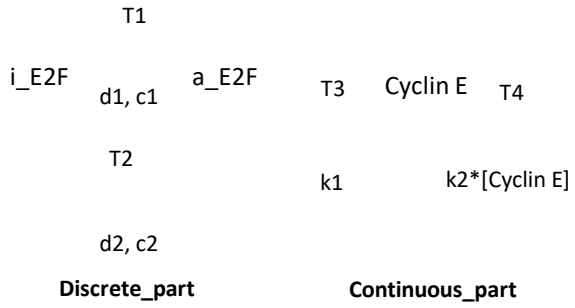

Figure 2.8 A demonstration of E2F-dependent production of Cyclin E through a Hybrid PN. E2F is presented discretely (using discrete Places and Transitions) while production and degradation of cyclin E are modelled continuously using continuous places and transitions (the degrader of cyclin is not shown here). Places iE2F and aE2F correspond to inactive and active E2Fs, respectively. Transitions T1, T2, T3, T4 denote activation, inactivation, synthesis, and degradation processes, respectively. Parameters k1 and k2 are synthesis and degradation rate constants, respectively.

Among all the research groups worked on PNs, two groups stand out: a Japanese group (Matsuno, Nagazaki, and colleagues) and Heiner's groups in Germany. Matsuno's group has developed a petri net tool for biological networks named "Genomic Object Net" in early 2000s. Later, they updated it into a more powerful graphical tool called "Cell-Illustrator" which helps modellers to create and simulate different types of biological systems in a very effective and user-friendly interface (Nagasaki, Fujita, et al., 2002; Nagasaki, Matsuno, et al., 2002; Nagasaki et al., 2009). They have also used their

tool to model cell cycle in Fission Yeast and Xenopus (Fujita et al., 2004; Matsui et al., 2004). Heiner and colleagues worked on Petri net modelling (not just on biological systems) from early 90's. They have also constructed a petri net tool called "Snoopy" in order to design and simulate hierarchical graphs. This tool had also the ability to convert different extensions, such as Qualitative, Continuous, Stochastic, Hybrid, etc. to each other (Heiner et al., 2010; Heiner et al., 2012; Heiner et al., 2008; Rohr et al., 2010). In one interesting Petri Net extension called "Coloured Petri Nets", it is possible to present each place with tokens in different colours. This capability is especially important in biological networks in which an entity may have different states, such as active and inactive (which can be represented with different colours) and this option is embedded in Snoopy as well (Lee et al., 2006; Liu & Heiner, 2010, 2013; Liu et al., 2014). Heiner's group have also developed a model of Eukaryotic cell cycle using Snoopy (Herajy et al., 2013).

Table 2.4 demonstrates mammalian as well as generic cell cycle models published in literature. The title of the article, the type of modelling, and the corresponding reference are presented in this summary table.

Table 2.4 Summary of Mammalian and Generic Cell Cycle Models

Article Title	Type of Model	Reference
Modeling the cell division cycle: cdc2 and cyclin interactions	Continuous Deterministic	(Tyson, 1991)
A minimal cascade model for the mitotic oscillator involving cyclin and cdc2 kinase	Continuous Deterministic	(Goldbeter, 1991)
A model for the adjustment of the mitotic clock by cyclin and MPF levels	Continuous Deterministic	(Norel & Agur, 1991)
Mathematical analysis of a model of the mitotic clock	Continuous Deterministic	(Thron, 1991)
A mathematical model for the G1/S transition of the mammalian cell cycle	Continuous Deterministic	(Hatzimanikatis et al., 1995)
A model of the G1 phase of the cell cycle incorporating cyclin E/cdk2 complex and retinoblastoma protein	Continuous Deterministic	(Obeyesekere et al., 1995)
A mathematical model of the regulation of the G1 phase of Rb+/+ and Rb-/- mouse embryonic fibroblasts and an osteosarcoma cell line	Continuous Deterministic	(Obeyesekere et al., 1997)
Bistable biochemical switching and the control of the events of the cell cycle	Continuous Deterministic	(Thron, 1997)

Functional capabilities of molecular network components controlling the mammalian G1/S cell cycle phase transition	Continuous Deterministic	(Kohn, 1998)
A theory for controlling cell cycle dynamics using a reversibly binding inhibitor	Continuous Deterministic	(Gardner et al., 1998)
Model scenarios for evolution of the eukaryotic cell cycle	Continuous Deterministic	(Novak et al., 1998)
A mathematical description of regulation of the G1-S transition of the mammalian cell cycle	Continuous Deterministic	(Hatzimanikatis et al., 1999)
A model of cell cycle behavior dominated by kinetics of a pathway stimulated by growth factors	Continuous Deterministic	(Obeyesekere et al., 1999)
The kinetic origins of the restriction point in the mammalian cell cycle	Continuous Deterministic	(Aguda & Tang, 1999)
A quantitative analysis of the kinetics of the G2 DNA damage checkpoint system	Continuous Deterministic	(Aguda, 1999b)
Shape-dependent control of cell growth, differentiation, and apoptosis: switching between attractors in cell regulatory networks	Discrete	(Huang & Ingber, 2000)
A model for a network of phosphorylation-dephosphorylation cycles displaying the dynamics of dominoes and clocks	Continuous Deterministic	(Gonze & Goldbeter, 2001)
Regulation of the eukaryotic cell cycle: molecular antagonism, hysteresis, and irreversible transitions	Continuous Deterministic	(Tyson & Novak, 2001)
Variability in the timing of G1/S transition	Stochastic	(Chiorino & Lupi, 2002)
Regulation of the mammalian cell cycle: a model of the G1-to-S transition	Continuous Deterministic	(Qu, Weiss, et al., 2003)
Simulation of the dynamics of gene networks regulating the cell cycle in mammalian cells	Continuous Deterministic	(Deineko et al., 2003)
A mathematical model for analysis of the cell cycle in cell lines derived from human tumors	Continuous Deterministic	(Basse et al., 2003)
Theoretical and experimental evidence for hysteresis in cell proliferation	Continuous Deterministic	(Bai et al., 2003)
Dynamics of the cell cycle: checkpoints, sizers, and timers	Continuous Deterministic	(Qu, MacLellan, et al., 2003)
A model for restriction point control of the mammalian cell cycle	Continuous Deterministic	(Novak & Tyson, 2004)
A mathematical model of the effects of hypoxia on the cell-cycle of normal and cancer cells.	Continuous Deterministic	(Alarcon et al., 2004)

Model predictions of MDM2 mediated cell regulation	Continuous Deterministic	(Obeyesekere et al., 2004)
Coordination of cell growth and cell division: a mathematical modeling study	Continuous Deterministic	(Qu et al., 2004)
Bifurcation analysis of the regulatory modules of the mammalian G1/S transition	Continuous Deterministic	(Swat et al., 2004)
Multisite phosphorylation and network dynamics of cyclin-dependent kinase signaling in the eukaryotic cell cycle	Continuous Deterministic	(Yang et al., 2004)
Dynamical analysis of a generic Boolean model for the control of the mammalian cell cycle	Discrete	(Fauré et al., 2006)
Using a mammalian cell cycle simulation to interpret differential kinase inhibition in anti-tumour pharmaceutical development	Continuous Deterministic	(Chassagnole et al., 2006)
Analysis of a generic model of eukaryotic cell cycle regulation	Continuous Deterministic	(Csikász-Nagy et al., 2006)
Linking cell division to cell growth in a spatiotemporal model of the cell cycle	Continuous Deterministic	(Yang et al., 2006)
Periodic forcing of a mathematical model of the eukaryotic cell cycle	Continuous Deterministic	(Battogtokh & Tyson, 2006)
Computational analysis of mammalian cell division gated by a circadian clock: quantized cell cycles and cell size control	Stochastic	(Zámborszky et al., 2007)
Minimal requirements for robust cell size control in eukaryotic cells	Continuous Deterministic	(Pfeuty & Kaneko, 2007)
Mathematical modelling of G2/M phase in the cell cycle involving the p53/Mdm2 oscillation system	Continuous Deterministic	(Tashima et al., 2007)
A systems biology dynamical model of mammalian G1 cell cycle progression	Continuous Deterministic	(Haberichter et al., 2007)
Cell cycle control in eukaryotes: A biospi model	Stochastic	(Lecca & Priami, 2007)
Underlying principles of cell fate determination during G1 phase of the mammalian cell cycle	Continuous Deterministic	(Pfeuty et al., 2008)
Prediction of Key Factor Controlling G1/S Phase in the Mammalian Cell Cycle Using System Analysis	Continuous Deterministic	(Tashima et al., 2008)
Mathematical modelling and sensitivity analysis of G1/S phase in the cell cycle including the DNA-damage signal transduction pathway	Continuous Deterministic	(Iwamoto et al., 2008)

A bistable Rb-E2F switch underlies the restriction point	Continuous Deterministic	(Yao et al., 2008)
Temporal self-organization of the cyclin/Cdk network driving the mammalian cell cycle	Continuous Deterministic	(Gérard & Goldbeter, 2009)
Sophisticated framework between cell cycle arrest and apoptosis induction based on p53 dynamics	Continuous Deterministic	(Hamada et al., 2009)
Modeling ERBB receptor-regulated G1/S transition to find novel targets for de novo trastuzumab resistance	Discrete	(Sahin et al., 2009)
Mitotic exit in mammalian cells	Stochastic	(Kapuy et al., 2009)
Towards a systems biology approach to mammalian cell cycle: modeling the entrance into S phase of quiescent fibroblasts after serum stimulation	Continuous Deterministic	(Alfieri et al., 2009)
Robustness of G1/S checkpoint pathways in cell cycle regulation based on probability of DNA-damaged cells passing as healthy cells	Continuous Deterministic	(Ling et al., 2010)
Restriction point control of the mammalian cell cycle via the cyclin E/Cdk2:p27 complex	Continuous Deterministic	(Conradie et al., 2010)
A skeleton model for the network of cyclin-dependent kinases driving the mammalian cell cycle	Continuous Deterministic	(Gérard & Goldbeter, 2010)
Modeling the cell cycle: From deterministic models to hybrid systems	Hybrid	(Alfieri et al., 2011)
Regulation of mammalian cell cycle progression in the regenerating liver	Continuous Deterministic	(Chauhan et al., 2011)
Mathematical modeling of cell cycle regulation in response to DNA damage: exploring mechanisms of cell-fate determination	Continuous Deterministic	(Iwamoto et al., 2011)
System-level feedbacks make the anaphase switch irreversible	Continuous Deterministic	(He et al., 2011)
A general framework for modelling growth and division of mammalian cells	Continuous Deterministic	(Gauthier & Pohl, 2011)
A hybrid model of mammalian cell cycle regulation	Hybrid	(Singhania et al., 2011)
An automaton model for the cell cycle	Stochastic	(Altinok et al., 2011)
Effect of positive feedback loops on the robustness of oscillations in the network of cyclin-dependent kinases driving the mammalian cell cycle.	Continuous Deterministic	(Gérard et al., 2012)
Strategic cell-cycle regulatory	Continuous	(Pfeuty, 2012)

features that provide mammalian cells with tunable G1 length and reversible G1 arrest	Deterministic	
From quiescence to proliferation: Cdk oscillations drive the mammalian cell cycle	Continuous Deterministic	(Gérard & Goldbeter, 2012)
Robustness and Backbone Motif of a Cancer Network Regulated by miR-17-92 Cluster during the G1/S Transition	Discrete	(Yang et al., 2013)
Hybrid Petri Nets for Modelling the Eukaryotic Cell Cycle	Petri Net	(Herajy et al., 2013)
A mathematical analysis of DNA damage induced G2 phase transition	Continuous Deterministic	(Zhang et al., 2013)
A Data-Driven, Mathematical Model of Mammalian Cell Cycle Regulation	Continuous Deterministic	(Weis et al., 2014)
Mathematical modeling of p53 pulses in G2 phase with DNA damage	Continuous Deterministic	(Zhang et al., 2014a)
A mathematical study of the robustness of G2/M regulatory network in response to DNA damage with parameters sensitivity	Continuous Deterministic	(Zhang et al., 2014b)
Modelling the onset of senescence at the G1/S cell cycle checkpoint	Discrete	(Mombach et al., 2014)
The balance between cell cycle arrest and cell proliferation: control by the extracellular matrix and by contact inhibition	Continuous Deterministic	(Gérard & Goldbeter, 2014)
Cyclin and DNA Distributed Cell Cycle Model for GS-NS0 Cells	Continuous Deterministic	(Münzer et al., 2015)
Dynamics of the mammalian cell cycle in physiological and pathological conditions	Continuous Deterministic	(Gérard & Goldbeter, 2015)
An application of invertibility of Boolean control networks to the control of the mammalian cell cycle	Discrete	(Zhang et al., 2017)
Modelling of the cancer cell cycle as a tool for rational drug development: A systems pharmacology approach to cyclotherapy	Continuous Deterministic	(Jackson et al., 2017)
Modelling T cell proliferation: Dynamics heterogeneity depending on cell differentiation, age, and genetic background	Continuous Deterministic	(Vibert & Thomas-Vaslin, 2017)
Logical modelling and analysis of cellular regulatory networks with GINsim 3.0	Discrete	(Naldi et al., 2018)
Mathematical modelling of reversible transition between quiescence and proliferation	Continuous Deterministic	(Pandey & Vinod, 2018)

A comprehensive model for the proliferation–quiescence decision in response to endogenous DNA damage in human cells	Continuous Deterministic	(Heldt et al., 2018)

2.4 Summary

Mammalian cell cycle is the least studied cell cycle system, experimentally or through modelling. The goal in this chapter was to review both biological regulatory system and computational modelling paradigms of mammalian cell cycle in order to understand its underlying mechanism and see how these methods have facilitated that understanding. We explained the mechanism of mammalian cell cycle regulation system by highlighting the important effect of Cyclin_Cdks as main controllers as well as their regulators. The role of checkpoints as the guardians of genome was also highlighted. Then, different modelling approaches (Discrete, Continuous-Deterministic, Stochastic, Hybrid and Petri Net-Based) that have been used in cell cycle modelling (fewer for mammalian) were presented with their pros and cons in terms of complexity and knowledge presentation. At the end of the chapter, a summary list of all computational models of mammalian cell cycle was presented where most of the models were Continuous-Deterministic type. There are many open questions that computational models can potentially answer through a variety of analyses that can be done on them. Increased understanding of different aspects of mammalian cell cycle systems and their operation as a whole system will greatly help future cancer treatments.

Chapter 3

A Comprehensive Complex Systems Approach to the Study of Mammalian Cell Cycle Control System in the Presence of DNA Damage Stress

In this chapter, we develop a comprehensive complex systems approach to the study of mammalian cell cycle control system in the presence of DNA damage. The proposed comprehensive mathematical model comprises 61 state variables and 148 kinetic parameters that together with the detailed description of sub-systems and their corresponding modules and interactions are explained in-depth in this chapter. This chapter comprises five sections. An overview of the chapter is provided in Section 3.1. The second section (Section 3.2) is about the current gaps in mammalian cell cycle modelling. Section 3.3 is devoted to four cell cycle sub-systems and their corresponding modules together with mathematical formulations. Results and discussion are given in Section 3.4. Finally, a summary of this chapter is provided in the last section (Section 3.5).

3.1 Overview

Not many models of mammalian cell cycle system exist due to its complexity. Some models are too complex and hard to understand, while some others are too simple and not comprehensive enough. Moreover, some essential aspects, such as the response of G1-S and G2-M checkpoints to DNA damage as well as the Growth Factor signalling, have not been investigated from a systems point of view in current mammalian cell cycle models. To address these issues, we bring a holistic perspective to cell cycle by mathematically modelling it as a complex system consisting of important sub-systems that interact with each other. This retains the functionality of the system and provides a clearer interpretation to the processes within it while reducing the complexity in comprehending these processes. To achieve this, we first update a published ODE mathematical model of cell cycle with current knowledge by adding the important missing components. Then the part of the mathematical model relevant to each sub-system is shown separately in conjunction with a diagram of the sub-system as part of this representation. The model sub-systems are Growth Factor, DNA damage, G1-S, and G2-M checkpoint signalling pathways. To further simplify the model and better explore the function of sub-systems, they are further divided into modules.

3.2 Current Gaps in Mammalian Cell Cycle Models

The state of current cell cycle models reveals a number of areas for improvement. G1-S and G2-M checkpoints play an important role in controlling cell cycle progression, particularly in the presence

of DNA damage, and their response mechanisms and corresponding inter-relationships should be properly investigated to understand DNA damage response in cell cycle more comprehensively. In the current literature, there is a lack of proper incorporation of G1-S and G2-M checkpoint sub-systems into a single mammalian cell cycle model, especially with DNA damage sub-system, where each sub-system comprises interconnected modules to give a better systems understanding of the whole cell cycle. The rationale for incorporation of G1-S and G2-M checkpoints are that during cell cycle both are crucial in checking if the conditions allow a proliferating cell to continue (Beishline & Azizkhan-Clifford, 2014). In fact, if there is any malfunction in either of these checkpoints, a damaged cell may be considered as normal and allowed to proliferate that can cause tumours and cancer. Furthermore, DNA response has two parts- rapid (*Chk-Related* module) and delayed (*p53* module) responses - and these parts need to be seamlessly integrated into a cell cycle model to aid our understanding of this important aspect of cell cycle and the crucial originator of uncontrolled cell proliferation. Additionally, it could be advantageous to incorporate some recently found new elements that show p53 pathway with greater clarity.

The Growth Factor signaling is another sub-system that has not been properly incorporated into mammalian cell cycle modelling yet and past models have assumed just a constant growth signal as cell cycle trigger (Iwamoto et al., 2011; Iwamoto et al., 2008). Growth Factor signaling is a crucial pathway that interacts with cell cycle system through a particular signaling cascade called MAPK and a transcription factor called c-Myc to initiate cell cycle machinery. It is this pathway that stimulates the production of D-type Cyclin which is the most critical controller in early-mid G1 phase of mammalian cell cycle (Adhikary & Eilers, 2005; Alberts et al., 2014; de Alboran et al., 2001; Morgan, 2007; Schmidt, 1999). Therefore, incorporation of Growth Factor signaling and especially c-Myc has value due to the biological significance of c-Myc to the cell cycle system. Also, as an extension to models, it gives a more complete description of cell cycle. Further, it allows the relationship (continuous dynamic) between c-Myc and Cyclin D to be realistically represented. Additionally, with c-Myc in the system, transcription factor of all Cyclins of cell cycle are represented in one model.

There are also a number of other pathways that can be incorporated to improve cell cycle models to allow greater and insightful understanding of cell cycle and meaningful investigation into cell cycle related diseases: Two Tyrosine phosphatase modules that are crucial for activating cell cycle controllers (Cyc_Cdk complexes) and also crucial in rapid and delay cell cycle arrest at both G1-S and G2-M checkpoints as cell cycle arrest involves inactivation of Cyc_Cdk complexes; Tyrosine Kinase module that plays the crucial role through Wee1 of inactivating nuclear version of CycB_Cdk1 to arrest transition to M phase; Plk1-Related module that plays a crucial role in both activating Tyrosine phosphatases and inactivating Tyrosine kinase in normal progression of cell cycle; and APC-Related module that includes two important steps in Cyclin B degradation.

The complexity of cell cycle system where many pathways interact calls for a clearer and simpler approach that still incorporates all the important facets so that future expansion and growth of models is manageable. Therefore, in this chapter, we incorporate all the above essential pathways into a comprehensive ODE mathematical model using a systems modelling paradigm. Specifically, mammalian cell cycle system is divided into four different functional sub-systems (Growth Factor, G1-S checkpoint, G2-M checkpoint, and DNA damage sub-systems) that cooperate with each other to effectively control accurate cell cycle progression. Moreover, each sub-system is divided into its constituent modules which link together to form the corresponding functional sub-system. Therefore, we add important new modules of: Chk-Related rapid cell cycle arrest, p53 modules expanded to seamlessly integrate with the rapid arrest module, Tyrosine phosphatase modules that activate Cyc_Cdk complexes and play a crucial role in rapid and delay arrest at both G1-S and G2-M, Tyrosine Kinase module that is important for inactivating nuclear transport of CycB_Cdk1 through Wee1 to resist M phase entry, Plk1-Related module that is crucial in activating Tyrosine phosphatases and inactivating Tyrosine kinase, and APC-Related module to show steps in Cyclin B degradation. This comprehensive system model is built, tested and further analysed to study cell cycle and DNA damage response as well as to verify the role of the newly added modules and elements in cell cycle.

3.3 A Comprehensive Mathematical Model of Mammalian Cell Cycle

We describe here a mathematical model comprising the four sub-systems, Growth Factor, G1-S checkpoint, G2-M checkpoint, and DNA damage signalling (each of which is divided into its constituent modules), developed to study the whole mammalian cell cycle control system, especially in the presence of DNA Damage Signal (DDS). Briefly, Growth Factor signals activate cell cycle proliferation. This sub-system, in turn, stimulates the activation of G1-S checkpoint sub-system by production of proteins that are crucial for cell cycle initiation. The G1-S checkpoint sub-system induces DNA replication (through interaction with DNA damage sub-system to ensure that DNA is intact), and then, sets the stage for the downstream activation of G2-M checkpoint sub-system. The G2-M checkpoint sub-system collaborates with DNA damage sub-system to check the existence of DNA damage and in the case of no damage, it allows transition to cell division phase. The proposed model is an extension of Iwamoto et al. (2011) ODE model with the above mentioned additions. The proposed model comprises 61 state variables and 148 kinetic parameters. A detailed description of sub-systems and their corresponding modules and interactions are explained in-depth in the following sub-sections. In this chapter, for the sake of brevity and clarity, ODE equations for only the newly added variables and modules are presented and all equations are presented in Appendix A. Some parameters are adopted from Iwamoto et al. (2011) model and others are estimated. The

initial concentration of proteins and value of kinetic parameters (with corresponding definitions) are given in Appendices B (in Table B. 1) and C (in Table C. 1), respectively.

3.3.1 Growth Factor Signalling Sub-System

Generally, a cell cycle begins when a cell receives Growth Factor signals. Upon receiving the signals, synthesis of Cyclin D (or G1 Cyclin) is initiated at G0-G1 transition (early G1) (Pardee, 1989). Growth Factor signals lead to an increase in cell size to a certain threshold without which cell cycle is not initiated. It has been proven that Growth Factor signals induce the synthesis of Cyclin D through a Ras-mediated pathway (Alberts et al., 2014; Morgan, 2007). The Growth Factor signalling sub-system (complete and simplified version) is shown in Figure 3.1. The activated Growth Factor receptors stimulate the activation of Ras by turning it into a form of GTP-bound Ras. Thereafter, a cascade of protein kinase activations is initiated which finally leads to phosphorylation and activation of MAP Kinase (MAPK). This kinase is translocated to the nucleus and it activates a transcription factor called c-Myc that eventually promotes the synthesis of Cyclin D (Adhikary & Eilers, 2005; Alberts et al., 2014; de Alboran et al., 2001; Morgan, 2007; Schmidt, 1999). Most of the previous models have represented Growth Factor as being present or absent and in this study for the first time (to the best of our knowledge) a Growth Factor model is incorporated into the mammalian cell cycle model. We use the minimal version of this sub-system shown at the bottom of Figure 3.1 to simplify the model while incorporating the most crucial aspect of Cyclin D synthesis.

According to our minimal version of the system, it is assumed that Growth Factor (GF) is available from early G1, and c-Myc is the most important link between GF and cell cycle machinery to trigger cell cycle initiation (by inducing Cyclin D synthesis): following the presence of GF, c-Myc becomes activated and subsequently stimulates the synthesis of Cyclin D. The corresponding dynamics of this sub-system are presented below where the bold letters refer to new elements/parameters.

$$\frac{d[\boldsymbol{icMyc}]}{dt} = \boldsymbol{k_1} \cdot [\boldsymbol{acMyc}] - \boldsymbol{k_2} \cdot GF \cdot [\boldsymbol{icMyc}] \tag{3-1}$$

$$\frac{d[\boldsymbol{acMyc}]}{dt} = \boldsymbol{k_2} \cdot \boldsymbol{GF} \cdot [\boldsymbol{icMyc}] - \boldsymbol{k_1} \cdot [\boldsymbol{acMyc}] \tag{3-2}$$

Within brackets is shown the concentration of respective proteins. We assumed c-Myc to be switched between active [acMyc] and inactive [icMyc] forms (Eq. (3-1) and Eq. (3-2)) in order to simplify the model. Parameters k_1 and k_2 are inactivation rate of acMyc and activation rate of icMyc, respectively.

Figure 3.1 Growth Factor Signalling Sub-System. Growth factor triggers the MAPK cascade that eventually activates transcription factor c-Myc which stimulates the synthesis of Cyclin D, the first cyclin in the cell cycle system. In this study, we use a minimal/compact version of Growth Factor signalling pathway shown as Minimal Growth Factor Sub-System at the bottom left corner in this figure. Green solid arrows denote biochemical reactions (i.e., synthesis of a protein or activation of an inactive element) while purple dashed arrows correspond to regulatory effects (i.e., enzymatic effect, transcriptional regulation through transcription factor).

3.3.2 DNA Damage Signalling Sub-System

During cell cycle, DNA damage is sensed by particular sensor proteins whose role is to ensure that the response is proportional to damage by appropriately activating some downstream elements. These elements trigger a variety of responses, such as damage repair, cell cycle arrest, or Apoptosis (if the damage is irreparable) (Fry et al., 2005; Nyberg et al., 2002). For Double-Strand Breaks (DSBs), Ataxia telangiectasia mutated (ATM) is the sensor protein (Shiloh & Ziv, 2013). Ataxia telangiectasia and Rad3-related protein (ATR) is responsible for sensing other types of breaks, such as Single-Strand Breaks (SSBs) (Smith et al., 2010). There are two important DNA damage signalling pathways, Chk-Related (rapid) and p53-Related (delayed), which become activated following DNA damage sensing.

Chk-Related Module

Upon DNA damage, Chk-Related (rapid) module becomes activated within a few minutes to arrest cell cycle progression. It is a transcription-independent process involving post-translational modifications, such as phosphorylation, that happens much faster than transcription. Upon sensing DSB (in this study, we focus on DSB), ATM becomes activated and then it phosphorylates Chk2 kinase. Eventually, Chk2 regulates the activity of Cyc_Cdks, the main controllers of cell cycle

progression (specially, in transition between cell cycle phases), by inhibiting the activity of Cdc25 phosphatases. These phosphatases remove the inhibitory phosphate from Cyc_Cdks, so they are necessary for activation of these complexes (Beishline & Azizkhan-Clifford, 2014; Morgan, 2007; Sancar et al., 2004). The diagram of Chk-Related module in the presence of DSB is shown in Figure 3.2. The proper definition of it as a rapid DNA damage module and its presentation within a sub-system is new in our model.

Figure 3.2 Chk-Related (rapid) DNA Damage Module. Active Cdc25 Tyrosine phosphatase is important in activation of Cyc_Cdks and cell cycle progression. DNA damage results in activation of Chk2 which in turn deactivates Cdc25. Therefore, through a number of relatively fast interactions (activation/inactivation), the DNA damage rapidly arrests the cell cycle. Green solid arrows denote biochemical reactions (i.e., synthesis of a protein or activation of an inactive element) while purple dashed arrows correspond to regulatory effects (i.e., enzymatic effect, transcriptional regulation through transcription factor, etc.).

p53-Related Module

A schematic of p53-Related (delayed) DNA damage module is illustrated in Figure 3.3. This module is transcription-dependent. In fact, the sensor protein ATM, which becomes activated following DSBs, phosphorylates and activates an important transcription factor p53. There is an important ubiquitin ligase (Mdm2) which inhibits p53 under no DNA damage condition. Mdm2 causes instability and nuclear export of p53, but Mdm2 becomes inactivated by ATM-mediated phosphorylation at Ser395 following the presence of DNA damage signal there by releasing p53. Thus, the negative feedback loop between p53 and Mdm2 is an essential part of this module (Bar-Or et al., 2000; Geva-Zatorsky et al., 2006; Kohn & Pommier, 2005; Meek, 2004; Nyberg et al., 2002; Zhang & Xiong, 2001). A putative (Imaginary) Factor (IF) is added to the model to account for the delay between activation of p53 and its transcriptional effect on Mdm2. Upon activation, p53 stimulates the synthesis of some downstream factors, like p21, 14-3-3σ, Gadd45α (see Figure 3.3), which further arrest cell cycle progression (Cann & Hicks, 2007; Zhan, 2005) by different means. Protein p21 is a Cyclin-Dependent

kinase Inhibitor (CKI) which binds to different Cyclin_Cdk complexes to inactivate them (see Sections 3.3.3 & 3.3.4. for details of the processes related to this binding). Another protein called 14-3-3σ is a phosphoserine binding protein that binds to Cdc25 phosphatases to further inhibit their activation of Cyc_Cdk complexes (see section 3.3.4 for details of this binding).

Gadd45α is another essential factor produced following DNA damage that has more impact on B-type Cyclin_Cdk complex (see Section 3.3.4 for more details). However, the way that 14-3-3σ and Gadd45α act upon CycB_Cdk1 inactivation is different. The first factor (14-3-3σ) inhibits Cdc25C (which is CycB_Cdk1 activator), while the second (Gadd45α) physically interacts with Cdk1 in order to stimulate CycB_Cdk1 unbinding (Jin et al., 2002; Zhan, 2005). Therefore, Gadd45α is an important player at G2-M checkpoint. The proper incorporation of Gadd45α into the p53-module and seamless integration of the rapid and delayed DNA damage responses are new additions in our model. The ODE highlighting the Gadd45α dynamics and its interactions with the rest of the system is presented below (the bold letters refer to new elements/parameters).

$$\frac{d[\mathbf{Gadd45\alpha}]}{dt} = \boldsymbol{k_{36}} + \boldsymbol{k_{37}} \cdot [p53] - \boldsymbol{k_{38}} \cdot [\mathbf{Gadd45\alpha}] \quad (3\text{-}3)$$

Figure 3.3 p53-Related DNA Damage Module. This module represents the delayed DNA damage signalling that centres on transcription factor p53, which stimulates the synthesis of p21, 14-3-3σ and Gadd45α. These products contribute to cell cycle arrest in different ways. Red solid round-ended arrows indicate inhibition; green solid arrows denote biochemical reactions (i.e., synthesis or degradation of a protein, etc.) and purple dashed arrows correspond to transcriptional regulation.

3.3.3 G1-S Checkpoint Signalling Sub-System

The G1-S checkpoint sub-system comprises the most important components and their interactions from initiation of Cyclin D synthesis until transition to S phase. In fact, this sub-system is made of four important modules (Cdk4-Related, E2F-pRb, Cdk2-Related, and Tyrosine Phosphatase) interacting with each other to induce cell cycle progression from G1 to S phase. An overview of interactions at

both sub-system and module levels is demonstrated in Figure 3.4. At the sub-system level, it is shown that Growth Factor and DNA damage signalling sub-systems affect G1-S checkpoint signalling, whereas G1-S influences G2-M checkpoint signalling (blue arrows in Figure 3.4). Indeed, all the aforementioned events take place through interactions among some modules inside the sub-systems. Therefore, it is also necessary to describe the system from module point of view. At the module level, the modules tightly interact with each other (black arrows in Figure 3.4) to contribute to the overall function of their corresponding sub-system (G1-S checkpoint signalling). The details of these modules are described in following sub-sections.

Figure 3.4 G1-S Checkpoint Signalling Sub-System in the context of the whole system and its four modules: Cdk4-Related, E2F-pRb, Cdk2-Related, Tyrosine Phosphatase modules. Black arrows indicate interactions between modules while blue arrows indicate interactions between G1-S checkpoint and other sub-systems.

Cdk4-Related Module

This module, basically, receives the growth signal from outside G1-S checkpoint signalling sub-system (through Growth Factor sub-system) and interacts with the next internal module (E2F-pRb module) to help release E2F that is necessary to induce the synthesis of a number of crucial cell cycle proteins, such as Cyclin E and A. The detailed diagram of the Cdk4-Related module is demonstrated in Figure 3.5. In the early G1 phase, Cdk4 is the protein kinase that is necessary for cell cycle initiation. Although Cdk4 is abundant during cell cycle, it needs to bind to Cyclin D to become functional toward its targets (Musgrove et al., 2011). As mentioned in Section 3.3.1, following the appearance of Growth Factors, c-Myc becomes activated and allows transcription of Cyclin D. Cyclin D, in turn, binds to Cdk4, to produce CycD_Cdk4 complex. Cyclin D is degraded by ubiquitin ligases “Skp_Cullin_F-box containing complex” (SCF) and APC_Cdc20 (Alao, 2007; Peters, 2002).

Another important group of proteins that play an essential role in regulation of CycD_Cdk4 complex (through binding to it) are CKIs, such as p27 and p21 (Figure 3.5). However, these two CKIs have contradictory effects toward different Cdk types. For example, p27 and p21 bind and activate CycD_Cdk4, but they inhibit CycE_Cdk2, CycA_Cdk2, and CycB_Cdk1 complexes. The main function of p27 is to keep the cell in quiescent mode (G0), so it exists in high levels during early G1 phase and it suppresses any activity of CycE_Cdk2, CycA_Cdk2 complexes. But upon availability of Growth Factor and accumulation of CycD_Cdk4 (as well as p27_ CycD_Cdk4), next module (E2F-pRb) is activated to release E2F - transcription factor that initiates the synthesis of Cyclin E and Cyclin A. This leads to accumulation of CycE_Cdk2 and CycA_Cdk2 which then triggers phosphorylation and degradation of p27 (Chu et al., 2008) that allows these latter complexes to break free from p27. Therefore, removal of p27 is one of the requirements for progression of cell cycle from G1 to S phase. In summary, the role of Cdk4-Related module is to prepare the conditions through CycD_Cdk4, p27_ CycD_Cdk4 and p21_ CycD_Cdk4 complexes to interact with the next module (E2F-pRb) to release E2F - transcription factor that initiates the synthesis of Cyclin E and Cyclin A.

Figure 3.5 **Cdk4-Related Module. The key elements of this module are Cyclin D, Cdk4, and p27. The effects of some other elements on production, degradation, and combination of these proteins have also been presented in this module. Transcription factor c-Myc triggers the synthesis of Cyclin D which in complex with Cdk4 forms the most crucial controller (CycD_Cdk4) of mammalian cell cycle during early to mid G1 phase. Elements in the rectangular boxes are the proteins in this module; whereas, the other elements belong to other modules (their dynamics are presented elsewhere in the corresponding modules). Green solid arrows denote the biochemical reactions (i.e., synthesis, degradation, association, dissociation, etc.) while purple dashed arrows correspond to regulatory effects (i.e., enzymatic effect, transcriptional regulation through transcription factor, etc.). Double-ended arrows represent reversible reactions. Elements in blue rectangular boxes are the proteins of this module whereas the other elements belong to other modules.**

The updated equation for Cyclin D is provided below (the bold letters refer to new elements/parameters).

$$\frac{d[CycD]}{dt} = k_{39} + \boldsymbol{k_{40}} \cdot [\boldsymbol{acMyc}] + k_{41} \cdot [CycD\_Cdk4] - (\, k_{44} + k_{42} \cdot [Cdk4] + \boldsymbol{k_{43}} \cdot [\boldsymbol{aSCF}] + \boldsymbol{k_{147}} \cdot [aAPC\_Cdc20]) \cdot [CycD] \quad (3\text{-}4)$$

E2F-pRb Module

E2F-pRb module is important in that it produces proteins (Cyclin E and A, Cdc25A, etc.) that are essential for G1-S transition. This is done through interaction of this module with two other internal modules, Cdk2-Related, and Tyrosine Phosphatase (as shown in Figures 3.4 & 3.6). This module centres on transcription factor E2F and a tumour suppressor protein, called Retinoblastoma protein (pRb), which binds to E2F and inhibits its activation (Figure 3.6). To become active and affect the said protein production, E2F needs to be released from pRb and this happens through phosphorylation of E2F_pRb by Cyc_Cdk complexes (Sherr & McCormick, 2002; Trimarchi & Lees, 2002).

Figure 3.6 E2F-pRb Module. The key factor in this module is transcription factor E2F. When active, this transcription factor stimulates the production of a number of crucial cell cycle proteins, such as Cyclin E, Cyclin A, Tyrosine phosphatase Cdc25A, another transcription factor called B-Myb and itself. E2F is initially inactivated by a tumour suppressor protein called pRb. The detail of the process which results in activation of E2F is well covered in this module. Green solid arrows denote biochemical reactions (i.e., synthesis, degradation, association, dissociation, phosphorylation, etc.) while purple dashed arrows correspond to regulatory effects (i.e., enzymatic effect, transcriptional regulation through transcription factor, etc.). Elements in blue rectangular boxes are the proteins of this module whereas the other elements belong to other modules.

According to wiring diagram of E2F-pRb module shown in Figure 3.6, following initial phosphorylation of E2F_pRb by CycD_Cdk4, p27_CycD_Ckd4, and p21_CycD_Ckd4, and then further phosphorylation of E2F_pRbPP by small amount of available CycE_Cdk2 and CycA_Cdk2, a number of E2F molecules are released. Then, these E2F proteins trigger the synthesis of Cyclin E and Cyclin A, which in complex with Cdk2, lead to more phosphorylation of pRb and thereby releasing more E2Fs (Deckbar et al., 2011; Helin, 1998). This positive feedback loop, resulting in an increase in concentration of CycE_Cdk2 as well as further release of E2F, is crucial for G1-S transition. The process of E2F degradation is mediated by aCycA_Cdk2 (Figure 3.6) upon G1-S transition (Ji & Dyson, 2010). At the end of cell cycle, pRbPPP becomes dephosphorylated (to pRb) by a crucial phosphatase called Protein Phosphatase 1 (PP1) (Berndt, 2002; Ludlow et al., 1993; Nelson et al., 1997; Trinkle-Mulcahy et al., 2003). We emphasise that Iwamoto et al. (2011) model was not cyclic because PP1 was missing in that model. Since PP1 is a newly added element in our model, the corresponding equations are presented below (the bold letters refer to new elements/parameters).

$$\frac{d[i\boldsymbol{PP1}]}{dt} = \boldsymbol{k_{62}} \cdot [\boldsymbol{aPP1}] - \boldsymbol{k_{63}} \cdot [\boldsymbol{iPP1}].[aCycB\_Cdk1\_Nuc] \quad (3\text{-}5)$$

$$\frac{d[\boldsymbol{aPP1}]}{dt} = \boldsymbol{k_{63}} \cdot [\boldsymbol{iPP1}].[\boldsymbol{a}CycB\_Cdk1\_Nuc] - \boldsymbol{k_{62}} \cdot [\boldsymbol{aPP1}] \quad (3\text{-}6)$$

$$\frac{d[pRb]}{dt} = k_{65} + \boldsymbol{k_{64}} \cdot [\boldsymbol{aPP1}].[pRbPPP] - (k_{56} \cdot [E2F] + k_{66}) \cdot [pRb] \quad (3\text{-}7)$$

In addition to the need to insert PP1, we further found that few original parameters related to E2F needed modification to make the model cyclic and they were updated accordingly. These changes were as follows: (i) Dephosphorylation of pRbPPP to pRb: The rate of dephosphorylation of pRbPPP to pRb has been updated from 5.0E-8 to 2.0E-3. In Iwamoto et al. (2011) model, there is no way that the model can be cyclic with such a small dephosphorylation rate as it leads to accumulation of pRbPPP and not produce enough pRb. There should be enough E2F_pRb for the new cell cycle to begin; (ii) Degradation of pRb: The degradation rate of pRb should be lowered (from 5.0E-3 to 5.0E-5) because for a new cell cycle to begin, enough E2F_pRb is needed and if the rate of pRb degradation is high, not enough E2F_pRb is produced; (iii) Synthesis of E2F: The basal synthesis rate of E2F should be higher for the cell cycle to be periodic (change from 5.0E-7 to 3.0E-4). This rate will guarantee that enough E2F is created and available to be bound to pRb to create E2F_pRb complex; (iv) Binding of pRb and E2F: To guarantee that enough E2F_pRb is available for a new cell cycle, the binding rate of pRb and E2F should be increased (from 5E-5 to 5E-2).

Cdk2-Related Module

Placed at the heart of G1-S checkpoint sub-system and known as its main driver, Cdk2-Related module has the most interactions with internal modules (E2F-pRb and Tyrosine Phosphatase) and external sub-systems (G2-M checkpoint & DNA damage). Cyclin E and Cyclin A are two important cyclins that bind to Cdk2 to activate it and the two resulting complexes (CycE_Cdk2 and CycA_Cdk2) help initiation of S phase (Murray, 2004). An overview of this module is given in Figure 3.7. After formation of CycE_Cdk2 and CycA_Cdk2, phosphatase Cdc25A activates them by removing the inhibitory phosphate added by Tyrosine kinases upon the complex formation. But these two complexes become inactive through binding to CKIs, p21 and p27, and stay inactive until CKIs are released. In fact, the concentration of p27 is high in early to mid G1 phase to prevent initiation of S phase (through inactivation of CycE_Cdk2 and CycA_Cdk2) until all conditions are appropriate. However, as stated before, accumulation of the two Cyc-Cdk complexes allows them to degrade p27 and break free from it thereby triggering G1-S transition.

Figure 3.7 **Cdk2-Related Module. The key players of this module are Cyclin E and Cyclin A whose synthesis and degradation depends on a number of transcription factors (E2F, B-Myb and NFY) and ubiquitin ligases (SCF, APC_Cdh1, and apc_Cdc20), respectively. Furthermore, the activity of CycE_Cdk2 and CycA_Cdk2 are affected by CKIs (p21 & p27) and Tyrosine phosphatase Cdc25A. Green solid arrows denote the biochemical reactions (i.e., synthesis, degradation, association, dissociation, etc.) while purple dashed arrows correspond to regulatory effects (i.e., enzymatic effect, transcriptional regulation through transcription factor, etc.). Double-ended arrows represent reversible reactions. Elements in blue rectangular boxes are the proteins of this module whereas the other elements belong to other modules.**

As stated previously, the amount of p21 increases in the presence of DNA damage (through transcription factor p53) to arrest cell cycle at G1-S checkpoint by forming p21_CycE_Cdk2 to inactivate the complex (Novák et al., 2001). It is important to emphasize that Cyclin E and Cyclin A are degraded differently (Figure 3.7). While Cyclin A is degraded by APC_Cdc20 and APC_Cdh1, the main degraders of Cyclins A and B, (abundance of APC-cdh1 at the beginning of cell cycle keeps respective cyclins levels at bay to supress cell cycle), degradation of Cyclin E is SCF-mediated. SCF (newly added in our model) is a ubiquitin ligase that has three different subunits (Fbw7, Skp2, and Btrc) which bind to it in order to activate it toward different substrates (Ang & Harper, 2004; Cardozo & Pagano, 2004; Nakayama & Nakayama, 2005). In this model, we assume that SCF switches between active and inactive forms and also its activation and inactivation rates depend on active CycE_Cdk2 and active APC_Cdh1, respectively. Cyc_Cdk2 complexes are also assumed to be slightly ubiquitinated and degraded to Cdk2.

Another important part of this module is a set of supplementary transcription factors (NFY and B-Myb). B-Myb, which is produced by E2F and activated by aCycA_Cdk2, induces the synthesis of Cyclin A (Fung & Poon, 2005; Joaquin & Watson, 2003; Zhu et al., 2004). However, NFY, which also becomes activated by aCycA_Cdk2, stimulates the production of both Cyclin A and Cyclin B (Chae et al., 2004; Chae & Shin, 2011; Fung & Poon, 2005; Yun et al., 2003). Therefore, Cyclin A indirectly helps production of next cyclin (Cyclin B) in the cell cycle system. The new and modified equations related to this module are presented below.

$$\frac{d[CycE]}{dt} = k_{70} \cdot [E2F] + k_{72} \cdot [iCycE\_Cdk2] - (k_{73} + k_{71} \cdot [Cdk2] + \boldsymbol{k_{74}} \cdot [\boldsymbol{aSCF}]) \cdot [CycE] \quad (3\text{-}8)$$

$$\frac{d[\boldsymbol{iSCF}]}{dt} = \boldsymbol{k_{91}} \cdot [\boldsymbol{aSCF}] \cdot [aAPC\_Cdh1] - \boldsymbol{k_{92}} \cdot [aCycE\_Cdk2] \cdot [\boldsymbol{iSCF}] \quad (3\text{-}9)$$

$$\frac{d[\boldsymbol{aSCF}]}{dt} = \boldsymbol{k_{92}} \cdot [aCycE\_Cdk2] \cdot [\boldsymbol{iSCF}] - \boldsymbol{k_{91}} \cdot [\boldsymbol{aSCF}] \cdot [aAPC\_Cdh1] \quad (3\text{-}10)$$

Tyrosine Phosphatase Module

The main function of Tyrosine Phosphatase module is to activate CycE_Cdk2 and CycA_Cdk2 (through connection to Cdk2-Related module) which is necessary for G1-S transition. The Tyrosine Phosphatase module is also influenced by another internal module, E2F-pRb (as E2F produces Cdc25A) and an external sub-system, DNA damage (DNA damage causes inactivation of Cdc25A). As shown in Figure 3.8, the central protein in this module is the phosphatase Cdc25A that induces the activation of iCycE_Cdk2 and iCycA_Cdk2 by removing the inhibitory phosphate from them. In fact, positive feedback loops between aCdc25A and these two Cyc_Cdks set the stage for G1-S transition.

It is important to note that following DNA damage, active Chk2 (rapid DNA response) phosphorylates Cdc25A and accelerates its degradation which eventually assists G1-S arrest (Bollen & Beullens, 2002; Boutros et al., 2007; Donzelli & Draetta, 2003; Karlsson-Rosenthal & Millar, 2006; Kiyokawa & Ray, 2008; Kristjansdottir & Rudolph, 2004). In Figure 3.8, Cdc25A is transformed between active and inactive forms and the processes of synthesis and degradation are also included.

Figure 3.8 Tyrosine Phosphatase Module. The main player of this module is Tyrosine phosphatase Cdc25A. Its synthesis and degradation are mediated through E2F and Chk2, respectively. Cdc25A has an important role in activating CycE_Cdk2 and CycA_Cdk2. The positive feedback loop between these Cyc_Cdks and Cdc25A triggers activation of more Cdc25A. Green solid arrows denote biochemical reactions (i.e., synthesis, degradation, association, dissociation, etc.) while purple dashed arrows correspond to regulatory effects (i.e., enzymatic effect, transcriptional regulation through transcription factor, etc.). Elements in blue rectangular boxes are the proteins of this module whereas the other elements belong to other modules.

3.3.4 G2-M Checkpoint Signalling Sub-System

B-type Cyclin complexes with Cdk1 (as CycB_Cdk1) and acts as the main regulator of G2-M checkpoint sub-system. This sub-system is divided into five inter-connected modules (Cdk1-Related, Tyrosine Kinase, Tyrosine Phosphatase, APC-Related and Plk1-Related). The corresponding interactions between these modules (together with interconnections between different sub-systems) are illustrated in Figure 3.9. As shown in this figure, G1-S checkpoint sub-system sends a signal to Cdk1-Related module of G2-M checkpoint sub-system. This leads to upregulation of CycB_Cdk1 complexes. But, the two modules, Tyrosine Phosphatase and Tyrosine Kinase, stimulate activation and inactivation of CycB_Cdk1s, respectively. Further, APC- and Plk1-Related modules are vital in M phase (the detailed description of each module is provided in following sub-sections). DNA damage signalling also interacts with G2-M checkpoint sub-system in a way that Chk-Related (rapid) and p53-Related (delayed) DNA damage modules interact with Tyrosine Phosphatase and Cdk1-Related modules, respectively, to arrest cell cycle in the case of any DNA damage, similar to corresponding processes at G1-S checkpoint.

Figure 3.9 G2-M Signalling Sub-System including its five modules: Cdk1-Related, APC-Related, Tyrosine Phosphatase, Tyrosine Kinase, and Plk1-Related modules. Black arrows indicate interactions between modules while blue arrows show interactions between G2-M checkpoint and other sub-systems.

Tyrosine Kinase Module

Tyrosine Kinase module interacts with two internal modules, Cdk1-Related (to inactivate CycB_Cdk1 complexes) and Plk1-Related (Wee1 becomes inactivated through Plk1) (Figure 3.9). Phosphorylation of Thr14 and Tyr15 residues in mammalian Cdks inhibits the activity of Cyc_Cdk complexes. In particular, the phosphorylation state of these sites is important in Cdk1 at the initiation of M phase. This phosphorylation is done by Tyrosine kinases. The most important Tyrosine kinase in mammalian cell cycle is Wee1 (Perry & Kornbluth, 2007). There is another kinase (Myt1) which phosphorylates both Tyr15 and Thr14 residues in vertebrates (in this module, Wee1 is used for both Myt1 and Wee1). Phosphorylation of Cdk1 on the above residues, which leads to CycB_Cdk1 inactivation, can be neutralized by de-phosphorylation via Cdc25C phosphatase. Balance of these activations is geared towards triggering a process that leads to activation of Cdk1 and onset of M phase. As demonstrated in Figure 3.10, Wee1 is phosphorylated and inactivated by Plk1, which itself becomes activated by CycB_Cdk1_Cyt (van Vugt & Medema, 2005). Inactivated Wee1 is ubiquitinated and then degraded by SCF (Nakayama & Nakayama, 2005; Smith et al., 2007; Watanabe et al., 2004).

Therefore, the double negative feedback loop between Wee1 and CycB_Cdk1 acts as an important suppressor of G2-M transition (Hamer et al., 2011). In this model, it is also assumed that aWee1 has a basal synthesis rate. Since SCF and Plk1 are newly added elements in our model, the corresponding

equations are presented below where the bold letters refer to new elements/parameters (all the equations of this module are provided in Appendix A).

$$\frac{d[iWee1]}{dt} = [aWee1] \cdot (\boldsymbol{k_{105}} \cdot [\boldsymbol{aPlk1}]) - (k_{106} + \boldsymbol{k_{107}} \cdot [\boldsymbol{aSCF}]) \cdot [iWee1] \quad (3\text{-}11)$$

$$\frac{d[aWee1]}{dt} = k_{108} + k_{106} \cdot [iWee1] - \boldsymbol{k_{105}} \cdot [\boldsymbol{aPlk1}] \cdot [aWee1] \quad (3\text{-}12)$$

Figure 3.10 Tyrosine Kinase Module. Tyrosine Kinase Wee1 plays the main role in this module where active Wee1 mediates inactivation of CycB_Cdk1 inside the nucleus. Wee1 becomes inactivated by Plk1 and then degraded by active ubiquitin ligase SCF. Green solid arrows denote the biochemical reactions (i.e., degradation, changing in the state of a protein by phosphorylation or dephosphorylation, etc.) while purple dashed arrows correspond to regulatory effects (i.e., enzymatic effect, etc.). Elements in blue rectangular boxes are the proteins of this module whereas the other elements belong to other modules.

Tyrosine Phosphatase Module

This module, which centres on Cdc25C phosphatase, interacts with internal Cdk1-Related module (to activate CycB_Cdk1 complexes), and with external DNA damage sub-system (to become inactivated in the presence of DNA damage). Unlike Tyrosine kinase Wee1, Tyrosine phosphatase Cdc25C removes the inhibitory phosphate from Cdk1 leading to activation of CycB_Cdk1 and M phase onset (Bollen & Beullens, 2002; Boutros et al., 2007; Perry & Kornbluth, 2007). As illustrated in Figure 3.11, inactive Cdc25C becomes phosphorylated and activated by active Plk1 and CycB_Cdk1 at G2-M transition and this positive feedback loop between CycB_Cdk1 and Cdc25C is crucial for M phase entry (Goulev & Charvin, 2011; Lindqvist et al., 2009; Trunnell et al., 2011; van Vugt & Medema, 2005).

It has also been shown that after DNA damage, Cdc25C is phosphorylated on Serine216 by Chk2 (rapid damage response) and then 14-3-3σ (in the p53-Related delayed damage response module) can bind to it in order to prevent M phase entry (Figure 3.11) (Chaturvedi et al., 1999; Hermeking &

Benzinger, 2006; Kumagai & Dunphy, 1999). These crucial elements were abstracted into a module in our model (see Appendix A for equations).

Figure 3.11 Tyrosine Phosphatase Module. This module covers the process of activation of Tyrosine phosphatase Cdc25C and its phosphorylated version Cdc25CP_S216. This phosphatase helps activation of CycB_Cdk1 which is the main controller of mammalian cell cycle during M phase. The effect of other regulatory proteins on different versions of this phosphatase is shown in this figure and explained in the text. Green solid arrows denote biochemical reactions (i.e., degradation, changing in the state of a protein by phosphorylation or dephosphorylation, etc.) while purple dashed arrows correspond to regulatory effects (i.e., enzymatic effect, etc.). Elements in blue rectangular boxes are the proteins of this module whereas the other elements belong to other modules.

Plk1-Related Module

This module, which mainly corresponds to Polo-like kinase-1 (Plk1), interacts with three internal modules, Tyrosine kinase (to inactivate it), Tyrosine phosphatase (to activate it), and Cdk1-Related modules (to mediate nuclear translocation of CycB_Cdk1) (as shown in Figure 3.9). Plk1 is one of the most important proteins in M-phase entry. Figure 3.12 shows the multiple functions of Plk1 including activation of Cdc25C phosphatase and APC_Cdc20 (degrader of Cyclins A & B), inactivation of Wee1 kinase, and translocation of CycB_Cdk1 from cytoplasm to nucleus (Golan et al., 2002; Lindqvist et al., 2009; Van De Weerdt & Medema, 2006; van Vugt & Medema, 2005; Zitouni et al., 2014). Plk1 is activated by cytoplasmic CycB_Cdk1 through induced phosphorylation and its degradation is mediated by ubiquitination through active APC_Cdh1 (Eckerdt & Strebhardt, 2006; Lindon & Pines, 2004). In this model, it is assumed (for simplification) that Plk1 is transformed between active and inactive forms and its inactivation is mediated by active APC_Cdh1 (Figure 3.12). Since Plk1 is a newly added element in our model, the Plk1 module is totally new and the corresponding equations are formulated as follows:

$$\frac{d[\boldsymbol{iPlk1}]}{dt} = \boldsymbol{k_{121}} \cdot [\boldsymbol{aPlk1}] \cdot [aAPC\_Cdh1] - \boldsymbol{k_{122}} \cdot [\boldsymbol{iPlk}] \cdot [aCycB\_Cdk1\_Cyto] \quad (3\text{-}13)$$

$$\frac{d[\boldsymbol{aPlk1}]}{dt} = \boldsymbol{k_{122}} \cdot [\boldsymbol{iPlk}] \cdot [aCycB\_Cdk1\_Cyto] - \boldsymbol{k_{121}} \cdot [\boldsymbol{aPlk1}] \cdot [aAPC\_Cdh1] \quad (3\text{-}14)$$

Figure 3.12 Plk1-Related Module. Plk1 is one of the key cell cycle elements prior to, and during, M phase where it activates Cdc25CP_S216 and mediates translocation of CycB_Cdk1 from cytoplasm to nucleus. It also helps activation and inactivation of APC_Cdc20 and Wee1, respectively. The effects of aPlk1 on elements from other modules are shown with outgoing dashed arrows from aPlk1. Green solid arrows denote biochemical reactions (i.e., degradation, changing in the state of a protein by phosphorylation or dephosphorylation, etc.) while purple dashed arrows correspond to regulatory effects (i.e., enzymatic effect, etc.). Elements in blue rectangular boxes are the proteins of this module whereas the other elements belong to other modules.

Cdk1-Related Module

The main driver of G2-M checkpoint sub-system is Cdk1-Related module which is majorly related to all the interactions that lead to CycB_Cdk1 production and activation. This module interacts with all internal modules as well as two external sub-systems (G1-S checkpoint and DNA damage sub-systems). In fact, the function of other modules in G2-M checkpoint sub-system is to control CycB_Cdk1 regulation (as shown in Figure 3.9). For example, Tyrosine kinase module has negative regulatory impact on Cdk1-Related module (through aWee1), while Tyrosine Phosphatase module positively regulates the same module (through aCdc25C). There are two different versions of CycB_Cdk1 which are vital for mitotic events (Cytoplasmic and Nuclear versions, as shown in Figure 3.13). CycB_Cdk1_Cyt, which is formed in the cytoplasm near the end of G2 phase, indirectly helps the initiation of mitosis. At the end of G2 phase, this complex is translocated into the nucleus (after phosphorylation by active Plk1) to form aCycB_Cdk1_Nuc marking G2-M transition. The aCycB_Cdk1_Nuc later (in Anaphase) helps Nuclear Envelope Breakdown (NEB) (Lindqvist et al., 2009; Morgan, 2007; van Vugt & Medema, 2005). It is also important to remind that existence of NFY in this module indicates interconnection between G1-S and G2-M checkpoint sub-systems so that the first system triggers the activation of the second one (through transcription factor NFY). In this model, it is assumed that different forms of CycB_Cdk complexes are ubiquitinated and degraded into Cdk1 by aAPC_Cdc20 and aAPC_Cdh1 in a two-step process. Now, in the presence of DNA

damage, p21, which is synthesised by p53, binds to active CycB_Cdk1 in the nucleus to inhibit its activity that eventually leads to prolonged G2-M arrest (Abbas & Dutta, 2009). As mentioned in Section 3.3.2, following DNA damage, Gadd45α (synthesised by p53) stimulates further dissociation of CycB_Cdk1 and this effect has been included as new in our model (Figure 3.13).

Figure 3.13 Cdk1-Related Module. CycB_Cdk1 is the main controller of cell cycle system during M phase. This module comprises Cyclin B, Cdk1, their complexes in cytoplasm and nucleus and the impact of other proteins on them. The detailed description of all the shown interactions is presented in the text. Green solid arrows denote biochemical reactions (i.e., degradation, changing in the state of a protein by phosphorylation or dephosphorylation, etc.) while purple dashed arrows correspond to regulatory effects (i.e., enzymatic effect, etc.). Double-ended arrows represent reversible reactions. Elements in blue rectangular boxes are the proteins of this module whereas the other elements belong to other modules.

The newly added equations associated with this module are provided below where the new elements/parameters are shown in bold (Refer to Appendix A for all equations).

$$\frac{d[CycB]}{dt} = k_{123} \cdot [NFY] + [iCycB\_Cdk1\_Cyto] \cdot (k_{124} + \boldsymbol{k_{125}} \cdot [\boldsymbol{Gadd45}]) - (k_{126} + k_{127} \cdot [Cdk1] + (k_{128} \cdot [aAPC\_Cdc20] + k_{129} \cdot [aAPC\_Cdh1])) \cdot [CycB] \quad (3\text{-}15)$$

$$\frac{d[Cdk1]}{dt} = k_{130} \cdot [iCycB\_Cdk1\_Cyto] \cdot ([aAPC\_Cdc20] + [aAPC\_Cdh1]) + [aCycB\_Cdk1\_Cyto] \cdot (k_{131} \cdot [aAPC\_Cdc20] + k_{132} \cdot [aAPC\_Cdh1]) + [iCycB\_Cdk1\_Cyto] \cdot (k_{124} + \boldsymbol{k_{125}} \cdot [\boldsymbol{Gadd45}]) - k_{127} \cdot [CycB \cdot Cdk1] \quad (3\text{-}16)$$

$$\frac{d[iCycB\_Cdk1\_Cyto]}{dt} = k_{127} \cdot [CycB] \cdot [Cdk1] + k_{133} \cdot [aCycB\_Cdk1\_Cyto] - (k_{124} + \boldsymbol{k_{125}} \cdot [\boldsymbol{Gadd45}] + k_{134} \cdot ([aCdc25C] + [aCdc25CP\_S216]) + k_{130} \cdot ([aAPC\_Cdc20] + [aAPC\_Cdh1])) \cdot [iCycB\_Cdk1\_Cyto] \quad (3\text{-}17)$$

$$\frac{d[aCycB\_Cdk1\_Cyto]}{dt} = k_{135} \cdot [aCycB\_Cdk1\_Nuc] + k_{134} \cdot [iCycB\_Cdk1\_Cyto] \cdot ([aCdc25C] + [aCdc25CP\_S216]) - (k_{133} + k_{131} \cdot [aAPC\_Cdc20] + k_{132} \cdot [aAPC\_Cdh1] - \boldsymbol{k_{136}} \cdot [\boldsymbol{aPlk1}]) \cdot [aCycB\_Cdk1\_Nuc] \quad (3\text{-}18)$$

$$\frac{d[aCycB\_Cdk1\_Nuc]}{dt} = \boldsymbol{k_{136}} \cdot [\boldsymbol{a}CycB\_Cdk1\_Cyto] \cdot [\boldsymbol{aPlk1}] + k_{138} \cdot [iCycB\_Cdk1\_Nuc] \cdot [aCdc25C] + k_{29} \cdot [p21\_aCycB\_Cdk1\_Nuc] - (k_{135} + k_{137} \cdot [aWee1] + k_{140} \cdot [aAPC\_Cdc20] + k_{141} \cdot [aAPC\_Cdh1] + k_{30} \cdot p21) \cdot [aCycB\_Cdk1\_Nuc] \quad (3\text{-}19)$$

APC-Related Module

This module is particularly important during mid to late M phase. In late Prometaphase, APC_Cdc20 (first degrader of Cyclins A & B) is phosphorylated and activated by CycB_Cdk1 complexes. Upon the deactivation of spindle assembly checkpoint (a control system that monitors the assembly of sister chromatids' kinetochores to the microtubules on the mitotic plate) in Metaphase, Mad2/BubR1 complex (not included in this model) is dissociated from APC_Cdc20 allowing APC_Cdc20 to attain its full activity and trigger the destruction of Cyclin B. Hence, Cyclin B is degraded in Anaphase and this leads to dephosphorylation of Cdh1 which results in formation of APC_Cdh1 (second degrader of Cyclins A & B). Active APC_Cdh1, in turn, stimulates the degradation of APC_Cdc20 and drives the final steps of M phase that lead to exit from cell cycle (Morgan, 2007). For the sake of simplicity, APC_Cdc20 and APC_Cdh1 were modelled as just active and inactive forms and their synthesis and degradation processes were excluded.

As shown in Figure 3.14, inactive APC_Cdc20 becomes active by aPlk1 and aCycB_Cdk1_Nuc, while its inactivation is mediated by aAPC_Cdh1. An important point about active APC_Cdh1 is that it is not only crucial in late M phase, but also in early G1 phase. During G1 phase, the function of aAPC_Cdh1 is to make sure that no new cell cycle starts unless environmental conditions favour proliferation and this is done through degradation of different entities, such as Cyclins A and B. However, following the appropriate conditions, activated CycE_Cdk2 complex promotes the deactivation of APC_Cdh1 (in late G1 phase) and it eventually results in higher expression of proteins needed for DNA synthesis, such as Cyclin A. APC_Cdh1 remains further deactivated till late M phase by aCycA_Cdk1 and

aCycB_Cdk1_Nuc (see Figure 3.14) (Berridge, 2014; Li & Zhang, 2009; Qiao et al., 2010; Yuan et al., 2014).

Figure 3.14 APC-Related Module. This module presents the process of activation/inactivation of ubiquitin ligases APC_Cdc20 and APC_Cdh1. These ligases are crucial ubiquitinators and their impact on CycB_Cdk1 is particularly important during M phase. Green solid arrows denote biochemical reactions (i.e., degradation, changing in the state of a protein by phosphorylation or dephosphorylation, etc.) while purple dashed arrows correspond to regulatory effects (i.e., enzymatic effect, etc.). Elements in blue rectangular boxes are the proteins of this module whereas the other elements belong to other modules.

The newly added element Plk1 affects this module through the equations provided below (Refer to Appendix A for all equations).

$$\frac{d[iAPC\_Cdc20]}{dt} = k_{142} \cdot [aAPC\_Cdc20] \cdot [aAPC\_Cdh1] - (k_{143} \cdot [aCycB\_Cdk1\_Nuc] + \boldsymbol{k_{148}} \cdot [\boldsymbol{aPlk1}]) \cdot [iAPC\_Cdc20] \quad (3\text{-}20)$$

$$\frac{d[aAPC\_Cdc20]}{dt} = (k_{143} \cdot [aCycB\_Cdk1\_Nuc] + \boldsymbol{k_{148}} \cdot [\boldsymbol{aPlk1}]) \cdot [iAPC\_Cdc20] - k_{142} \cdot [aAPC\_Cdh1] \cdot [aAPC\_Cdc20] \quad (3\text{-}21)$$

3.4 Results and Discussion

In this section, we simulate the dynamic behaviour of the proposed model with and without DNA damage and demonstrate the effect of some newly added elements as well. The model is first simulated under no DNA damage condition (we call the cells under this condition healthy cells). In this condition, the parameter DDS (DNA Damage Signal) equals zero. Here, the temporal dynamics of newly added elements (c-Myc, PP1, SCF, and Plk1), indicators of G1-S and G2-M checkpoints (CycE_Cdk2, aCycB_Cdk1_Nuc) and some other significant proteins (p27, E2F, CycD_Cdk4, CycA_Cdk2, APC_Cdc20, APC_Cdh1) are discussed. As shown in Figure 3.15, p27 and aAPC_Cdh1 are predominant factors that suppress the initiation of cell cycle and this is in good agreement with experiments (Chu et al., 2008; Massagué, 2004; Sheaff et al., 1997; Yuan et al., 2014) (in our model,

we have highlighted the importance of p27 and APC_Cdh1 and represented them in sub-systems G1-S and G2-M checkpoints, respectively). Following the presence of Growth Factor, c-Myc becomes activated (through our added Growth Factor signalling sub-system) and then it induces the production of Cyclin D which is consistent with biological findings (Adhikary & Eilers, 2005; de Alboran et al., 2001; Schmidt, 1999). Thus, as shown in Figure 3.15, CycD_Cdk4 starts to increase and this, in turn, causes a drop in concentration of p27 throughout the mid G1 phase (because some CycD_Cdk4 complexes bind to p27). However, CycD_Cdk4 level has a slight decrease in the middle of cell cycle, which is mediated by SCF, and a dramatic drop at the end of cell cycle through ubiquitination by aAPC_Cdc20 (Alao, 2007) (this and the processes below highlight the well represented role of the APC module).

The model simulation properly shows that aAPC_Cdh1 remains at high level till late G1 phase where it is phosphorylated and deactivated by aCycE_Cdk2. The processes leading to this are as follows: At the beginning of cell cycle, the level of E2F_pRb is high for the reason that phosphatase PP1 mediates dephosphorylation of pRb leading to formation of complex E2F_pRb which has been well proven through experiments (Berndt, 2002; Ludlow et al., 1993; Nelson et al., 1997; Trinkle-Mulcahy et al., 2003). In fact, activation of CycE_Cdk2 happens following the release of transcription factor E2F from pRb through multiple phosphorylation of E2F_pRb complex by different Cyc_Cdks (see Section 3.3.3 for details). As shown in Figure 3.15, upon activation, CycE_Cdk2 stimulates further degradation of its inhibitor p27 (p27 concentration increases again at the end of cell cycle where the level of Cyc_Cdks is low) as well as phosphorylation and deactivation aAPC_Cdh1 (degrader of Cyclin A & B). In this way, aCycE_Cdk2 controls cell cycle transition from G1 to S phase and its peak time can be considered as an indicator of G1-S transition (Ohtsubo et al., 1995). Therefore, in the case of no DNA damage, the G1-S transition occurs at time-point 1095.

The ubiquitin ligase SCF (solid brown line), which becomes activated after activation of CycE_Cdk2 and inactivation of aAPC_Cdh1, functions as the main ubiquitinator of cell cycle until mid M phase where it is deactivated by aAPC_Cdh1 (dashed red line) which itself is activated around the same time (Figure 3.15). As shown in the simulated results, after G1-S transition, aCycE_Cdk2 starts to decrease and the reason is SCF-mediated degradation of Cyclin E. This behaviour is also in good agreement with biological findings (Nakayama & Nakayama, 2005). We compared Cyclin E behaviour in our model with SCF and without it (as in Iwamoto et al. (2011) model that does not incorporate the corresponding biological details of Cyclin E degradation). Results showed that with SCF, aCycE_Cdk2 peaks sooner and gets degraded more quickly than without it (Peak time of aCycE_Cdk2 (which indicates G1-S transition) with SCF is 1095 and without SCF is 1133, indicating a time difference of 38). These differences are shown in Figure 3.16. Therefore, we can assume that Cyclin E degrades more realistically in our model.

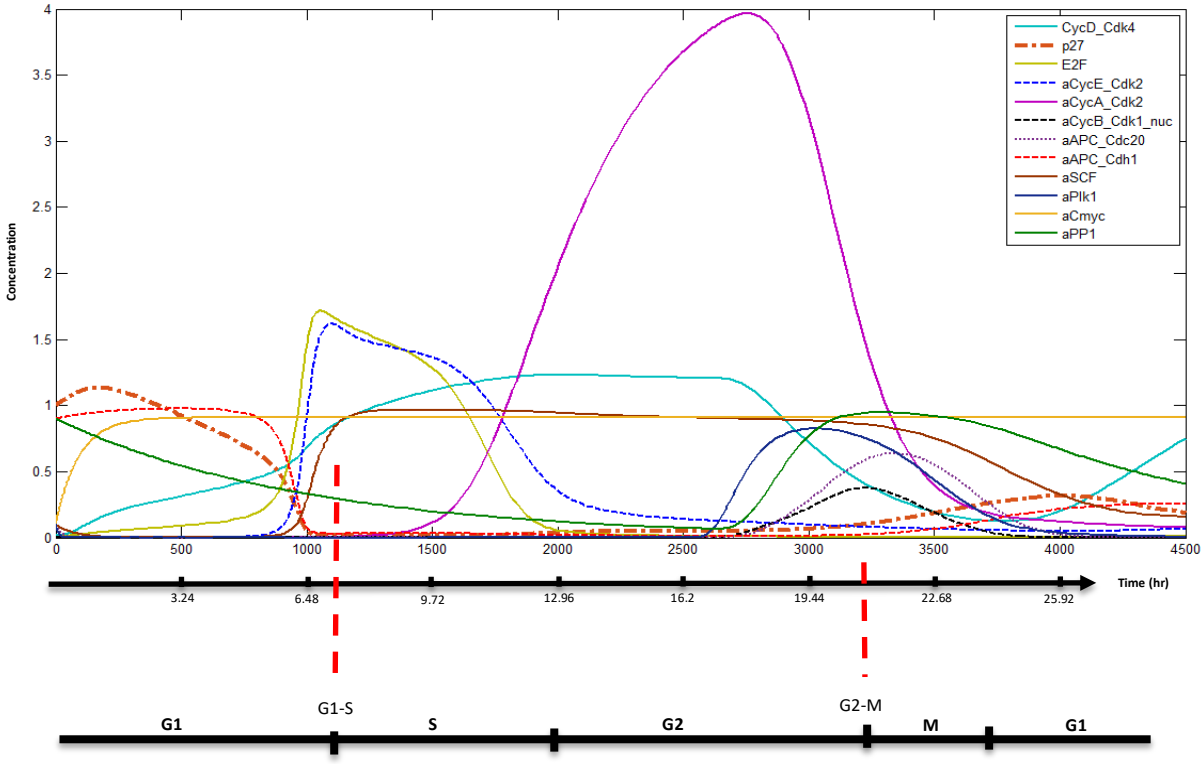

Figure 3.15 Temporal dynamics of the key players of mammalian cell cycle control system including newly added elements (c-Myc, PP1, SCF, and Plk1), indicators of G1-S and G2-M checkpoints (CycE_Cdk2, aCycB_Cdk1_Nuc) and some other significant proteins (p27, E2F, CycD_Cdk4, CycA_Cdk2, APC_Cdc20, APC_Cdh1). Cyc_Cdks are at the centre of this control system and the other elements regulate their concentration. G1-S and G2-M transitions under no DNA damage are denoted on the horizontal axis. The peak time (PT) of active CycE_Cdk2 and CycB_Cdk1_Nuc correspond to G1-S and G2-M transition, respectively [x-axis indicates time (simulation time units as well as hours); y-axis indicates protein concentration (mg/ml)].

Now, the concentration of aCycA_Cdk2 increases from S phase and keeps increasing throughout G2 phase before decreasing at late G2 phase. For G2-M transition, active version of nuclear CycB_Cdk1, which is translocated from cytoplasm into nucleus by aPlk1, is selected as the indicator of this transition. As can be seen in Figure 3.15, Plk1 becomes activated preceding CycB_Cdk1_Nuc and these dynamics are in agreement with the corresponding biological findings (Lindqvist et al., 2009; van Vugt & Medema, 2005) (which highlights the value of incorporation of Plk1 in our model). Therefore, the peak time of aCycB_Cdk1_Nuc as the indicator of G2-M transition is justified. This peak time occurs at time-point 3208 in our model. Further, a deeper investigation into the behaviour of the two versions of CycB_Cdk1 in the presence of aPlk1 as in our model and without it as in Iwamoto et al. (2011) model showed that Plk1 modified the concentrations and temporal dynamics of the two CycB_Cdk1 versions. In particular, the peak time of CycB_Cdk1_Nuc (indicator of G2-M

transition) with Plk1 and without it was 3208 and 3238, respectively, indicating that Plk1 accelerates the peak time by 30 time points. These results are shown in Figure 3.17.

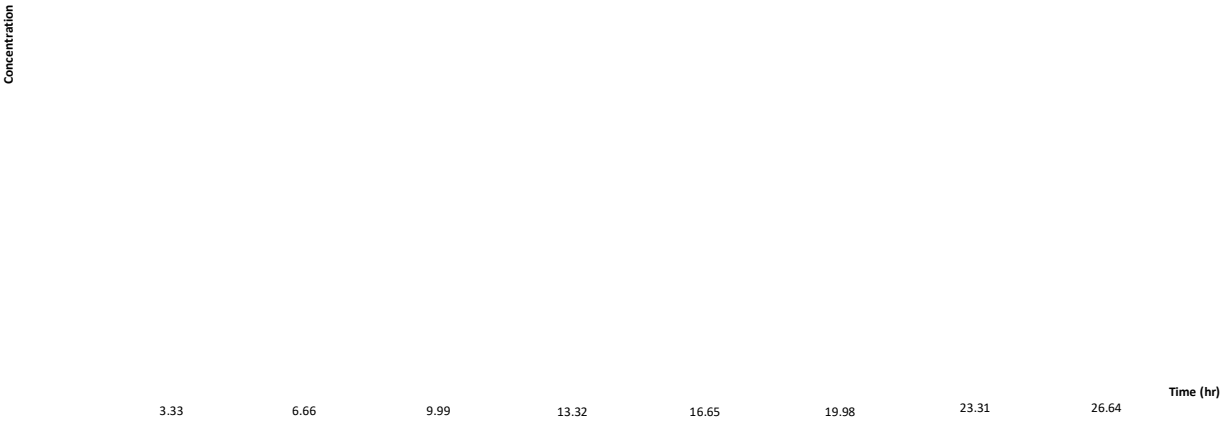

Figure 3.16 Impact of newly added Cyclin E degrader SCF on Cyclin E dynamics (solid line – with SCF and dashed line – without SCF). Figure shows that in the presence of SCF, Cyclin E peaks slightly sooner and degrades quicker than without SCF. Peak time (PT) of aCycE_Cdk2 indicates G1-S transition (with SCF: PT =1095, without SCF: PT= 1133; PT difference is 38) [x-axis indicates time (simulation time units as well as hours); y-axis indicates protein concentration (mg/ml)].

It is also important to note that at the end of cell cycle, first APC_Cdc20 and then APC_Cdh1 become activated as shown in Figure 3.15 to degrade all cyclins and help cell cycle exit (for detailed information, see Section 3.3.4). We also assessed the cyclic behaviour of the model over more than one cell proliferation cycles and the model produces cyclic behaviour reasonably well (see Appendix D for more details). In the case of DNA damage, the parameter DDS (DNA Damage Signal), is changed from zero (no DNA damage) to 0.012 (corresponds to 400-800 (J/m^2) dose of UV) to assess the effect of DNA damage on cell cycle progression.

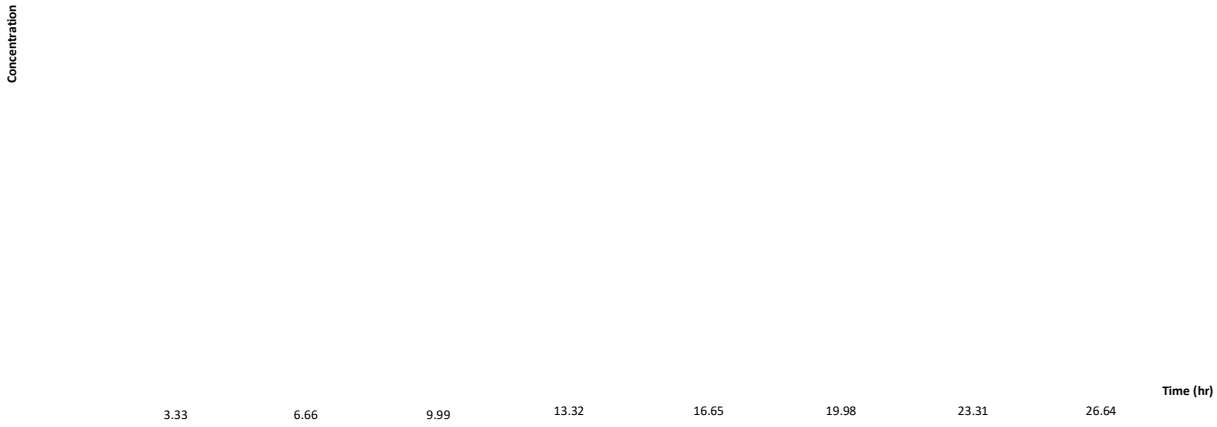

Figure 3.17 Impact of newly added Plk1 on Cyclin B dynamics (solid line – with Plk1; and dashed line – without Plk1). Figure shows that Plk1 alters the concentration and Peak time (PT) of CycB_Cdk1_Cyt and CycB_Cdk1_Nuc complexes. PT of CycB_Cdk1_Nuc indicates G2-M transition (PT with Plk1 is 3208 and without Plk1 is 3238; PT difference is 30) [x-axis indicates time (simulation time units as well as hours); y-axis indicates protein concentration (mg/ml)].

Figure 3.18 shows the dynamics of some important, including the newly added, elements of the rapid and delayed DNA response modules. In particular, Chk-Related (rapid) module is activated immediately and then p53 (delayed response) reaches peak activating other elements in the delayed module, in particular p21 and Gadd45α (newly added). The p53 shows oscillatory behaviour which agrees with findings in the literature (Batchelor et al., 2008) and Gadd45α increases while p53 is active. These results point to the integrated response of the two DNA damage modules and the value of Gadd45α in the expansion of the delayed DNA damage response in the model. Further, both G1-S and G2-M transitions take place with a delay indicating the occurrence of cell cycle arrest at these checkpoints. In this condition, G1-S and G2-M transitions happen at time-points 1125 and 3330, respectively, and the corresponding arrest durations are 30 and 122 time-points, respectively. This finding that G2-M arrest is longer than that of G1-S is consistent with experiments done on mouse Swiss3T3 cells revealing prolonged G2-M cell cycle arrest compared to G1-S after DNA damage (Siu et al., 1999). More analysis will be done on the proposed model in the next two chapters.

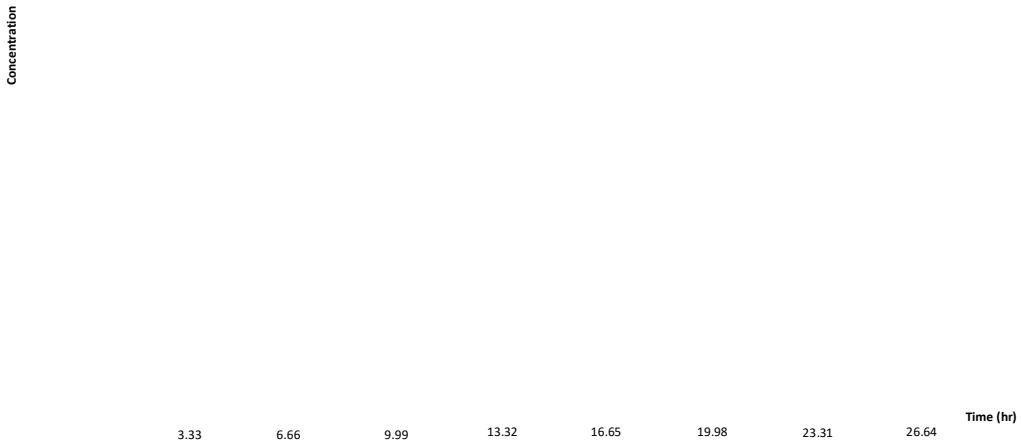

Figure 3.18 Temporal dynamics of important elements in the rapid and delayed DNA damage response in cell cycle arrest. Chk2 is the key player in rapid DNA damage signalling (explained in Section 3.3.2) which becomes activated after the presence of DNA damage and inhibits the progression of cell cycle. This is followed by the delayed response centred on transcription factor p53. Since transcription is slower than activation (of Chk2), this module is called delayed DNA damage response. These results show the integrated response of the rapid and delayed pathways as proposed in this study. Transcription factor p53 induced the synthesis of Cyclin-dependent Kinase Inhibitor p21 and the newly added Gadd45α showing latter's close correspondence to p53 and the joint activity of the delayed module (the significance of these elements is described in Section 3.3.2) [x-axis indicates time (simulation time units as well as hours); y-axis indicates protein concentration (mg/ml)].

3.5 **Summary**

In this chapter, a comprehensive system based mathematical model of mammalian cell cycle with new additions and extensions was proposed based on Iwamoto et al. (2011) ODE cell cycle model and analysed for determining the most influential sub-systems and parameters and for comparing the relative efficiency of G1-S and G2-M checkpoints. We developed our model based on four abstracted functional sub-systems: Growth Factor (newly added), G1-S, G2-M, and DNA damage signalling sub-systems. The four sub-systems, abstracted from the existing cell cycle knowledge, were further enriched with some important new modules and elements: G1-S was abstracted into four interconnected modules (Cdk4-Related, E2F-pRb, Cdk2-Related and Tyrosine phosphatase where the latter is a novel addition to this sub-system and E2F-pRb module is expanded and modified to make

the model cyclic); G2-M was abstracted into five modules (Cdk1-Related, Tyrosine phosphatase, Tyrosine kinase, Plk1-Related and APC-Related where the latter four are novel additions and contained new elements); and DNA damage was abstracted into two modules including Chk-Related (rapid) and newly added elements in p53-Related (delayed) modules.

This model enabled us to seamlessly and realistically study the function of sub-systems as well as the influence of sub-systems on each other where the Growth Factor sub-system senses the Growth Factor signals and triggers the activation of subsequent sub-systems. Past models have considered Growth Factor to be a binary signal - on or off. We represented it as a continuous signal and now the relationship (continuous dynamic) between c-Myc and Cyclin D is realistically represented. The function of Growth Factor signal is to activate c-Myc that in essence initiates the cell cycle by triggering the synthesis of Cyclin D. We added the Growth Factor signalling and especially c-Myc due to its biological significance to the cell cycle system and our numerical analysis in fact showed that c-Myc is the most significant element in the whole system. Thus, the Growth Factor sub-system is a crucial part from a systems perspective and adding it is beneficial. Further, as an extension to the cell cycle model, Growth Factor signalling system gives a more complete description of cell cycle. Also, with c-Myc in the system, we now have the Transcription factors of all Cyclins in one model. Therefore, we have presented a more realistic description of cell cycle initiation through Growth Factor signalling sub-system that can also be used in future studies to investigate the impact of perturbation to growth signal on system behaviour.

Our intuitive approach to breaking down the sub-systems into their constituent modules enabled us to determine the function of each module and correctly formulate their effects on each other using ODEs. For example, in the G1-S checkpoint signalling sub-system: (1) Cdk4-Related module (receives the signal from Growth Factor sub-system to initiate the cell cycle); (2) E2F-pRb module (receives the signal from Cdk4-Related module and induces the production of some critical cell cycle proteins through transcription factor, E2F); (3) Cdk2-Related module (talks to other internal and external modules and sub-systems to prepare the cell for entering into S phase); and (4) Tyrosine Phosphatase module (stimulates the activation of Cyc_Cdk2 complexes which are crucial for G1-S transition).

The dynamic simulation of the model under no DNA damage conditions reveals the role and value of the newly added elements in filling the gaps and giving a fuller description of cell cycle. One of the newly added elements is phosphatase PP1 that dephosphorylates Retinoblastoma protein (pRb) at the end of cell cycle and helps a new cell cycle to begin which has been biologically proven (Berndt, 2002; Ludlow et al., 1993; Nelson et al., 1997; Trinkle-Mulcahy et al., 2003). It should be noted that Iwamoto et al. model was not cyclic because PP1 was missing in that model. Plk1 is another newly added element which is one of the most important proteins in m-phase entry. In Iwamoto et al.

model, there were two types of CycB-Cdk1: nucleus and cytoplasmic versions; but there was no explanation for the translocation of the cytoplasmic version into nucleus version (Iwamoto et al., 2011). Our model provides this explanation through Plk1. Plk1 has multiple functions including activation of Cdc25C phosphatase and APC_Cdc20 (degrader of Cyclin A and Cyclin B), inactivation of Wee1 kinase, and translocation of CycB_Cdk1 from cytoplasm to nucleus (Golan et al., 2002; Lindqvist et al., 2009; Van De Weerdt & Medema, 2006; van Vugt & Medema, 2005; Zitouni et al., 2014). Plk1 is activated by cytoplasmic CycB_Cdk1 through induced phosphorylation and its degradation is mediated by ubiquitination through active APC_Cdh1 (Eckerdt & Strebhardt, 2006; Lindon & Pines, 2004). With Plk1 added, the model now incorporates correctly a process that explains an important cell cycle stage transition.

SCF is another newly added element that is a ubiquitin ligase whose function in cell cycle system is to degrade a number of key elements in the cell cycle control system. The reason for adding SCF to our model is that there is biological evidence that Cyclin E, which is the key player of cell cycle during G1 phase, is degraded by SCF (Ang & Harper, 2004; Cardozo & Pagano, 2004; Nakayama & Nakayama, 2005). In Iwamoto et al. model, the process of Cyclin E degradation is not complete and we believe that adding SCF to the model makes it more accurate. In Iwamoto et al. model, biologically relevant CycE degradation details are not incorporated as in our model and therefore, CycE-Cdk2 degradation happens over a longer time. Therefore, we can assume that Cyclin E degrades more realistically in our model.

Furthermore, the dynamic behaviour of the system was investigated where the cell cycle arrest occurred in the presence of DNA damage. Under this condition, both the Chk-Related (rapid) and p53-Related (delayed) modules were activated with p53 showing the expected oscillatory behaviour and the contributory role of new element being shown in perspective. The DNA damage part in Iwamoto et al. model had p53 as a transcription factor that induces synthesis of a number of proteins. One of them was 14-3-3σ that affects (inactivates) B-type Cyclin_Cdk complex to arrest cell cycle in the case of DNA damage. However, that does not represent the complete picture of impact of p53 on CycB_Cdk1. To make that picture more complete, we found another product of p53, Gadd45α, that also inactivates CycB_Cdk1 (as the main controller of cell cycle during M-phase) (Jin et al., 2002; Zhan, 2005). Furthermore, biological evidence shows that the way that 14-3-3σ and Gadd45α act upon CycB_Cdk1 inactivation is different. The first factor (14-3-3σ) inhibits Cdc25C (which is the CycB_Cdk1 activator), while the second (Gadd45α) physically interacts with Cdk1 in order to stimulate CyclinB_Cdk1 unbinding (Jin et al., 2002; Zhan, 2005). Therefore, Gadd45α is added to the model to present a more complete picture of G2-M checkpoint. As shown in Figure 3.18, Gadd45α is produced throughout the period of activity of p53. We also noticed from the dynamic simulation results that G1-S and G2-M transitions occurred with a delay of 30 and 122 time-

points, respectively, in comparison to no DNA damage condition thus revealing that the arrest duration at G2-M is longer than that of G1-S that has biological support (Siu et al., 1999).

Therefore, this chapter provides an approach to represent and analyse a complex system, in particular, mammalian cell cycle, from a holistic systems perspective incorporating sub-systems and modules along with a number of new additions. Newly added elements provide an opportunity for biologists to set up new hypothesis to experiment in their lab for targeted cancer therapies. For example, PP1 can be used for cancer therapy as its knocking out can halt the cell proliferation by stopping the system from cycling. This chapter also gives a clearer view of cell cycle and provides new insights into systems dynamics, influential sub-systems/modules/parameters (will be presented in Chapter 4), and checkpoint efficiency (will be presented in Chapter 5).

Chapter 4

Investigation of the Effect of Sub-Systems, Modules, and Parameters on Cell Cycle Control System Response

In this chapter, the most effective sub-systems, modules, and parameters on cell cycle control system response associated with the comprehensive mathematical model presented in the last chapter are identified through Global Sensitivity Analysis (GSA), which focuses on global impact of parameters. A model called Self-Organizing Map with Correlation Coefficient Analysis (SOMCCA) is developed to perform GSA which shows that Growth Factor and G1-S checkpoint sub-systems and seven parameters in the modules within them are crucial for G1-S and G2-M transitions. An overview of the chapter is presented in the first section. In the second section, the GSA formulation through the SOMCCA model is presented. The third section of this chapter is devoted to identification of the most influential parameters, sub-systems, and modules of the comprehensive model on system response. Finally, a summary of the chapter is presented in Section 4.4.

4.1 Overview

An effective way to investigate the system behaviour is to analyse the system parameters. The behaviour that we are investigating here is G1-S and G2-M transitions. Therefore, in this chapter, we describe a numerical analysis that is applied to the proposed model in Chapter 3 to identify the parts of the system that have the highest impact on G1-S and G2-M transitions. Thanks to our systems modelling scheme, it is possible to find these parts as sub-systems and modules in order to investigate the system response from a functional perspective. The Global Sensitivity Analysis (GSA) is performed to explore the changes in system behaviour with respect to variation of all parameters and to find a region of parameter space where the system response is highly disrupted. The rationale for using GSA instead of Local Sensitivity Analysis (LSA), which is based on perturbation of just one individual parameter at a time, is that GSA is closer to reality where all the system parameters are affected by environmental or other perturbations. A hybrid model is developed to perform GSA that has two main phases. In the first phase, an Artificial Neural Network (ANN) approach called Self-Organizing Map (SOM) (Samarasinghe, 2006) is implemented to explore the space of parameter vectors and their relations. Then, the output of SOM goes through the second phase called Correlation Coefficient Analysis (CCA) to reveal the correlation between parameters and system response. The proposed hybrid model is called SOMCCA. It should be noted that the Peak Times (PTs) of aCycE_Cdk2 and aCycB_Cdk1_Nuc are considered as *in silico* indicators of G1-S and G2-M transitions, respectively.

4.2 GSA Formulation through SOMCCA Model

GSA determines the collective impact of parameters on system response and reveals the effective parameters from a global perspective. It is based on perturbation of all parameters around their fixed values and then checking the impact of this change on system response. The fixed value for each parameter is its value in unperturbed condition and the output is the PT of the interested biological indicator, such as aCycE_Cdk2. We develop a model based on Self-Organizing Map and Correlation Coefficient Analysis called SOMCCA to perform GSA. Some of the benefits of using Self-Organizing Map are dimensionality reduction, visualisation, handling nonlinear relationships in data and showing similar entities closer to each other (topology preservation) (Samarasinghe, 2006). Using the SOMCCA model, we can demonstrate the global spectrum of parameters (in the form of 2D maps) and find the correlation between these parameters and system response. A flowchart of the proposed model is illustrated in Figure 4.1.

Figure 4.1 A flowchart of the SOMCCA model. This model comprises two main phases, SOM and CCA. During the SOM phase, the SOM network is constructed and then trained using cell samples. The parameters are first qualitatively assessed through SOM input planes and then the input weight matrix (W) is extracted. The W matrix is used as input to CCA phase in order to calculate the Covariance (Cov) matrix. Using the Cov matrix, Pearson Correlation Coefficient (PCC) can be calculated and used to assess the parameters quantitatively. Finally, by sorting the effective parameters, we identify the most effective parameters from a global perspective.

According to the SOMCCA model (Figure 4.1), all parameters are perturbed simultaneously and sampled 2000 times to produce 2000 cells (the assumed perturbation range is $\pm 10\%$). The parameter vectors of these cells are inputs to SOM phase. SOM is an unsupervised ANN in which the topology of the data is exactly preserved and presented in a rectangular or hexagonal (depending on selected topology) 2D map of neurons (Samarasinghe, 2006). This allows visualisation of high

dimensional data (i.e., parameters and PT) and their relations on a 2D plane. A schematic diagram of an SOM model is shown in Figure 4.2.

As demonstrated in Figure 4.2, m input variables, $y_1, y_2, \dots, y_m$, which are the parameters and PT of the cell cycle system, are connected to a feature map by a set of weighted arrows. In fact, each neuron j in feature map corresponds to a vector of m weights $wt_j = (wt_{1j}, wt_{2j}, \dots, wt_{mj})$ coming from m inputs. Each weight vector after training represents a cluster of input vectors. Training an SOM is a repetitive process. For each input vector, neurons compete with each other to represent the input vector and be the winner that allows them to modify their weights. The winner of the competition is the neuron that has the closest distance (there are different distance functions, such as Euclidian, Manhattan, etc.) to the input vector.

Figure 4.2 **A schematic diagram of SOM. It includes a set of input variables, $y_1, y_2, \dots, y_m$, (parameters and PT) and a set of neurons arranged in a 2D Feature Map. Each neuron is represented by a weight vector linking it to input vectors. Input vectors are presented to the SOM and the output (activation level) of each neuron is the weighted sum of the input vector. The neuron with the highest activation is declared the winner and its weight vector is adjusted along with that of the neurons in its neighbourhood. This learning process continues until there is no or minimal weight adjustment.**

The corresponding formula for Euclidian measure is expressed as follows:

$$Dist_j = y - wt_j = \sqrt{\sum_{i=1}^{m} (y_i - wt_{ij})^2} \quad (4\text{-}1)$$

Then the winner weights are brought closer to the input vector. For topology preservation that preserves relations in input data, the neighbours of winner neuron are also moved toward the input (by a smaller amount than that of winner). This is expressed through a function called Neighbour Strength (NS). The function can take different forms, such as Gaussian, Exponential, etc. For example, the Exponential NS function is shown in Eq. (4-2):

$$NS_{exp} = Exp\left(-C \times dist_{i,j}\right) \quad (4\text{-}2)$$

where $dist_{i,j}$ is the distance between winner neuron i and any neighbour neuron j, and C is a constant between 0 and 1. The weight update for both winner and neighbours is presented below:

$$\Delta_{wt_j} = {wt_j}^{New} - {wt_j}^{Old} = \beta eta \times NS \times (y_i - {wt_j}^{Old}) \quad (4\text{-}3)$$

where Δ_{wt_j} is the weight update or difference between new and old weight values, βeta is learning rate that can be defined as a constant or variable through different functions. The training process is halted when Δ_{wt_j} becomes zero or below a user-defined threshold over iterations (Samarasinghe, 2006). In a trained SOM, individual neuron weights represent the centre of gravity or centre of a cluster of parameter vectors. After training, the results of SOM are usually presented through a Unified Matrix (U-Matrix). The U-Matrix is a map of the distance between neighbour neurons. One of the results that is of interest in this study is the spread of individual parameters separately on the map (map planes). Through these maps, it is possible to qualitatively evaluate the effect of different parameters on system response (PT).

The topology preservation characteristic of SOM enables us to conduct a quantitative evaluation of parameters as well. To do this, the weight matrix W is extracted from the trained SOM and imported to the next phase, CCA phase, to perform a statistical analysis in order to find the correlation coefficient between parameters and system response (see Figure 4.1). For example, if SOM has 25 neurons (5×5 map) and the number of input variables is 10, W will be a 25×10 matrix. The first step in CCA phase is to calculate the covariance of W. Basically, covariance matrix shows how much two variables y_m and y_n change together or behave similarly (Wasserman, 2013) and it can be represented as:

$$Cov_{m,n} = E\left(\left(y_m - E(y_m)\right) \times \left(y_n - E(y_n)\right)\right) \quad (4\text{-}4)$$

where E corresponds to the expected value of variables. Considering the aforementioned example where W was a 25×10 matrix, the corresponding covariance matrix becomes a 10×10 symmetric matrix whose diagonal elements are the variance of variables. To find the correlation coefficient between parameters and system response (PT), Pearson Correlation Coefficient (PCC) is used (Benesty et al., 2009). The elements of PCC matrix can be calculated as follows:

$$PCC_{m,n} = \frac{Cov(m,n)}{\sqrt{Cov(m,m) \times Cov(n,n)}} \quad (4\text{-}5)$$

For the above example, PCC is a 10×10 symmetric matrix whose diagonal elements are one and the other elements indicate the correlation between variables in the range of ± 1 where -1 corresponds to complete negative correlation, whereas $+1$ signifies total positive correlation.

4.3 Most influential Parameters/Sub-Systems/Modules

Using SOMCCA model, it is possible to perform a quantitative analysis and sort the effective parameters from a global point of view based on correlation coefficient values (parameters with correlation coefficient value greater than 0.05 are considered as significant; the corresponding correlation coefficient values of the most significant parameters with respect to PTs of G1-S and G2-M indicators are shown in the last row of Table 4.1). The 2D maps of the most significant parameters of the system with respect to PTs of G1-S indicator (aCycE_Cdk2) under No DDS is shown in Figure 4.3. Here, the location of a particular neuron in the planes corresponds to each other, so by following a neuron location in two map planes, the relation (negative or positive) between two inputs can be assessed using the colour code. In this case, PT of aCycE_Cdk2, is mainly influenced by (in order of significance – the corresponding correlation coefficient values are shown in Table 4.1): $\boldsymbol{k_{40}}$ (synthesis rate of Cyclin D through transcription factor c-Myc), $\boldsymbol{k_{64}}$ (rate of dephosphorylation of pRbPPP to pRb through PP1), $\boldsymbol{k_{49}}$ (synthesis rate of p27), $\boldsymbol{k_{60}}$ (dissociation rate of E2F_pRbPP complex through aCycE_Cdk2), $\boldsymbol{k_{50}}$ (dissociation rate of p27_aCycE_Cdk2 complex), $\boldsymbol{k_{52}}$ (association rate of p27 and aCycE_Cdk2), $\boldsymbol{k_{98}}$ (synthesis rate of iCdc25A through E2F), $\boldsymbol{k_{88}}$ (activation rate of iCycE_Cdk2 through aCdc25A), $\boldsymbol{k_{101}}$ (activation rate of iCdc25A through aCycE_Cdk2 and aCycA_Cdk2), $\boldsymbol{k_{48}}$ (association rate of p27 and CycD_Cdk4), $\boldsymbol{k_{70}}$ (synthesis rate of Cyclin E through transcription factor E2F), $\boldsymbol{k_2}$ (activation rate of ic-Myc through Growth Factor), $\boldsymbol{k_{83}}$ (degradation rate of iCycE_Cdk2 to Cdk2), and $\boldsymbol{k_{100}}$ (degradation rate of iCdc25A). As shown in Figure 4.3, the parameters $\boldsymbol{k_{64}}$, $\boldsymbol{k_{49}}$, $\boldsymbol{k_{52}}$, $\boldsymbol{k_{83}}$ and $\boldsymbol{k_{100}}$ positively correlate with PT of G1-S indicator, while others have negative correlation. For instance, the higher the synthesis rate of p27 ($\boldsymbol{k_{49}}$), the longer the G1 phase. Overall, the positive correlations are with parameters of processes that increase PT due to their negative effect on CycE_Cdk2 production, activation (in particular through promoting p27 binding and inhibiting activation by Cdc25A) and degradation; whereas, the negative correlations are with parameters of processes that have the opposite effect on CycE_Cdk2 and Cyclin D.

Based on our systems modelling approach, after identification of the most effective parameters, it is possible to identify the most impactful sub-systems and modules too. The impact of the aforementioned parameters on G1-S Transition under No DDS in terms of sub-systems and modules is demonstrated in Figure 4.4. As shown in this figure, under No DDS, just two sub-systems have impact on G1-S transition, Growth Factor and G1-S checkpoint sub-systems. Growth Factor sub-system regulates the G1-S transition through two c-Myc-related Parameters, $\boldsymbol{k_{40}}$ and $\boldsymbol{k_2}$ and our

model has correctly identified them. This is in agreement with experiments that have shown that c-Myc has an important role in S phase induction (Baluchamy et al., 2003; Berns et al., 2000). Furthermore, biological findings have suggested that c-Myc has an essential impact on cell growth and its down-regulation leads to prolonged G1 and G2 phases (Dang, 1999; Iritani & Eisenman, 1999).

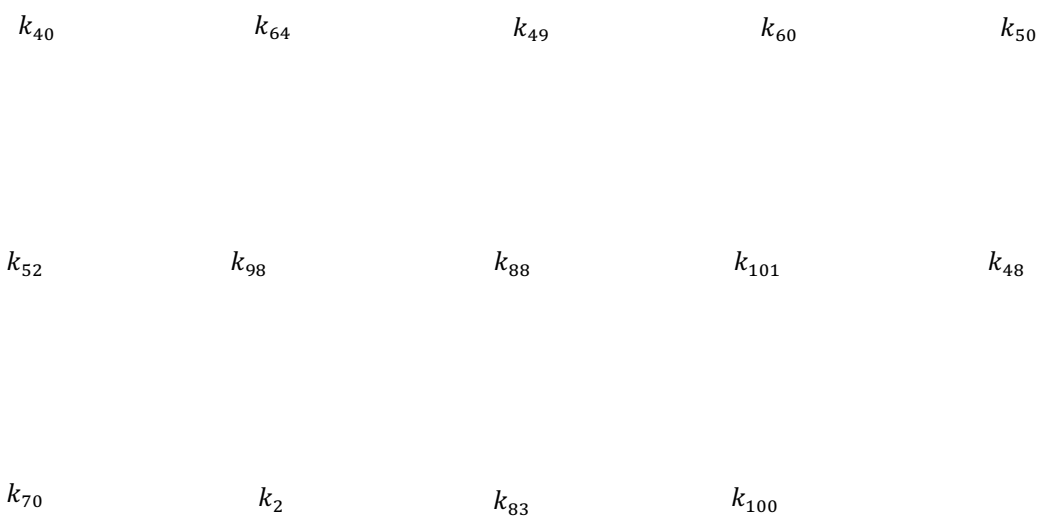

Figure 4.3 **SOM planes showing the spread of the most significant parameters sorted through SOMCCA (in order of significance - parameters with correlation coefficient value greater than 0.05 are considered as significant) with respect to PT of G1-S indicator (the last figure). It shows the relationship of variables/parameters to the output PT and relationship of parameters to each other. Darker colours indicate lower values of a parameter and lighter ones indicate higher values. By comparing the colour pattern in the output plane with those in the input plane it is easy to see which parameter have similar patterns to the output (positive relationship = positive correlation) and which ones have opposite colour pattern (negative correlation) and which ones have weak or no correlation to the output. This is considered as qualitative evaluation. Also, comparing the parameter planes to each other, it can be determined which variables are positively, negatively, weakly, or not correlated. Parameters k_{64} (rate of dephosphorylation of pRbPPP to pRb through PP1), k_{49} (synthesis rate of p27), k_{52} (association rate of p27 and aCycE_Cdk2), k_{83} (degradation rate of iCycE_Cdk2 to Cdk2) and k_{100} (degradation rate of iCdc25A) have positive correlation with PT of G1-S indicator, while others (k_{40} (synthesis rate of Cyclin D through transcription factor c-**

Myc), k_{60} (dissociation rate of E2F_pRbPP complex through aCycE_Cdk2), k_{50} (dissociation rate of p27_aCycE_Cdk2 complex), k_{98} (synthesis rate of iCdc25A through E2F), k_{88} (activation rate of iCycE_Cdk2 through aCdc25A), k_{101} (activation rate of iCdc25A through aCycE_Cdk2 and aCycA_Cdk2), k_{48} (association rate of p27 and CycD_Cdk4), k_{70} (synthesis rate of Cyclin E through transcription factor E2F) and k_2 (activation rate of ic-Myc through Growth Factor)) have negative correlation.

The G1-S checkpoint sub-system has also a crucial effect on G1-S transition through its four modules (Figure 4.4). As the first module that becomes functional following the presence of Growth Factor, Cdk4-Related module controls G1-S transition through its two p27-related parameters, $\boldsymbol{k_{48}}$ and $\boldsymbol{k_{49}}$. These two parameters (together with two other p27-related significant parameters, $\boldsymbol{k_{50}}$ and $\boldsymbol{k_{52}}$, which are associated with Cdk2-Related module) are correctly identified as effective in our model, confirming the findings that showed the importance of p27 repressor in G1-S transition (Chu et al., 2008). E2F-pRb module, which comes to the picture after activations of Cdk4-Related module, affects G1-S transition through E2F-related parameters, $\boldsymbol{k_{60}}$ and $\boldsymbol{k_{64}}$ (Figure 4.4). Parameter $\boldsymbol{k_{64}}$, which corresponds to a newly added protein PP1, is identified as one of the most significant parameters in our model. PP1 was biologically proven to be a crucial element in the cell cycle system as it dephosphorylates Retinoblastoma Protein (pRb) during late Mitosis and early G1 phase (Berndt, 2002; Nelson et al., 1997; Trinkle-Mulcahy et al., 2003).

Figure 4.4 Influential parameters, sub-systems and modules on G1-S transition under No DDS. Growth Factor sub-system and all the modules of G1-S checkpoint have impact on G1-S transition. The significant parameters are shown on the corresponding arrows.

During G1 phase, E2F acts as the main transcription factor and directs the cell toward G1-S transition by synthesis of some important target proteins including Cyclin E, which in turn stimulates the

release of more E2F (E2F is initially in locked mode by association with pRb). The release of E2F is an important process as correctly identified by the significant role of $\boldsymbol{k_{60}}$ (dissociation rate of E2F_pRbPP complex through aCycE_Cdk2). Experiments have demonstrated the key role of Tyrosine phosphatase Cdc25A as one of the most essential regulators of G1-S checkpoint (through its positive feedback loop with aCycE_Cdk2 as activator of iCycE_cdk2) (Blomberg & Hoffmann, 1999; Sexl et al., 1999). That is why our simulation results show the vital effect of Tyrosine Phosphatase module on G1-S transition through three Cdc25A-related parameters, $\boldsymbol{k_{98}}, \boldsymbol{k_{100}}$ and $\boldsymbol{k_{101}}$ (Figure 4.4). It is important to note that other experiments have also suggested that this phosphatase may mediate G2-M transition as well (Chen et al., 2003; Mailand et al., 2002; Timofeev et al., 2010). Cdk2-Related module, which comprises the reactions that regulate Cyclin E and CycE_Cdk2 complex through parameters, $\boldsymbol{k_{50}}, \boldsymbol{k_{52}}, \boldsymbol{k_{70}}, \boldsymbol{k_{83}}$ and $\boldsymbol{k_{88}}$, also shows significant effect on G1-S transition (Figure 4.4).

The SOMCCA analysis was also conducted for G2-M transition under no DNA damage with PT of CycB_Cdk1_Nuc as the indicator of transition. Under this condition, most of the aforementioned parameters remain significant and some new parameters are also recognized as significant (the corresponding correlation coefficient values of the most significant parameters with respect to PTs of G1-S and G2-M indicators are shown in the last row of Table 4.1). The reason is that the cell cycle system consists of a sequence of events which are tightly connected to each other and when something is wrong in one part (sub-system/module), it directly or indirectly affects the subsequent parts as well. In fact, from a high-level point of view, three different sub-systems have impact on G2-M transition: Growth Factor, G1-S, and G2-M checkpoint sub-systems (Figure 4.5). The newly added/identified significant parameters are shown in bold in Figure 4.5. As shown in Figures 4.4 & 4.5, the first two sub-systems (Growth Factor and G1-S checkpoint) have more or less the same effect on G1-S and G2-M transitions. In fact, parameters $\boldsymbol{k_{76}}$ (synthesis rate of Cyclin A through BMyb), $\boldsymbol{k_{80}}$ (association rate of Cyclin A and Cdk2), $\boldsymbol{k_{93}}$ (synthesis rate of iBMyb through E2F) and $\boldsymbol{k_{96}}$ (activation rate of NFY through aCycA_Cdk2), which correspond to Cdk2-realated module of G1-S checkpoint sub-system, are also found significant for G2-M transition. The reason for this is that during S and G2 phases, Cyclin A, which is synthesised through BMyb and NFY, sets the stage for G2-M transition through its indirect effect on CycB_Cdk1 complex (Chae & Shin, 2011; Joaquin & Watson, 2003). Therefore, our simulation results are consistent with experimental findings reported on the role Cdk2 function in activating Cdk1 and M phase entry (Hu et al., 2001).

Cyclin B (which in complex with Cdk1 makes CycB_Cdk1) and Cdc25C are also found to be significant through G2-M checkpoint sub-system (through Cdk1-Related and Tyrosine phosphatase modules, respectively) which is consistent with biological findings (Boutros et al., 2007; De Souza et al., 2000; Lindqvist et al., 2009; Su et al., 2006; Trunnell et al., 2011). Tyrosine phosphatase module stimulates the G2-M transition through two parameters, $\boldsymbol{k_{109}}$ and $\boldsymbol{k_{112}}$, which correspond to synthesis rate of

Cdc25C and activation rate of iCdc25C through aCycB_Cdk1_Cyto and aCycB_Cdk1_Nuc, respectively (Figure 4.5). As for the effect of Cdk1 related module, it controls G2-M transition through three Cyclin B-related parameters, $\boldsymbol{k_{123}}$ (synthesis rate of Cyclin B through NFY), $\boldsymbol{k_{127}}$ (association rate of Cyclin B and Cdk1) and $\boldsymbol{k_{134}}$ (activation rate of iCycB_Cdk1_Cyto through aCdc25C and aCdc25CP_S216).

Figure 4.5 The most Influential parameters, sub-systems and modules in G2-M transition under No DDS. The parameters are shown on the corresponding arrows. The newly found significant parameters (in comparison to those found significant for G1-S) are bolded.

The SOMCCA analysis was also conducted on DNA damage condition. In the presence of DNA damage (in comparison with No DDS), some other new parameters related to DNA damage sub-system are identified and added to the list of significant parameters (see Table 4.1). The newly identified significant parameters on both G1-S and G2-M transitions are as follows: $\boldsymbol{k_6}$ (rate of DNA damage repair), $\boldsymbol{k_{31}}$ (degradation rate of p21), $\boldsymbol{k_{22}}$ (synthesis rate of p21 through p53), $\boldsymbol{k_{26}}$ (association rate of aCycE_Cdk2 and p21), $\boldsymbol{k_5}$ (rate of DNA damage signal production), $\boldsymbol{k_9}$ (activation rate of p53 through ATM), $\boldsymbol{k_{11}}$ (p53 degradation rate through Mdm2), $\boldsymbol{k_{14}}$ (synthesis rate of Mdm2), and $\boldsymbol{k_{17}}$ (degradation rate of Mdm2). These simulation results are consistent with experimental findings which suggest that following the presence of DNA damage, p53, p21 and Mdm2 (through negative feedback with p53) are the key players of cell cycle arrest and DNA damage response (Agarwal et al., 1995; Carvajal et al., 2005; Vassilev et al., 2004). A summary of significant parameters, sub-systems, and modules in different conditions (No DDS, with DDS) for both G1-S and G2-M transitions is demonstrated in Table 4.1. Parameters with correlation coefficient value greater than 0.05 are considered as significant. As shown in this table, G1-S checkpoint and Growth Factor sub-systems are

identified as significant in all conditions. Furthermore, G2-M checkpoint sub-system does not impact G1-S transition.

Table 4.1 List of effective parameters as well as sub-systems and modules for G1-S & G2-M transitions with and without DNA damage (italicised modules in columns 3 and 5, respectively, indicate the additional modules for DDS compared to No DDS condition for G1-S and G2-M shown in columns 2 and 4; and underlined modules in columns 4 and 5 are additional modules for G2-M compared to G1-S shown in columns 2 and 3). The value of the correlation coefficient of parameters with respect to PTs of G1-S and G2-M indicators are shown in brackets in the last row next to the corresponding parameter. Parameters with correlation coefficient value greater than 0.05 are considered as significant parameters.

	G1-S Transition (No DDS)	**G1-S Transition (with DDS)**	**G2-M Transition (No DDS)**	**G2-M Transition (with DDS)**
Effective Sub-Systems	G1-S checkpoint Signalling, Growth Factor signalling	G1-S checkpoint Signalling, Growth Factor signalling, DNA damage signalling	G1-S checkpoint signalling, G2-M checkpoint signalling, Growth Factor signalling	G1-S checkpoint signalling, G2-M checkpoint signalling, Growth Factor signalling, DNA damage signalling
Effective Modules	Cdk4-Related, E2F-pRb, Tyrosine Phosphatase, Cdk2-Related, Growth Factor signalling	Cdk4-Related, E2F-pRb, Tyrosine Phosphatase, Cdk2-Related, Growth Factor signalling, *Chk-Related DNA damage signalling, p53-Related DNA damage signalling*	Cdk4-Related, E2F-pRb, Tyrosine Phosphatase (in G1-S sub-system), Cdk2-Related, Growth Factor signalling, Cdk1-Related, Tyrosine Phosphatase (in G2-M sub-system)	Cdk4-Related, E2F-pRb, Tyrosine Phosphatase (in G1-S sub-system), Cdk2-Related, Growth Factor signalling, Cdk1-Related, Tyrosine Phosphatase (in G2-M sub-system), *Chk-Related DNA damage signalling, p53-Related DNA damage signalling*
Effective Parameters (In order of Significance)	k_{40} [-0.624], k_{64} [+0.512], k_{49} [+0.420], k_{60} [-0.322], k_{50} [-0.289], k_{52} [+0.239], k_{98} [-0.191], k_{88} [-0.169], k_{101} [-0.160], k_{70} [-0.139], k_{48} [-0.138], k_{2} [-0.126], k_{83} [+0.095], k_{100} [+0.073]	k_{40} [-0.582], k_{64} [+0.471], k_{49} [+0.375], k_{60} [-0.328], k_{50} [-0.255], k_{52} [+0.241], k_{88} [-0.204], k_{98} [-0.181], k_{101} [-0.169], k_{70} [-0.151], k_{48} [-0.145], k_{83} [+0.140], k_{2} [-0.138], k_{100} [+0.114] k_{6} [-0.112], k_{31} [-0.111],	k_{40} [-0.567], k_{64} [+0.443], k_{49} [+0.360], k_{60} [-0.280], k_{50} [-0.271], k_{52} [+0.197], k_{98} [-0.177], k_{76} [-0.170], k_{93} [-0.167], k_{134} [-0.166], k_{109} [-0.165], k_{96} [-0.161], k_{123} [-0.159], k_{101} [-0.156], k_{88} [-0.147], k_{70} [-0.129],	k_{40} [-0.540], k_{64} [+0.412], k_{49} [+0.327], k_{60} [-0.292], k_{50} [-0.258], k_{52} [+0.232], k_{98} [-0.181], k_{76} [-0.180], k_{93} [-0.167], k_{101} [-0.165], k_{88} [-0.164], k_{70} [-0.145], k_{109} [-0.141], k_{134} [-0.137], k_{96} [-0.134], k_{123} [-0.129],

		k_{26} [+0.092], k_{22} [+0.091], k_5 [+0.063], k_9 [+0.061], k_{99} [+0.059], k_{11} [-0.055], k_{14} [-0.052], k_{17} [+0.051]	k_{48} [-0.127], k_2 [-0.114], k_{80} [-0.089], k_{112} [-0.071] k_{100} [+0.059], k_{127} [-0.059]	k_6 [-0.123] k_{48} [-0.111], k_5 [+0.107] k_2 [-0.102], k_{100} [+0.085], k_{80} [-0.081], k_{83} [+0.076], k_9 [+0.075], k_{31} [-0.074], k_{22} [+0.072] k_{26} [+0.061]

For comparison, we also conducted the same GSA analysis on Iwamoto et al. (2011) model and found that the significant parameters in that model are mostly the same as ours, with the exception that in our model the parameters related to the two newly added elements c-Myc and PP1 - $\boldsymbol{k_{40}}$ (synthesis rate of Cyclin D through transcription factor c-Myc) and $\boldsymbol{k_{64}}$ (rate of dephosphorylation of pRbPPP to pRb through PP1) - have become the most significant. These parameters are missing in Iwamoto et al. (2011) model. The list of significant parameters from their model is provided in Appendix E.

4.4 Summary

In this chapter, we performed Global Sensitivity Analysis (GSA) as a numerical analysis on the comprehensive mathematical model (proposed in the previous chapter) to find the most influential parameters and functional sub-systems on G1-S and G2-M transitions. To do this, we chose the biological indicators for checkpoints (G1-S and G2-M sub-systems) and then developed a Global Sensitivity Analysis model called SOMCCA to identify the kinetic parameters with the largest effect on the indicators. The analysis results showed that Growth Factor and G1-S signalling sub-systems have impact on G1-S and G2-M transitions in all (with or without DNA damage) conditions. In fact, the two most significant parameters of the system correspond to two newly added elements in our model that shows the importance of newly added proteins for cell cycle modelling. The first element is transcription factor c-Myc and its corresponding parameter is $\boldsymbol{k_{40}}$ (a parameter in the Growth Factor signalling sub-system) which is related to synthesis rate of Cyclin D through c-Myc. The second significant element is phosphatase PP1 whose related parameter is $\boldsymbol{k_{64}}$ (a parameter in the G1-S checkpoint sub-system) which corresponds to the effect of PP1 on pRb (i.e., dephosphorylation rate of pRbPPP into Rb by PP1). The other significant parameters in the G1-S checkpoint sub-system are: $\boldsymbol{k_{49}}$ (a parameter in Cdk4-Related module) which is related to synthesis rate of p27 that inhibits Cyc-Cdk cell cycle controllers), $\boldsymbol{k_{60}}$ (a parameter in E2F-pRb module) which is related to dissociation rate of E2F_pRbPP complex through aCycE_Cdk2 to release E2F), $\boldsymbol{k_{50}}$ (a parameter in Cdk2-Related module) which is related to dissociation rate of p27_aCycE_Cdk2 complex to release the cell cycle

controller), $\boldsymbol{k_{52}}$ (a parameter in Cdk4-Related module) which is related to association rate of p27 and aCycE_Cdk2), $\boldsymbol{k_{98}}$ (a parameter in Tyrosine Phosphatase module) which is related to activation rate of iCdc25A through E2F to activate cell cycle controllers. Accordingly, half of these parameters are related to p27 (the main Cdk inhibitor) indicating the crucial role it plays in cell cycle. This is in agreement with the current hypothesis that the release of p27 from Cyc-Cdk complexes triggers cell cycle phase transition (Chu et al., 2008). Results also indicate the importance of initial triggering of cell cycle (through Growth Factor signalling), production of two main cell cycle controllers (through E2F) and activation of these controllers (through Tyrosine Phosphatase).

Chapter 5

Efficiency of Cell Cycle Checkpoints in Detecting Damaged Cells

In this chapter, we probe deeply into the relationship between DNA damage and cell cycle progression and test the biological evidence that G1-S checkpoint is relatively inefficient in arresting damaged cells compared to G2-M checkpoint using the comprehensive mathematical model presented in Chapter 3. To study the relative efficiency of DNA damage checkpoints, a Checkpoint Efficiency Evaluation (CEE) model is developed based on perturbation studies and statistical Type II error. In the first section of this chapter, an overview of the chapter is presented. The CEE model is presented in the second section of the chapter. Section 5.3 is devoted to the checkpoint efficiency based on the number of damaged cells passing G1-S and G2-M checkpoints as normal cells. Section 5.4 presents the checkpoint efficiency based on the number of healthy cells getting sacrificed as damaged cells at G1-S and G2-M checkpoints. Finally, a summary of the chapter is presented in Section 5.5.

5.1 Overview

Since it has been reported that G1-S checkpoint does not always perform efficiently in detecting damaged cells under DNA damage conditions (Beishline & Azizkhan-Clifford, 2014; Di Leonardo et al., 1994), we conduct a comparative study of the efficiency of G1-S and G2-M checkpoints in their response to DNA damage through a proposed Checkpoint Efficiency Evaluation (CEE) model. The CEE model is applied to the comprehensive mathematical model presented in Chapter 3 under two different scenarios. The first one is regarding the number of damaged cells that pass each of the G1-S and G2-M checkpoints as normal cells under DNA damage and different perturbation levels. The second scenario is related to the number of healthy cells that get sacrificed as damaged cells at G1-S and G2-M checkpoints for different perturbation levels. The results demonstrate that G2-M checkpoint is more efficient than G1-S in correctly identifying damaged cells. Moreover, both checkpoints are near perfect in passing healthy cells. Biological findings have shown that cancer cells relay more on G2-M checkpoint in order to repair their excess DNA damage and avoid Apoptosis as their G1-S checkpoint is usually deficient which causes accumulation of mutations (Bucher & Britten, 2008; Chen et al., 2012). Therefore, having a model that can represent the behaviour of checkpoints is beneficial for targeted cancer therapies. New hypotheses can be formulated by scientists to test in their lab, such as knocking out G2-M proteins in order to push cancer cells into unscheduled M-phase which leads to Apoptosis through mitotic catastrophe.

5.2 Checkpoint Efficiency Evaluation Model

As the scientific aim of systems biology is not only to develop precise and detailed models but also to understand the underlying structural and fundamental principles of biological systems, it is important to gain deep insights into principles that govern the behaviour of complex systems (Kitano, 2007). One of the less investigated aspects of cell cycle checkpoints is the comparison of the efficiency of checkpoints in the presence of DNA damage. It has been reported that G1-S checkpoint is relatively inefficient compared to G2-M checkpoint in detecting damaged cells (Beishline & Azizkhan-Clifford, 2014; Di Leonardo et al., 1994) and therefore, for the first time in cell cycle modelling (to the best of our knowledge), we develop a model to investigate the efficiency of checkpoints in capturing damaged cells under DNA damage condition. We also test the efficiency of checkpoints in correctly identifying healthy cells. We call the model Checkpoint Efficiency Evaluation (CEE) model (demonstrated in Figure 5.1).

As shown in Figure 5.1, the most significant parameters extracted through SOMCCA are identified (Step 1) and then perturbed simultaneously in order to simulate real situations that cells may confront (within five ranges of $\pm 5\%, \pm 10\%, \pm 15\%, \pm 20\%$ and $\pm 30\%$) and sampled 2000 times for each level of perturbation (Step 2). Then, 2000 PTs are calculated for each indicator (Step 3) and the Probability Density Function (PDF) of PTs is estimated by normal distribution (Step 4). The procedure is repeated for DNA damage condition and the PDF of PTs of the indicators in the presence of DNA damage is obtained. Then, using Type II Error with significance level of 10% (Type II Error is the probability of accepting a null hypothesis while it is not true (Weiers, 2010)), the damaged cells passing each checkpoint as healthy/normal cells are labelled to calculate the efficiency of checkpoints in detecting damaged cells passing each checkpoint as healthy cells (Step 5). The efficiency of checkpoints in correctly detecting damaged cells is calculated using the number of correctly identified damaged cells and the total number of damaged cells (the formula is shown in the last step in Figure 5.1). This idea of identifying damaged cells from normal cells is depicted in Figure 5.2 for a hypothetical case where five damaged cells pass G1-S checkpoint as normal cells, while four out five cells are captured correctly at G2-M checkpoint. Using the CEE model, it is also possible to calculate the efficiency of each checkpoint in not arresting healthy cells. To do that, in step 5 of the CEE model, the healthy cells arrested at each checkpoint as damaged cells are labelled. Then, in step 6, the efficiency of checkpoints in correctly letting the healthy cells pass each checkpoint is calculated using the number of identified healthy cells (those healthy cells correctly classified as healthy by the checkpoint) and the total number of healthy cells.

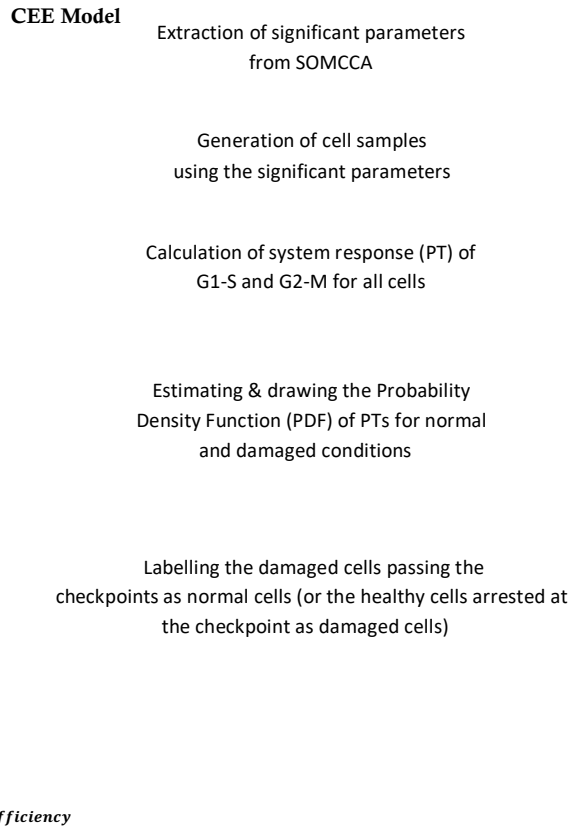

Figure 5.1 Diagram of the Checkpoint Efficiency Evaluation (CEE) Model. The CEE model evaluates the performance of checkpoints in correctly identifying cells. Using the significant parameters identified through SOMCCA model, the CEE generates a cell population (by perturbing the significant parameters within a particular range) for both normal (healthy) and damage conditions and then calculates PTs of G1-S and G2-M checkpoint indicators for all the cells in the population. Then it draws the probability Density Function (PDF) of PTs for normal and damaged conditions for each checkpoint and labels the damaged cells passing each checkpoint as healthy cells (to calculate the efficiency of checkpoints in correctly identifying/arresting the damaged cells) or alternatively labels the healthy cells arrested as damaged at checkpoints (to calculate the efficiency of checkpoints in correctly letting the healthy cells pass the checkpoints) based on Type II error. Finally, it calculates the efficiency of checkpoints in correctly arresting the damaged cells using the number of identified damaged cells (those damaged cells correctly classified as damaged by the checkpoint) and the total number of damaged cells. To calculate the efficiency of checkpoints in correctly letting the healthy cells pass checkpoints, the number of identified healthy cells (those healthy cells correctly classified as healthy by the checkpoint) and the total number of healthy cells are used.

Figure 5.2 **A hypothetical example of PDF of PT of Normal and Damaged cells for G1-S (left figure) and G2-M (right figure) checkpoints showing how Type II Error is used to estimate the checkpoint efficiency. The figure shows a hypothetical case of a number of damaged cells (red dots) that pass each checkpoint as normal cells (the vertical line shows the significance level, 10%). In this example, G1-S checkpoint could not identify five damaged cells while G2-M checkpoint identified all but 1 of those damaged cells that escape G1-S. In this hypothetical case, G2-M checkpoint performs better than G1-S in detecting damaged cells. The concept of healthy cells arrested at each checkpoint as damaged cells can be shown with a similar example but in the opposite direction.**

5.3 Checkpoint Efficiency Based on the Number of Damaged Cells Passing Checkpoints as Healthy Cells

The simulation results for the efficiency of G1-S and G2-M checkpoints under DNA damage and different perturbation ranges are presented in Table 5.1. For this analysis, PDFs of PTs for normal and damaged cells for both G1-S and G2-M checkpoints similar to those in Figure 5.2 were developed. From these two tests, we first assessed the number of damaged cells that escaped the two checkpoints. Then, the damaged cells (i.e., the corresponding parameter vectors) that escaped G2-M checkpoint were compared with those passing G1-S to determine the proportion of the latter that also escapes G2-M. For clarity, we only show the number of cells passing G1-S and the portion of these cells that also escapes G2-M.

As demonstrated in Table 5.1, G2-M checkpoint is capable of identifying and arresting a greater percentage of damaged cells than G1-S. For example, under ±5% perturbation, 543 out of 2000 damaged cells pass G1-S checkpoint as healthy cells and then only 78 out of these 543 damaged cells are not caught at G2-M checkpoint. Therefore, the efficiency of G1-S is $\frac{2000-543}{2000} = 72.85\%$, while the efficiency of G2-M is $\frac{543-78}{543} = 85.63\%$ (the efficiency of G2-M is higher than that of G1-S). The rate at which damage cells pass the combined checkpoint system as healthy cells is 3.9% (78/2000) (False Negative rate) making the whole system efficiency $\frac{2000-78}{2000} = 96.1\%$ (True Positive rate).

Table 5.1 **Efficiency of checkpoints based on the number of damaged cells that pass each of the G1-S and G2-M checkpoints as normal cells under DNA damage and different perturbation levels (the total number of damaged cells is 2000). [For example, for ±5% perturbation, the number of damaged cells passing G1-S as healthy is shown in the second column (i.e., 543 out of 2000); the number of these damaged cells that are not caught at G2-M is in the fourth column (i.e., 78 out of 543); therefore, the efficiency of G1-S and G2-M are $\frac{2000-543}{2000} = 72.85\%$ and $\frac{543-78}{543} = 85.63\%$, respectively. The combined checkpoint efficiency is $\frac{2000-78}{2000} = 96.1\%$].**

Perturbation Range	*Damaged Cells Passing G1-S as Normal*	*G1-S Efficiency (%)*	*Portion of G1-S Escaped Damaged Cells Passing G2-M as Normal*	*G2-M Efficiency in Capturing Damaged Cells Escaping G1-S (%)*	*Combined-Checkpoint System Efficiency (%)*
±5%	543	72.85	78	85.63	96.1
±10%	1270	36.5	741	41.65	62.95
±15%	1478	26.1	1049	29.02	47.55
±20%	1586	20.7	1208	23.83	39.6
±30%	1694	15.3	1427	15.76	28.65

5.4 Checkpoint Efficiency Based on the Number of Healthy Cells Getting Sacrificed as Damaged Cells

While it is more important for damaged cells to be stopped at checkpoints, it is not beneficial to sacrifice too many healthy cells. Therefore, we also conducted another analysis to study checkpoint efficiency in correctly recognising healthy cells. Here, we allowed 2000 healthy cells to go through the checkpoints and counted the number of healthy cells incorrectly identified as damaged and arrested at checkpoints. The results are provided in Table 5.2 which shows that both checkpoints are highly efficient and near perfect in recognising healthy cells at ±5% perturbation (99.15% for G1-S and 99.49% for G2-M). As the perturbation level increases, both checkpoints drop in efficiency in recognising healthy cells but G2-M not only remains more efficient but also is more robust against sacrificing healthy cells.

Table 5.2 **Efficiency of checkpoint based on the number of healthy cells that get sacrificed as damaged cells at G1-S and G2-M checkpoints for different perturbation levels (the total number of healthy cells is 2000). [For example, for ± 5% perturbation, the number of healthy cells incorrectly identified and arrested at G1-S is shown in the second column (i.e., 17 out of 2000 are sacrificed); the number of incorrectly arrested cells at G2-M is shown in the 4th column (i.e., 2000-17=1983 healthy cells go to G2-M checkpoint and just 10 cells (10 out of 1983) get incorrectly arrested as damaged). Therefore, the efficiency of G1-S and G2-M is $\frac{2000-17}{2000} = 99.15\%$ and $\frac{1983-10}{1983} = 99.49\%$, respectively. The combined checkpoint efficiency in releasing healthy cells is $\frac{2000-(10+17)}{2000} = 98.65\%$].**

Perturbation Range	*Healthy Cells Arrested at G1-S as Damaged*	*G1-S Efficiency (%)*	*Portion of G1-S Released Healthy Cells Arrested at G2-M as Damaged*	*G2-M Efficiency in Releasing Healthy Cells that Pass G1-S (%)*	*Combined Checkpoint Efficiency in Releasing Healthy Cells (%)*
±5%	17	99.15	10	99.49	98.65
±10%	601	69.95	185	86.77	60.7
±15%	1064	46.8	372	60.25	28.2
±20%	1329	33.55	358	46.64	15.65
±30%	1706	14.7	213	27.55	4.05

5.5 **Summary**

we conducted numerical and statistical analyses to assess the relative efficiency of checkpoints in arresting damaged cells as some biological findings indicate that G1-S is less efficient than G2-M checkpoint. In this regard, the checkpoint efficiency analysis model called CEE model was developed to determine the efficiency of the two cell cycle checkpoints in arresting damaged cells. Using this model, we were able to quantify the number of damaged cells that passed each checkpoint as healthy. The simulation results showed that in the presence of DNA damage and under different parameter perturbations, the efficiency of G2-M checkpoint was always higher than that of G1-S. We also analysed the potential of the two checkpoints to sacrifice normal cells as damaged and the results revealed that they are highly efficient in correctly recognising normal cells. The simulation results under ±5% parameter perturbation showed that cell cycle is about 96% efficient in arresting damaged cells with G2-M checkpoint being more efficient than G1-S. Further, both checkpoint systems are near perfect (98.6%) in passing healthy cells (under ±5% parameter perturbation).

Therefore, this study has shown the efficacy of the proposed systems approach to gain a better understanding of different aspects of mammalian cell cycle system separately and as an integrated system that will open new doors for further experiments and also be useful in investigating targeted therapy in future cancer treatments.

Chapter 6

Towards Abstraction of Computational Modelling of Mammalian Cell Cycle: A Petri Net Approach

In this chapter, an abstract Petri Net-based model of the mammalian cell cycle is developed which is extracted from the comprehensive mathematical model presented in Chapter 3. Therefore, a model with 61 ODEs and 148 parameters is downsized to just four equations and 31 parameters. An overview of the chapter is presented in Section 6.1. The details of the most significant components used in the abstract model are presented in Section 6.2. Section 6.3 is devoted to the abstract model development through Petri Nets (in this section, the key elements of the model are described in Sub-section 6.3.1. The next three sub-sections are devoted to High-level, Stage-level, and Low-level views of Multi-Level Hybrid Petri Net (MLHPN) model, respectively). In Section 6.4, the kinetics of the model are presented. The model Results are presented in Section 6.5 and the analysis of Checkpoint Efficiency Evaluation (CEE) on the MLHPN model is given in Section 6.6. Finally, a summary of the chapter is presented in Section 6.7.

6.1 Overview

In Chapter 3, we proposed a comprehensive mathematical model of mammalian cell cycle control system and showed that the dynamical behaviour of the model is consistent with biological findings. Now, it is of interest to develop an abstract/minimised model of mammalian cell cycle in a way that the main characteristics (dynamics of the previously identified key players) and system response (G1-S and G2-M transitions as well as response to DNA damage) remain intact. To do this, in this chapter, we propose a novel abstract systems approach to modelling mammalian cell cycle to gain deep insights into how it coordinates such an intricate system of interactions in a robust and timely manner. It involves incorporation of the most essential controllers of mammalian cell cycle (as primary elements) and regulators of these controllers (as secondary elements) at different levels of abstraction. Furthermore, the concept of cell cycle sub-systems is incorporated in this model same as the one introduced in Chapter 3 for the comprehensive model where cell cycle system was presented through four inter-connecting sub-systems (Growth Factor signalling, G1-S and G2-M checkpoints, and DNA damage signalling).

The MLHPN model, which is a graphical Petri Net-based model, is proposed to model the mammalian cell cycle regulation system. Intuitive nature of the MLHPN makes it possible to present biological properties and processes with different time scales through a combination of continuous and discrete paradigms at different levels of abstraction. The goal is to gain a deep understanding of the

mechanism of mammalian cell cycle regulation in the presence of Growth Factor with and without DNA damage. The MLHPN model has just four equations and 31 parameters while the comprehensive mathematical model presented in Chapter 3 had 61 ODEs and 148 parameters. Further analysis is done on the MLHPN using Checkpoint Efficiency Evaluation (CEE) model to investigate the efficiency of checkpoints based on detecting either damaged cells incorrectly passing checkpoints as healthy cells or healthy cells incorrectly arrested at checkpoints as damaged cells. The results of the CEE analysis on the MLHPN model is consistent with those of the comprehensive mathematical model presented in Chapter 5.

6.2 Identification of the Most Significant Components

The first step towards model abstraction is to identify the core components with the highest impact on system response (G1-S and G2-M transitions). In Chapter 4, we identified the most effective parameters using the "Self-Organizing Map with Correlation Coefficient Analysis" (SOMCCA) model. Therefore, it is possible to identify the most significant components in the cell cycle system. These components are presented in Table 6.1 categorised based on the component type and sub-system.

Table 6.1 The most significant components of mammalian cell cycle based on component type and corresponding sub-system.

Components	Component Type	Sub-System
c-Myc	*Transcription Factor*	*Growth Factor signalling*
E2F		*G1-S signalling*
NFY		*G1-S & G2-M signalling*
p53		*DNA damage signalling*
CycD_Cdk4	*Cyc_Cdks*	*G1-S signalling*
CycE_Cdk2		*G1-S signalling*
CycA_Cdk2		*G1-S signalling*
CycB_Cdk1		*G2-M signalling*
p27	*Cyclin-Dependent Kinase Inhibitor*	*G1-S signalling*
p21		*DNA damage signalling*

Cdc25A	*Tyrosine Phosphatase*	*G1-S signalling*
Cdc25C		*G2-M signalling*
SCF	*Ubiquitin Ligase*	*G1-S signalling*
APC_Cdc20		*G2-M signalling*
APC_Cdh1		*G2-M signalling*
Chk2	*Kinase*	*DNA damage signalling*

The components in Table 6.1 mainly correspond to production and degradation of Cyc_Cdks which have been known as key players of mammalian cell cycle control system (Berridge, 2014; Malumbres & Barbacid, 2009; Morgan, 1997; Ruddon, 2007; Satyanarayana & Kaldis, 2009). In fact, it is periodic synthesis and degradation of cyclins that regulates activity of Cdks in a timely manner (Malumbres & Barbacid, 2009). Therefore, whenever we talk about the effect of cyclins on other species here in this chapter, we mean the effect of Cyc_Cdk complexes. It should be noted that although PP1 was identified as one of the significant components of the comprehensive model in Chapter 3, since it doesn't have a direct effect on Cyc_Cdks and it mainly affects E2F through pRb (and we already have E2F in the abstract model which represents the transcription factor E2F together with the total effect of all the absent elements on E2F), it is not included in the abstract model. Having the most significant players of the system, we develop a schematic of the abstract model (Figure 6.1). As shown in Figure 6.1, at the beginning of cell cycle, transcription factor c-Myc becomes activated (within Growth Factor signalling sub-system following the presence of Growth Factor) which eventually stimulates the synthesis of Cyclin D (Adhikary & Eilers, 2005; Alberts et al., 2014; Morgan, 2007). Initiation of CycD_Cdk4 production is an indication of G0-G1 transition (START) and cell cycle initiation (Adhikary & Eilers, 2005). CycD_Cdk4, in turn, stimulates production of Cyclin E (next cyclin in the series of cyclins) through activation of transcription factor E2F (Ji & Dyson, 2010). Tyrosine phosphatase Cdc25A is also necessary for activation of CycE_Cdk2 (and CycA_Cdk2) that eventually results in G1-S transition (Boutros et al., 2007; Donzelli & Draetta, 2003; Karlsson-Rosenthal & Millar, 2006; Kristjansdottir & Rudolph, 2004). These active Cyc_Cdks lead to phosphorylation and SCF-mediated degradation of p27 (Chu et al., 2008).

Transcription factor E2F also induces synthesis of next Cyclin, Cyclin A. Another transcription factor NFY also triggers the synthesis of Cyclin A and Cyclin B (Chae & Shin, 2011). Cyclin B has a key role at

G2-M transition as well as during M phase where its degradation through two ubiquitin ligases (APC_Cdc20 and APC_Cdh1) triggers the M-G1 transition event ("END" of one cell cycle). It is important to note that SCF ubiquitin ligase degrades Cyclin D and Cyclin E, while APC ubiquitin ligases degrade all cyclins excluding Cyclin E (Nakayama & Nakayama, 2005; Peters, 2002). In the case of DNA damage (Double-Strand Breaks (DSBs)), the key controllers of DNA damage signalling (p53, p21, and Chk2) trigger cell cycle arrest through their interactions with different Cyc_Cdks (Beishline & Azizkhan-Clifford, 2014; Meek, 2004; Morgan, 2007; Nyberg et al., 2002; Sancar et al., 2004).

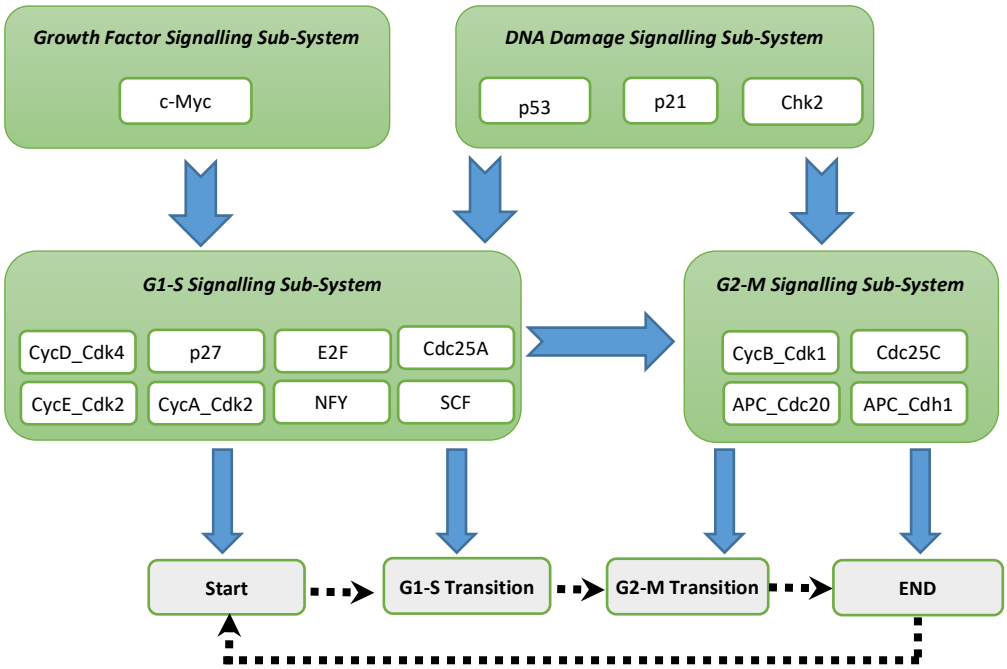

Figure 6.1 A schematic of the most significant components of mammalian cell cycle categorized under different sub-systems, and corresponding effects on ordered sequence of cell cycle transitions.

6.3 Abstract Cell Cycle Model Development: A Petri Net Approach

We develop an abstract model based on the most significant identified components under different cell cycle sub-systems (the Growth Factor, G1-S, G2-M checkpoints, and DNA damage sub-systems). Since synthesis and degradation of cyclins are slow reactions but activation and inactivation of regulators of cyclins (transcription factors, ubiquitin ligases and Tyrosine Phosphatases) are by far faster, a hybrid modelling approach will be implemented. In this hybrid paradigm, we incorporate deterministic continuous (for slow reactions, such as synthesis/degradation of Cyc_Cdks) and discrete (for fast biochemical reactions, such as activation/inactivation) modelling schemes. We adopt Petri Net (PN) modelling approach to present this hybrid modelling in the most intuitive way.

Moreover, to further extend our hybrid PN in terms of granularity, a multi-level extension is implemented and added to hybrid PN scheme. Thus, this Multi-Level Hybrid Petri Net (MLHPN) model is able to describe the whole mammalian cell cycle control system in an abstract intuitive yet comprehensive manner at three different levels of abstraction (High, Low, and Stage-levels). At High-level of abstraction, the focus is on Cyc_Cdks as main controllers of the system. At Low-level, the regulators of cyclins are investigated. And the focus of Stage-level is on transition between different cell cycle stages/phases and the corresponding impact of Cyc_Cdks on them.

6.3.1 Key Elements of the MLHPN Model

Over the recent years, PN-based modelling started to be implemented for modelling biological networks and cell cycle, in particular (Fujita et al., 2004; Gilbert & Heiner, 2006; Grunwald et al., 2008; Hardy & Robillard, 2004; Herajy & Heiner, 2012; Herajy et al., 2013; Liu et al., 2012; Matsui et al., 2004; Matsuno et al., 2003; Mura & Csikász-Nagy, 2008; Windhager & Zimmer, 2008). Among all these models, Hybrid Petri Net has been more promising due to its ability to represent different time-scales which suits the nature of cell cycle system. As a Petri Net-based model, the MLHPN comprises four key elements: Places, Transitions, Arcs, and Marking (shown in Table 6.2). Places represent species (such as proteins), while transitions indicate biochemical reactions. Arcs, on the other hand, denote the type of interaction between species and carry numbers (thresholds) that correspond to stoichiometric coefficients. Marking is used to represent the value of places. If a place is discrete, the marking is in the form of tokens, whereas, the marking for a continuous place is expressed as a real number. A list of elements utilized in the MLHPN model is shown in Table 6.2.

Table 6.2 Elements used in the proposed model.

Places	Transitions		Arcs	Marking	
Discrete:	Discrete Delayed:	<D>	Standard:	Discrete (tokens):	
Continuous:	Continuous:		Read:	Continuous	Real
Macro:	Macro:				
Logical:	Logical:		Inhibitor:		

Discrete Delayed transitions are fired after a pre-defined delay if the markings of their pre-places (the places that enter into a transition) are more than the corresponding arcs' thresholds. However, continuous transitions are fired continuously as long as the marking of their pre-places is non-zero. Macro elements are used for multi-level presentation of the system. The main feature of macro

elements is that they appear at High-level of abstraction, while the elements inside them appear at Low-level. Generally, a macro place represents a place-bounded set of elements, whereas a macro transition signifies a set of transition-bounded elements. Logical elements are also utilised to represent a particular node (place or transition) in different reactions in a model and they are represented in grey colour (see Table 6.2). Standard arcs denote regular biochemical reactions with corresponding stoichiometric coefficients. Read arcs are used to represent reactions in which the marking is not consumed, such as enzymatic reactions, and a transition with an inhibitory arc can take place only if the marking of the corresponding pre-place is less than the arc's threshold (Blätke et al., 2011). For a more detailed description of Petri Nets, the reader is referred to the book written by (Koch et al., 2010). It should be noted that the rules for firing transitions, thresholds of arcs and transition delays are intuitively perceived from the model figures throughout this chapter. Furthermore, the values of the model parameters, the initial values of places and the definition of transitions (together with firing rule for each transition) are provided in Appendices F, G, and H, respectively (in Tables F. 1, G. 1 and H.1, respectively). In the next three sub-sections, we explain the details of three different levels of abstraction.

6.3.2 High-level of Abstraction

The High-level view of the MLHPN presents a big picture of the model in which the control system is based on an ordered sequence of synthesis and degradation of Cyc_Cdks (Figure 6.2 - the details of the elements inside each macro elements are presented in Section 6.3.4). As shown in Figure 6.2, following the presence of Growth Factor, first, the Growth Factor sub-system comes to the picture where G0_G1_Activation macro transition (this macro transition centres around G0_G1_TF which refers to transcription factor c-Myc) triggers the production of CycD_Cdk4 through continuous transition T1 (see details in Figure 6.4). Then, as a part of G1-S sub-system, CycD_Cdk4 interacts with a macro transition called G1_S_TF_Activation (mainly associated with G1_S_TF, transcription factor E2F). This macro transition, in turn, stimulates the synthesis of CycE_Cdk2 and CycA_Cdk2. Then, G2-M sub-system comes to the picture where CycA_Cdk2 interacts with the last macro transition, G2_M_TF_Activation (this macro transition centres around G2_M_TF which refers to transcription factors NFY and b-Myb), which encompasses a set of elements that results in synthesis of CycB_Cdk1 & CycA_Cdk2 itself. The degradation of Cyc_Cdks, on the other hand, is mediated through macro places UBQ_D, UBQ_E, UBQ_A and UBQ_B where these macro places are associated with a set of elements mediating the degradation of CycD_Cdk4, CycE_Cdk2, CycA_Cdk2 and CycB_Cdk1, respectively, throughout the cell cycle (Figure 6.2).

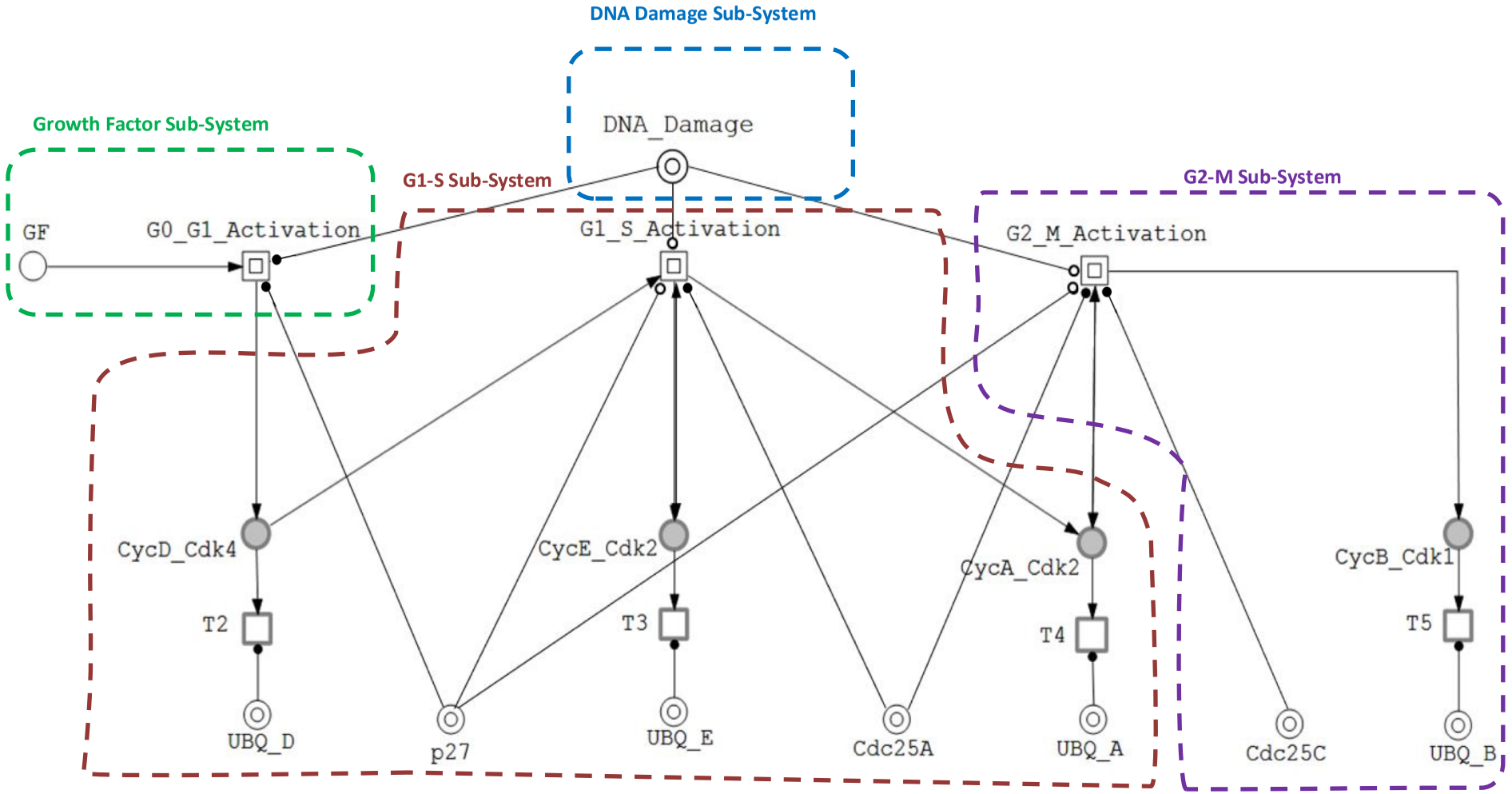

Figure 6.2 High-level view of the MLHPN model. For all Cyc_Cdks, the active form is considered.

As shown in Figure 6.2, The relationship between p27 and CycD_Cdk4, CycE_Cdk2 and CycA_Cdk2 has been presented through p27 macro place where its effect on CycD_Cdk4 is activation (by an activating effect on G1_S_Activation macro transition) while the corresponding effect on CycE_Cdk2 and CycA_Cdk2 is towards inhibiting their activation (through inhibiting G1_S_Activation macro transition). Furthermore, as shown in Figure 6.2, Cdc25A macro place represents the positive impact of Cdc25A on activation of CycE_Cdk2 and CycA_Cdk2 while Cdc25C macro place demonstrates the positive effect of Cdc25C on activation of CycB_Cdk1. Thus, these two macro places have crucial effect on G1-S and G2-M transitions that will be explained in detail in Section 6.3.4. Another crucial sub-system shown in Figure 6.2 is DNA damage which comprises a macro place called DNA_Damage. This macro place includes the key controllers of DNA damage signalling, such as p53, p21 and Chk2. The effect of this macro place on three other sub-systems is as follows: it has positive effect on Growth Factor sub-system because p21 can eventually activate CycD_Cdk4; on the other hand, the effect of this macro place on G1-S and G2-M sub-systems is inhibitory where the DNA damage controllers directly/indirectly suppress the activity of CycE_Cdk2, CycA_Cdk2, and CycB_Cdk1.

6.3.3 Stage-level of Abstraction (Temporal Progression)

At the stage-level, the different stages (and sub-stages) of mammalian cell cycle and the corresponding impact of different Cyc_Cdks on temporal progression of cell cycle are modelled. The important stages in mammalian cell cycle (Early_G1, Mid_G1, Late_G1, S, G2, Late_G2, Prophase, Metaphase, Anaphase, and Telophase) are modelled as discrete places (as shown in Figure 6.3). The transition between stages is either controlled by the level of Cyc_Cdks or takes place after a specific delay. Some details, such as duration of phases and sub-phases, are adopted from an article published by Singhania et al. (2011) in which flow cytometry data of cyclin levels have been utilised for model development.

First, the system is assumed to be in stationary stage G0 which we call Early_G1. Then following the presence of Growth Factor (GF), Sensing_GF transition is fired and the state of the system is changed to Mid_G1 (Figure 6.3). In this stage, G0_G1_TF (mainly corresponds to transcription factor c-Myc) becomes activated and induces the synthesis of Cyclin D, which eventually leads to an increase in concentration of CycD_Cdk4. When the level of CycD_Cdk4 passes a threshold, G1_S_TF (mainly associated with transcription factor E2F) becomes activated and stimulates synthesis of some target proteins including Cyclin E & Cyclin A (this is represented by R_Point transition). The increase in the level of CycE_Cdk2 and CycA_Cdk2 sets the stage for beginning of DNA replication process. Hence, the level of CycE_Cdk2 is an indicator of transition from G1 to S which alters the system state from Late_G1 to S (Figure 6.3).

Figure 6.3 **Stage-level view of the MLHPN model. It is assumed that at the beginning, the system is in G0 or Early_G1 state. The black squares demonstrate discrete transitions while the circles represent discrete/continuous places. For example, the cell cycle state switches from Late_G1 phase (modelled by a discrete place) to S phase (also modelled as a discrete place) through discrete transition G1_S when the level of continuous place CycE_Cdk2 is more than a threshold (8.5 simulation time units). The grey elements (places/transitions) are logical elements which may appear somewhere else in the model (it may be at the same level or at another level of abstraction). The weights for the arcs whose weight value is not equal to one are shown in the figure. For instance, the time it takes for the cell cycle to perform DNA replication (which happens during S phase) is assumed to be seven hours shown under S_G2 discrete transition in the figure.**

DNA replication happens during S phase and it is assumed that this process takes around seven hours Singhania et al. (2011). Afterwards, S_G2 transition is fired and system state changes from S to G2. CycA_Cdk2 triggers the activation of G2_M_TF (transcription factors NFY and b-Myb) whose activation stimulates further synthesis of CycA_Cdk2 as well as synthesis of CycB_Cdk1. The next transition is G2_M transition whose firing is controlled by CycB_Cdk1. It is important to emphasize that the transitions between M phase events (Prophase, Metaphase, Anaphase, and Telophase) occur according to some pre-defined delays adopted from Singhania et al. (2011). As seen in Figure 6.3, The effect of CycB_Cdk1 on G2_M transition is mediated through a read arc because this

transition is fired if the level of CycB_Cdk1 becomes higher than a threshold (5.6 simulation time units). On the other hand, CycB_Cdk1 impacts the last cell cycle transition (M_G1) through an inhibitory arc as this transition takes place if the concentration of CycB_Cdk1 falls down below another threshold (0.15 simulation time units).

6.3.4 Low-level of Abstraction

At low-level of abstraction, the elements inside all macro places and transitions will be described in detail and categorised based on the sub-system they belong to. The first sub-system is Growth Factor sub-system which includes G0_G1_Activation macro transition (will be explained in Growth Factor Sub-System section). The second sub-system (G1-S checkpoint) comprises G1_S_Activation macro transition as well as p27, Cdc25A, UBQ_D, UBQ_E, and UBQ_A macro places (will be described in G1-S Sub-System section). The third sub-system is G2-M checkpoint which includes G2_M_Activation macro transition as well as Cdc25C, and UBQ_B macro places (will be presented in G2-M Sub-System section). The last sub-system is DNA damage which includes DNA damage macro place (will be described in DNA Damage Sub-System section). It should be noted that in the next sub-sections, continuous transitions are presented with capital letter (i.e. T1) while discrete transitions are shown with lower-case letters (i.e. t1_1).

Growth Factor Sub-System

As shown in Figure 6.4, the Growth Factor sub-system comprises one macro transition (G0_G1_Activation) whose constituting elements will be explained in this section.

Figure 6.4 Growth Factor Sub-System (inside dashed green rectangle) which includes GF as a discrete place and G0_G1_Activation macro transition. The connections between this sub-system and other cell cycle sub-systems have already been demonstrated in Figure 6.2.

G0_G1_Activation Macro Transition

As described in Chapter 3, the Growth Factor signalling pathway comprises MAPK signalling cascade that eventually results in activation of G0_G1_TF, which in turn induces the synthesis of Cyclin D and starts the cell cycle engine (Blain, 2008; Pardee, 1989). The first state of the system is that Growth Factor is available and G0_G1_TF is inactive (shown as iG0_G1_TF in Figure 6.5). G0_G1_Activation Macro Transition is the main part of Growth Factor signalling sub-system in the MLHPN model in which the existence of Growth Factor (GF), which is modelled as a discrete place, triggers the firing of discrete transition t1_1 (through a read arc) that leads to activation of G0_G1_TF. In other words, Growth Factor signal stimulates the activation of transcription factor required for cell cycle start. Then active G0_G1_TF (shown as aG0_G1_TF in Figure 6.5) induces the synthesis of Cyclin D through continuous transition T1. In the absence of GF, discrete transition t1_2 is fired (through an inhibitory arc) and G0_G1_TF becomes inactive again (Figure 6.5).

Figure 6.5 Elements of G0_G1_Activation macro transition as the main part of Growth Factor signalling sub-system. Active and inactive forms of transcription factor c-Myc are presented as aG0_G1_TF and iG0_G1_TF, respectively. At the beginning (initial state), Growth Factor (GF) is present and G0_G1_TF is inactive. Following the presence of GF, G0_G1_TF becomes active through discrete transition t1_1 and aG0_G1_TF, in turn, triggers the synthesis of CycD_Cdk4 through continuous transition T1. The absence of GF results in inactivation of G0_G1_TF through discrete transition t1_2.

G1_S Sub-System

As shown in Figure 6.6, the G1-S sub-system comprises one macro transition (G1_S_Activation), five macro places (UBQ_D, UBQ_E, UBQ_A, p27 and Cdc25A), three continuous places (CycD_Cdk4, CycE_Cdk2 and CycA_Cdk2) and three continuous transitions (T2, T3 and T4). The constituting elements of macro places/transitions will be explained in this section.

Figure 6.6 **G1-S Sub-System (inside dashed brown enclosure) which includes G1_S_Activation macro transition, five macro places (UBQ_D, UBQ_E, UBQ_A, p27 and Cdc25A), three continuous places (for CycD_Cdk4, CycE_Cdk2 and CycA_Cdk2) and three continues transitions associated with degradation of Cyc_Cdks. The connections between this sub-system and other cell cycle sub-systems have already been demonstrated in Figure 6.2.**

UBQ_D Macro Place

As a part of G1-S sub-system, UBQ_D macro place corresponds to the ubiquitination process of Cyclin D (CycD_Cdk4) through continuous transition T2 (as shown in Figure 6.7). As described in Chapter 3,

Figure 6.7 **Elements of UBQ_D macro place which is a part of G1-S sub-system. This macro place is mainly associated with degradation of Cyclin D (CycD_Cdk4) through different ubiquitin ligases.**

SCF and APC_Cdc20 are ubiquitin ligases that induce degradation of Cyclin D. Similar to the assumption made by Singhania et al. (2011), we distinguish between the activity of APC_Cdc20 towards Cyclin A (called APC_Cdc20A - active from late G2 until the end of cell cycle) and Cyclin B (called APC_Cdc20B – active throughout M phase). It is also assumed that both APC_Cdc20 types affect Cyclin D degradation.

G1_S_Activation Macro Transition

G1_S_Activation macro transition is one of the major parts of G1-S sub-system that centres around transcription factor E2F (here called G1_S_TF). At the beginning of cell cycle, G1_S_TF is inactive because a tumour suppressor protein, called Retinoblastoma protein (pRb – not shown in the abstract model) binds to it and inhibits its activation. At late G1, G1_S_TF is released from pRb and becomes activated through phosphorylation by CycD_Cdk4 and CycE_Cdk2 (Sherr & McCormick, 2002; Trimarchi & Lees, 2002). This process is presented through discrete transition t6_1 (Figure 6.8) where the weight values of CycD_Cdk4 and CycE_Cdk2 are 4.25 and 0.4, respectively (the weights are estimated so that the model dynamics are qualitatively similar to biological findings). Then active G1_S_TF (aG1_S_TF) triggers the production of CycE_Cdk2 and CycA_Cdk2 (Deckbar et al., 2011; Helin, 1998). This is modelled as continuous transitions T6 and T7, respectively. Finally, G1_S_TF becomes inactivated by CycA_Cdk2 (through discrete transition t6_2) when the level of CycA_Cdk2 passes a particular threshold (2.3 simulation time units) (Ji & Dyson, 2010). It should be noted that in all figures throughout this chapter, the weight values equal to one are not shown.

Figure 6.8 Elements of G1_S_Activation macro transition as a part of G1-S sub-system. Active and inactive G1_S_TF are demonstrated as aG1_S_TF and iG1_S_TF, respectively. The weight values for the arcs whose weight is other than one are shown in the figure.

p27 Macro Place

One of the parts of G1-S sub-system that has impact on the activity of Cyc_Cdks is p27 macro place which is mainly associated with Cyclin-Dependent Kinase Inhibitor p27. From the beginning of cell cycle, p27 is active (modelled through discrete transition t3_1 in Figure 6.9) and affects the activity of CycD_Cdk4, CycE_Cdk2, CycA_Cdk2 (Chu et al., 2008). Since in the abstract model Cyc_Cdks are presented as active components, the effect of p27 is modelled on production of these components. CycD_Cdk4 is further activated by p27 while CycE_Cdk2 and CycA_Cdk2 are inhibited following binding to p27 (the full description was presented in Chapter 3). The effect of p27 on CycD_Cdk4, CycE_Cdk2, and CycA_Cdk2 is modelled through continuous transitions T1, T6 and T7, respectively. When cell cycle enters Late_G1 phase, p27 becomes inactivated again (this is modelled through discrete transition t3_2) (Chu et al., 2008).

Figure 6.9 Elements of p27 macro place as a part of G1-S sub-system. Active and inactive p27 are shown as ap27 and ip27, respectively.

Cdc25A Macro Place

Cdc25A is a Tyrosine phosphatase which has a key role in activating CycE_Cdk2 and CycA_Cdk2 (Boutros et al., 2007; Kiyokawa & Ray, 2008; Kristjansdottir & Rudolph, 2004). The activation of these two Cyc_Cdks is modelled through continuous transitions T6 and T7 (as shown in Figure 6.10). Through positive feedback loops, CycE_Cdk2 and CycA_Cdk2 stimulate activation of Cdc25A at late G1 which is modelled through discrete transition t6_3 (Bollen & Beullens, 2002; Donzelli & Draetta, 2003; Karlsson-Rosenthal & Millar, 2006).

Figure 6.10 Elements of Cdc25A macro place as a part of G1-S sub-system. Active and inactive Cdc25A are presented as aCdc25A and iCdc25A, respectively. The weights for the arcs whose weight value is other than one are shown in the figure.

UBQ_E Macro Place

UBQ_E macro place models the process of activation/inactivation of SCF, which has the primary role in degradation of CycE_Cdk2 (Cardozo & Pagano, 2004; Nakayama & Nakayama, 2005). The ubiquitin ligase SCF becomes activated upon S phase entry (modelled through discrete transition t3_3) and then active SCF (aSCF) induces the degradation of CycE_Cdk2 through continuous transition T3 (Figure 6.11). At the next cell cycle, SCF becomes inactive again from Mid G1 (through discrete transition t3_4).

Figure 6.11 Elements of UBQ_E macro place as a part of G1-S sub-system. Active and inactive SCF are demonstrated as aSCF and iSCF, respectively.

UBQ_A Macro Place

As demonstrated in Figure 6.12, UBQ_A macro place models degradation of CycA_Cdk2 through two ubiquitin ligases APC_Cdc20A and APC_Cdh1 (Mateo et al., 2009). APC_Cdc20A becomes activated when the level of CycB_Cdk1 passes a threshold (3.9 simulation time units) which is modelled through discrete transition t4_3. Later in M phase (at Telophase), APC_Cdh1 also becomes activated (through discrete transition t4_1) and induces the full degradation of CycA_Cdk2 (via continuous transition T4).

Figure 6.12 Elements of UBQ_A macro place as a part of G1-S sub-system. Active and inactive APC_Cdc20A are shown as aAPC_Cdc20A and iAPC_Cdc20A, respectively. The same prefixes are used for APC_Cdh1. The weights for the arcs whose weight value is other than one are shown in the figure.

G2-M Sub-System

As shown in Figure 6.13, the G2-M sub-system comprises G2_M_Activation macro transition, UBQ_B and Cdc25C macro places, CycB_Cdk1 continuous place and a continues transition associated with degradation of CycB_Cdk1. The constituting elements of macro places/transitions will be explained in this section.

G2_M _Activation Macro Transition

G2_M_Activation macro transition is one of the main players of G2-M sub-system. As illustrated in Figure 6.14, when the level of CycA_Cdk2 increased sufficiently (at the end of S phase), G2_M_TF becomes activated (shown as discrete transition t7_1) and triggers production of more CycA_Cdk2 and CycB_Cdk1 (Transition T7 and T8, respectively) (Chae et al., 2011; Chae et al., 2004; Fung & Poon, 2005; Joaquin & Watson, 2003; Zhu et al., 2004). Therefore, the increased level of CycB_Cdk1 results in G2-M transition (Fung & Poon, 2005). At the end of cell cycle (Telophase), G2_M_TF becomes inactivated again through discrete transitions t7_2 (Figure 6.14).

Figure 6.13 **G2-M Sub-System (inside dashed purple enclosure) which includes G2_M_Activation macro transition, two macro places (UBQ_B and Cdc25C), one continuous place (for CycB_Cdk1) and one continues transition associated with degradation of CycB_Cdk1. The connections between this sub-system and other cell cycle sub-systems have already been demonstrated in Figure 6.2.**

Figure 6.14 **Elements of G2_M_Activation macro transition as a part of G2-M sub-system. Active and inactive G2_M_TF are demonstrated as aG2_M_TF and iG2_M_TF, respectively. The weights for the arcs whose weight value is other than one are shown in the figure.**

Cdc25C Macro Place

As described in Chapter 3, at the beginning of M phase (prophase), CycB_Cdk1 stimulates the activation of Cdc25C and then Cdc25C leads to formation of more CycB_Cdk1 through a positive feedback loop (Bollen & Beullens, 2002; Boutros et al., 2007; Goulev & Charvin, 2011; Perry & Kornbluth, 2007). In the abstract model and as demonstrated in Figure 6.15, Cdc25C becomes activated through discrete transition t8_1 when the cell cycle enters Prophase modelled as a logical place. The active Cdc25C then stimulates production of more CycB_Cdk1 presented as continuous transition T8 in the model (Figure 6.15). On the other hand, Cdc25C becomes deactivated when cell cycle enters Mid_G1 (through t8_2 in Figure 6.15).

Figure 6.15 Elements of Cdc25C macro place as a part of G2-M sub-system. Active and inactive Cdc25C are demonstrated as aCdc25C and iCdc25C, respectively.

UBQ_B Macro Place

UBQ_B macro place models the degradation of CycB_Cdk1 through two ubiquitin ligases APC_Cdc20B and APC_Cdh1 (Mateo et al., 2009). As shown in Figure 6.16, the effect of these ubiquitin ligases on CycB_Cdk1 is modelled through continuous transition T5. APC_Cdc20B is inactive from Mid G1 (modelled through discrete transition t5_2) but it becomes activated at the beginning of M phase (through discrete transition t5_1). Later in M phase (at Telophase), the second ubiquitin ligase, APC_Cdh1, also becomes activated (modelled through discrete transition t4_1) and induces the full degradation of CycB_Cdk1 (through continuous transition T5).

Figure 6.16 Elements of UBQ_B macro place as a part of G2-M sub-system. Active and inactive APC_Cdc20B are demonstrated as aAPC_Cdc20B and iAPC_Cdc20B, respectively. The same prefixes are used for APC_Cdh1.

DNA Damage Sub-System

As shown in Figure 6.17, the DNA damage sub-system comprises one macro place (DNA_Damage) whose constituting elements will be explained in this section.

Figure 6.17 DNA Damage Sub-System (inside dashed blue rectangle) which includes DNA_Damage macro place. The connections between this sub-system and other cell cycle sub-systems has already been demonstrated in Figure 6.2.

DNA_Damage Macro Place

The DNA damage sub-system centres around DNA_Damage Macro place where the total effect of rapid and delayed DNA damage pathways on Cyc_Cdks is presented in a simplified version because the main purpose of developing the MLHPN model is to present an abstract minimised model of cell cycle. As demonstrated in Figure 6.18, DNA Damage Signal is presented as a discrete place (DDS). Furthermore, the key controllers of DNA damage signalling, p53, p21 and Chk2 (Beishline & Azizkhan-Clifford, 2014; Meek, 2004; Morgan, 2007; Nyberg et al., 2002; Sancar et al., 2004), are modelled as one discrete place called DDS_Ctrls (DNA Damage Signalling Controllers) whose state switches between active and inactive depending on existence of DDS (Figure 6.18).

As illustrated in Figure 6.18, following the presence of DNA Damage Signal, DDS_Ctrls place becomes activated through discrete transition t9_1 and then aDDS_Ctrls place affects different Cyc_Cdks. Since p21_CycD_Cdk4 helps the process of E2F activation (described in Chapter 3), the effect of aDDS_Ctrls on CycD_Cdk4 is positive (modelled through transition T1) while the corresponding effect on other Cyc_Cdks is negative and it is towards their inactivation (modelled through transition T6, T7, and T8). The absence of DNA damage triggers discrete transition t9_2 which makes aDDS_Ctrls inactive again (iDDS_Ctrls).

Figure 6.18 Elements of DNA_Damage macro place which presents the DNA damage sub-system in the MLHPN model.

6.4 Kinetics of the Abstract Model

In the previous section, the MLHPN model was described from three different levels of abstraction. The High-level of abstraction presented a big picture of the abstract model where the level of

Cyc_Cdks (as the main controllers of cell cycle system) is regulated through a number of macro places and transitions located within four different sub-systems, namely, Growth Factor, G1-S, G2-M, and DNA damage sub-systems. The details of the constituent macro places and transitions of the cell cycle sub-systems were presented in the section devoted to Low-level of abstraction. At the Stage-level, the effect of different Cyc_Cdks on transition between different cell cycle stages was modelled. Now, the continuous transitions associated with Cyc_Cdks (as key controllers of cell cycle system) are presented below where the value of model parameters (together with corresponding parameter definition) and initial values of model elements (places) are provided in Tables F. 1 (in Appendix F) and G. 1 (in Appendix G), respectively. The value/state of the elements on the right side of equations is determined through interaction of the corresponding element with different elements in the system at different levels of abstraction. For example, elements that have positive effect on increasing the level of CycE_Cdk2 are aG1_S_TF and aCdc25A, where the first element is G1_S transcription factor whose state is determined through G1_S_Activation Macro Transition (shown in Figure 6.8) and the state of aCdc25A is determined through interactions shown in Figure 6.10. Parameters k_1 to k_{31} are parameters that are used to calibrate the output of the abstract model according to the corresponding dynamics from the comprehensive model and Multilayer Neural Network (MLP) algorithm is used to perform parameter estimation (with two hidden layers each of which having 10 neurons, Sigmoid activation function, and Back Propagation learning algorithm).

$$\frac{d(CycD\_Cdk4)}{d(t)} = (k_1 + k_2 * aG0\_G1\_TF + k_3 * aDDS\_Ctrls + k_4 * ap27) - aCycD\_Cdk4 * (k_5 + k_6 * aSCF + k_7 * aAPC\_Cdc20A + k_8 * aAPC\_Cdc20B) \quad (6\text{-}1)$$

$$\frac{d(CycE\_Cdk2)}{d(t)} = (k_9 + k_{10} * aG1\_S\_TF + k_{11} * aCdc25A) - aCycE\_Cdk2 * (k_{12} + k_{13} * aSCF + k_{14} * ap27 + k_{15} * aDDS\_Ctrls) \quad (6\text{-}2)$$

$$\frac{d(CycA\_Cdk2)}{d(t)} = (k_{16} + k_{17} * aG1\_S\_TF + k_{18} * aG2\_M\_TF + k_{19} * aCdc25A) - aCycA\_Cdk2 * (k_{20} + k_{21} * aAPC\_Cdc20A + k_{22} * aAPC\_Cdh1 + k_{23} * ap27 + k_{24} * aDDS\_Ctrls) \quad (6\text{-}3)$$

$$\frac{d(CycB\_Cdk1)}{d(t)} = (k_{25} + k_{26} * aG2\_M\_TF + k_{27} * aCdc25C) - aCycB\_Cdk1 * (k_{28} + k_{29} * aAPC\_Cdc20B + k_{30} * aAPC\_Cdh1 + k_{31} * aDDS\_Ctrls) \quad (6\text{-}4)$$

6.5 **MLHPN Simulation Results**

With the system equations provided in the last section, it is possible to present the dynamics of Cyc_Cdks as the main controllers of cell cycle system. These dynamics are demonstrated in Figure 6.19(A). As shown in this figure, first, CycD_Cdk4 level increases and in late_G1 phase, the concentrations of CycE_Cdk2 and CycA_Cdk2 start increasing (because of activation of G1_S_TF) and when the level of CycE_Cdk2 reaches a threshold, G1-S transition occurs at 6.0756 simulation time units (shown with a vertical dashed pink line in Figure 6.19(A)). Then the levels of CycA_Cdk2 and CycB_Cdk1 increase and when the concentration of CycB_Cdk1 crosses a threshold, G2-M transition occurs at 17.2901 (shown with a vertical dashed pink line in Figure 6.19(A)). At the end of cell cycle, the level of CycB_Cdk1 decreases through degradation by aAPC_Cdc20B and aAPC_Cdh1 and cell cycle ends at simulation time point 20.57.

When comparing the simulation results of the abstract MLHPN model (Figure 6.19(A)) with that of the comprehensive mathematical model presented in Chapter 3 (Figure 6.19(B)), we should not expect that the MLHPN model to be exactly the same as the comprehensive model and qualitative similarities in Cyc_Cdk dynamics would suffice as the MLHPN is an abstract model with just four equations in comparison to the comprehensive model with 61 ODEs. As shown in Figures 6.19(A) and 6.19(B), the trends of Cyc_Cdks are qualitatively similar. In order to compare the MLHPN results with the corresponding results of the comprehensive model, we need to convert the figures to the scale of the comprehensive model (or vice versa) as each cell cycle of the MLHPN model is 20.57 simulation time units while that of the comprehensive model is approximately 3700 units (they can also be converted to hours as shown in the simulation figures). Therefore, the G1-S transition happens at 6.0756 for the MLHPN model and the corresponding converted time point for the comprehensive model is $(1095) \times \frac{20.57}{3700} = 6.0876$ which shows the closeness of the results. The corresponding values for the G2-M transition are 17.2901 and $(3208) \times \frac{20.57}{3700} = 17.8347$ for the MLHPN and the comprehensive model, respectively, which also shows that the results of the two models are close to each other.

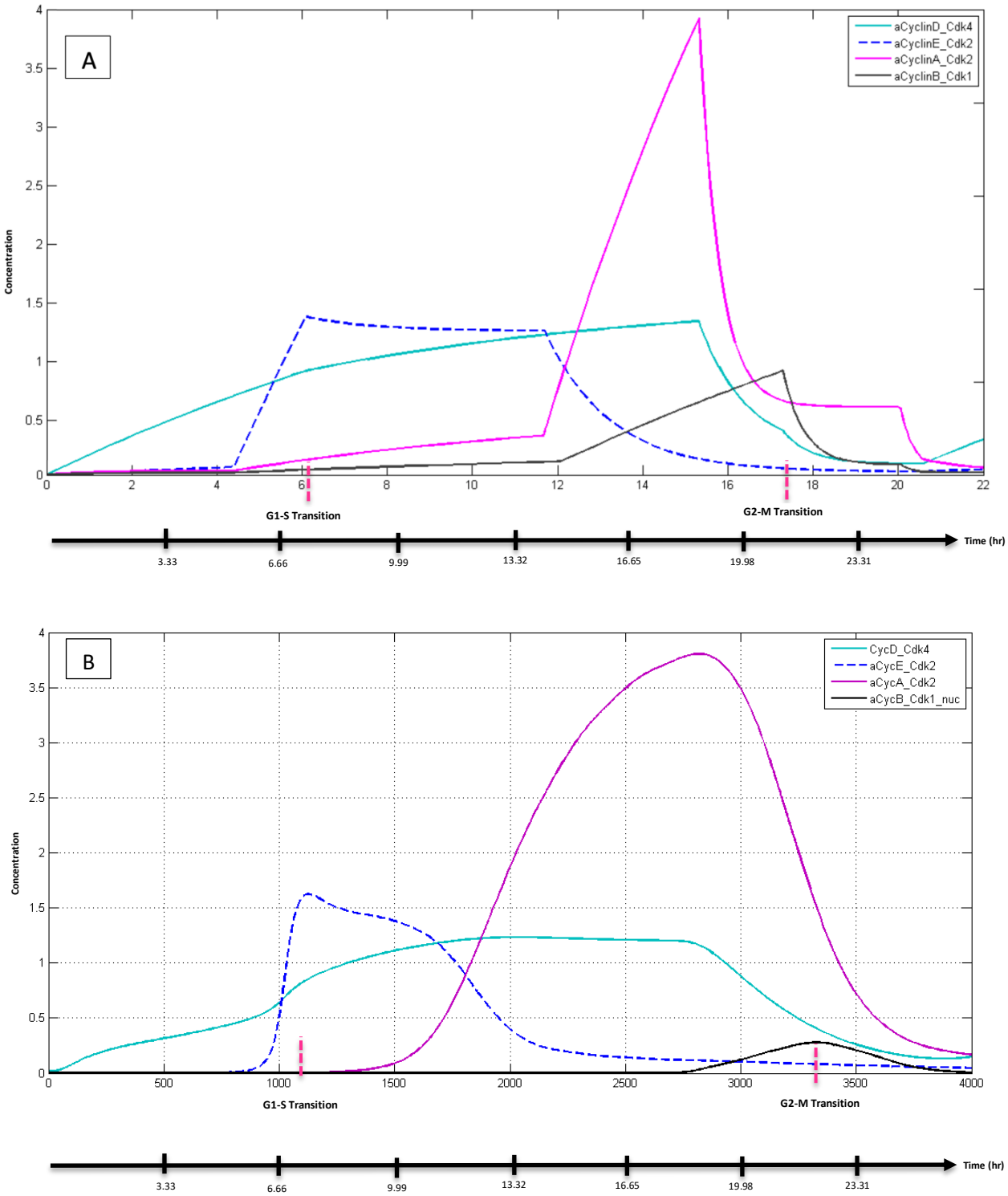

Figure 6.19 **Temporal dynamics of Cyc_Cdks as key controllers of mammalian cell cycle system under no DNA damage for (A) the MLHPN model and (B) the comprehensive mathematical model. The vertical dashed pink lines show the G1-S and G2-M transitions in both top and bottom figures [x-axis indicates time (both simulation time units and hour); y-axis indicates protein concentration].**

The simulation results also show that following the DNA damage (100 units of damage), the G1-S transition time shifts from 6.0756 (no damage) to 6.2232. Furthermore, the G2-M transition shifts from 17.2901 (no damage) to 17.9438 (damage condition). After converting the results of the MLHPN model, the G1-S and G2-M arrest durations are $(6.2232 - 6.0756) \times \frac{3700}{20.57} = 26.54$ and $(17.9438 - 17.2901) \times \frac{3700}{20.57} = 117.58$ units, respectively, which are close to the corresponding arrest durations for the comprehensive model (30 and 122, respectively). Therefore, similar to the comprehensive model presented in Chapter 3, the proposed MLHPN model can qualitatively present the cell cycle arrest under DNA damage condition. There are also some differences between the two models which is not surprising as the abstract model has not been designed to be the exact same as the comprehensive model and rather, it is an abstract/minimised version of the comprehensive model and qualitatively presents the behaviour of cell cycle controllers, so the values and concentrations are not the main concern. For example, the dynamic behaviour of CycA_Cdk2 is a little bit different between the two models where the corresponding dynamics in the comprehensive model is smoother which may be due to the existence of all the elements contributing to the formation of CycA_Cdk2, such as Cyclin A, Cdk2, and all the other components associated with CycA_Cdk2 presented in the comprehensive mathematical model but not in the MLHPN model (the same condition applies to other Cyc_Cdks as well).

6.6 Checkpoint Efficiency Evaluation on the MLHPN Model

As there is biological evidence that G1-S checkpoint is not as efficient as G2-M checkpoint in detecting damaged cells (Beishline & Azizkhan-Clifford, 2014; Di Leonardo et al., 1994), in Chapter 5, we developed Checkpoint Efficiency Evaluation (CEE) model and applied it on the comprehensive mathematical model presented in Chapter 3 and showed that the comprehensive model results are in good agreement with biological findings. Now, having developed the abstract MLHPN model for mammalian cell cycle based on the most significant parameters of the comprehensive model, we aim to conduct a checkpoint efficiency evaluation analysis on the abstract model to evaluate the performance of G1-S and G2-M checkpoints in detecting damaged cells. Therefore, according to the CEE model, the MLHPN model parameters are perturbed simultaneously in order to simulate real situations that cells may confront (within five ranges of $\pm 5\%, \pm 10\%, \pm 15\%, \pm 20\%$ and $\pm 30\%$) and sampled 2000 times for each level of perturbation. Then, 2000 Peak Time (PT) values are calculated for each checkpoint indicator (aCycE_Cdk2 and aCycB_Cdk1) and the Probability Density Function (PDF) of PTs is estimated by normal distribution. The procedure is repeated for DNA damage condition and the PDF of PTs of the indicators in the presence of DNA damage is obtained. Then, using Type II Error with significance level of 10% (Type II Error is the probability of accepting a null hypothesis while it is not true (Weiers, 2010)), the damaged cells passing each checkpoint as healthy

cells are labelled. The efficiency of checkpoints is calculated as the number of correctly identified damaged cells to the total number of damaged cells. Therefore, it is possible to check how many damaged cells are identified and captured at each checkpoint.

6.6.1 Checkpoint Efficiency Based on the Number of Damaged Cells Passing Checkpoints as Healthy Cells

The checkpoint efficiency is evaluated based on the number of damaged cells that pass checkpoints as healthy cells and the results are demonstrated in Table 6.3. As shown in this table, G2-M checkpoint captures more damaged cells than G1-S under all different perturbation levels and DNA damage condition. As a case in point, under perturbation level of ±5%, 614 out of 2000 damaged cells pass G1-S checkpoint as healthy cells and then only 118 out of these 614 damaged cells are not caught at G2-M checkpoint. Therefore, the efficiency of G1-S is $\frac{2000-614}{2000} = 69.3\%$, whereas the efficiency of G2-M is $\frac{614-118}{614} = 80.78\%$. The rate at which damage cells pass the combined checkpoint system as healthy cells is 5.9% (118/2000) (False Negative rate) making the whole system efficiency $\frac{2000-118}{2000} = 94.1\%$ (True Positive rate). Although the difference between the efficiency of G2-M and G1-S decreases when the level of perturbation increases, the efficiency of G2-M checkpoint in capturing damaged cells is higher than that of G1-S. This is in good agreement with experiments showing relative inefficiency of G1-S checkpoint in arresting damaged cells (Beishline & Azizkhan-Clifford, 2014; Di Leonardo et al., 1994). Another important point to mention is that the trend of efficiency percentages for the comprehensive model (presented in Table 5.1 in Chapter 5; for example, the G1-S efficiencies for *±5%, ±10%, ±15%, ±20%* and *±30%* perturbations are *72.85%, 36.5%, 26.1%, 20.7% and 15.3%*, respectively) and the MLHPN model (Table 6.3) is similar. In other words, the efficiencies of both checkpoints as well as combined efficiency decrease when the perturbation level increases. However, Increasing the perturbation level results in lower efficiency in the MLHPN model. This is due to the lower number of parameters in the MLHPN model that makes the model more sensitive to parameter perturbations.

Table 6.3 Efficiency and the number of damaged cells that pass each of the G1-S and G2-M checkpoints as normal cells under DNA damage and different perturbation levels (the total number of damaged cells is 2000) for the MLHPN model.

Perturbation Range	*Damaged Cells Passing G1-S as Normal*	*G1-S Efficiency (%)*	*Portion of G1-S Escaped Damaged Cells Passing G2-M as Normal*	*G2-M Efficiency in Capturing Damaged Cells Escaping G1-S (%)*	*Combined-Checkpoint System Efficiency (%)*
±5%	614	69.3	118	80.78	94.1

±10%	1408	29.6	917	34.87	54.15
±15%	1616	19.2	1266	21.65	36.7
±20%	1766	11.7	1521	13.87	23.95
±30%	1832	8.4	1645	10.2	17.75

6.6.2 Checkpoint Efficiency Based on the Number of Healthy Cells Getting Sacrificed as Damaged Cells

Although it is crucial to investigate the number of damaged cells passing cell cycle checkpoints as healthy cells, it is also important to check the number of healthy cells arrested at checkpoints incorrectly. Thus, we conduct another analysis on the MLHPN model to study the checkpoint efficiency in correctly recognising healthy cells. Here, we allow 2000 healthy cells to go through the checkpoints and count the number of healthy cells incorrectly identified as damaged and arrested at checkpoints. The results of this analysis are shown in Table 6.4. For example, at ±5% perturbation level, the number of healthy cells incorrectly identified and arrested at G1-S is shown in the second column (i.e., 55 out of 2000 are sacrificed); the number of incorrectly arrested cells at G2-M is shown in the fourth column (i.e., 2000-55=1945 healthy cells go to G2-M checkpoint and just 37 cells (37 out of 1945) get incorrectly arrested as damaged). Therefore, the efficiency of G1-S and G2-M is $\frac{2000-55}{2000} = 97.25\%$ and $\frac{1945-37}{1945} = 98.09\%$, respectively. The combined checkpoint efficiency in releasing healthy cells is $\frac{2000-(55+37)}{2000} = 95.4\%$.

The results shown in table 6.4 indicate that both checkpoints are highly efficient and near perfect in recognising healthy cells at ±5% perturbation. As the perturbation level increases, both checkpoints drop in efficiency in recognising healthy cells but G2-M not only remains more efficient but also is more robust against sacrificing healthy cells. If we compare the results in Table 6.4 with the same results from the comprehensive model (presented in Table 5.2 in Chapter 5; for example, the G1-S efficiencies for *±5%, ±10%, ±15%, ±20%* and *±30%* perturbations are *99.15%, 69.95%, 46.8%, 33.55% and 14.7%*, respectively), we notice that the trend of efficiencies is similar for both the MLHPN and the comprehensive models. However, the corresponding figures for the MLHPN are less than those of the comprehensive model which indicates that the abstract the MLHPN model is more sensitive to parameter perturbation which is normal because in the MLHPN, cell cycle is modelled with lower number of elements and parameters.

Table 6.4 **Checkpoint efficiency and the number of healthy cells that get sacrificed as damaged cells at G1-S and G2-M checkpoints for different perturbation levels (the total number of healthy cells is 2000) for the MLHPN model.**

Perturbation Range	*Healthy Cells Arrested at G1-S as Damaged*	*G1-S Efficiency (%)*	*Portion of G1-S Released Healthy Cells Arrested at G2-M as Damaged*	*G2-M Efficiency in Releasing Healthy Cells that Pass G1-S (%)*	*Combined Checkpoint Efficiency in Releasing Healthy Cells (%)*
±5%	55	97.25	37	98.09	95.4
±10%	907	54.65	323	70.44	38.5
±15%	1356	32.20	366	43.16	13.9
±20%	1561	21.95	305	30.52	6.7
±30%	1762	11.9	191	19.74	2.35

6.7 Summary

In this chapter, we developed an abstract model of mammalian cell cycle (the MLHPN model) based on the most significant parameters (of the comprehensive model presented in Chapter 3) identified through GSA and SOMCCA model. Using Petri Nets (PNs), we introduced a novel intuitive approach to modelling the mammalian cell cycle by presenting the system in three levels of abstraction: High-level, Stage-level, and Low-level. The High-level of abstraction rendered a big picture of the model. At the Stage-level, the function of Cyc_Cdks in controlling transitions between different cell cycle stages was described. Finally, the details of regulators of Cyc_Cdks were presented at Low-level of abstraction. Furthermore, all the cell cycle sub-systems introduced in Chapter 3 for the comprehensive model (Growth Factor signalling, G1-S and G2-M checkpoints, and DNA damage signalling) also existed in the MLHPN model where the number of the corresponding elements inside each sub-system was less due to model abstraction. The proposed abstract model comprised just four equations and 31 parameters while the comprehensive mathematical model presented in chapter 3 had 61 ODEs and 148 parameters. Therefore, the MLHPL model provided ease of understanding of a process that has temporal and organizational complexity in a simpler and intuitive way while making it possible to easily access and assess either temporal or higher or lower (detail) view of the process.

The simulation results based on simple mass action kinetic equations in the MLHPN were qualitatively in agreement with simulations of the comprehensive mathematical model. The significance of this study is mainly related to developing a minimal model that can represent the behaviour of Cyc_Cdks as key controllers of mammalian cell cycle. It was shown that the temporal development of all Cyc-Cdk complexes were qualitatively in agreement with the ODE counterpart. In conclusion, the proposed model in this chapter provided an intuitive approach to represent the complex system of mammalian cell cycle from different levels of abstraction where the sub-systems and their constituent elements (different places and transitions) interact with each other. More importantly, using the MLHPN, we were able to conduct the Checkpoint Efficiency Evaluation (CEE) analysis and the results were consistent with those of the comprehensive model showing that the MLHPN model can be used to gain similar insights into mammalian cell cycle control system as the ODE model but with much less model complexity and greater computational efficiency.

Chapter 7

Conclusions

In this thesis, we used Ordinary Differential Equations (ODEs) and Petri Nets (PNs) modelling approaches to achieve a better understanding of underlying mechanisms in cell cycle control system in the presence of DNA damage from a systems point of view. The major focus of the current study was to explore the current knowledge of mammalian cell cycle through developing a comprehensive mathematical model incorporating all cell cycle sub-systems introduced in this study (Growth Factor signalling, G1-S checkpoint signalling, G2-M checkpoint signalling, and DNA damage pathway) as well as performing a model abstraction through a PN-based approach. Numerical analyses were conducted to identify the most significant parameters, modules, and sub-systems of the cell cycle system on system responses (G1-S and G2-M transitions). Moreover, the efficiency of cell cycle checkpoints was investigated to gain more insights into performance of both G1-S and G2-M checkpoints in arresting damaged cells and not sacrificing healthy cells. Simulations have shown that our models are beneficial in attaining new insights into the behaviour of mammalian cell cycle system. This chapter is organized as follows: An overall overview of our achievements is given in Section 7.1. The research highlights are provided in Section 7.2. Section 7.3 is devoted to recommendations for future research. And section 7.4 provides a conclusion of our research.

7.1 Research Overview

The first goal of this research was to gather the most recent knowledge of mammalian cell cycle control system in order to identify missing essential elements and pathways. Therefore, we did a thorough research on current understanding of mammalian cell cycle system and its computational modelling (presented in Chapter 2) which was published in an International Conference paper titled "A Review of Computational Models of Mammalian Cell Cycle" (Abroudi et al., 2015). Based on information gathered on the current cell cycle knowledge, we developed a comprehensive systemic mathematical model that enabled us to perform further analyses to gain more insights into mammalian cell cycle system behaviour. The associated study presented in Chapter 3 has been published in Journal of Theoretical Biology (JTB) with the title "A comprehensive complex systems approach to the study and analysis of mammalian cell cycle control system in the presence of DNA damage stress" (Abroudi et al., 2017). In order to develop our comprehensive model, we updated the most complete model of mammalian cell cycle at the time which was a model developed by Iwamoto et al. (2011). We identified the missing elements in that model according to the latest knowledge of mammalian cell cycle system. We added some crucial elements, such as c-Myc (a transcription factor which is vital for cell cycle initiation by inducing the synthesis of Cyclin D), PP1 (a vital phosphatase

whose addition made the Iwamoto et al. (2011) model cyclic. This phosphatase mainly functions through dephosphorylation of Retinoblastoma protein pRb), Plk1 (one of the essential proteins in mitotic entry which activates Cdc25C phosphatase and APC_Cdc20, inactivates Wee1 kinase, and helps translocation of CycB_Cdk1 from cytoplasm to nucleus), SCF (a crucial ubiquitin ligase which has impact on G1-S transition through degradation of Cyclin E), and Gadd45α (this protein is one of the bi-products of transcription factor p53, and it physically interacts with Cdk1 in order to stimulate CycB_Cdk1 unbinding). The simulation results of the model showed the effect of newly added elements on system response (G1-S and G2-M transitions).

We also introduced the concept of functional sub-systems where the whole system was divided into four inter-connected sub-systems (Growth Factor signalling, G1-S & G2-M checkpoints, and DNA damage signalling). Unlike previous models that presented Growth Factor as a constant signal, we presented a more realistic Growth Factor signalling by introducing Growth Factor signalling sub-system centring around transcription factor c-Myc. G1-S and G2-M checkpoints were two other essential sub-systems presented along with their functional modules in our model. G1-S checkpoint sub-system consisted Cdk4-Related, E2F-pRb, Cdk2-Related, and Tyrosine phosphatase modules where the latter is a novel addition to this sub-system and E2F-pRb module is expanded and modified to make the model cyclic. G2-M checkpoint sub-system was presented as five inter-connected modules: Cdk1-Related, Tyrosine phosphatase, Tyrosine kinase, Plk1-Related, and APC-related where the latter four are novel additions and contained new elements. We also expand the DNA damage sub-system into two modules including Chk-Related (rapid) and newly added elements in p53-Related (delayed) modules. The detailed description of the abovementioned elements, sub-systems, and modules as well as the corresponding equations of our comprehensive mathematical model were presented in Chapter 3.

The second goal of this study was to investigate the behaviour of cell cycle system under different circumstances including different perturbation levels and DNA damage in order to identify the most significant parameters, sub-systems and modules of the system. To accomplish this objective, we first determined the indicators of G1-S and G2-M transitions (PT of CycE_Cdk2 and CycB_Cdk1_Nuc, respectively). Then, we introduced an analytical method involving Global Sensitivity Analysis (GSA) based on Self-Organizing Map with Correlation Coefficient Analysis (SOMCCA) to find the most significant parameters, modules and sub-systems which showed that Growth Factor and G1-S checkpoint sub-systems and seven parameters in the modules within them were crucial for G1-S and G2-M transitions (Chapter 4). Having identified the most influential parameters and their corresponding proteins, we were able to take a step forward to develop an abstract minimal model based on the identified significant components and see if this new abstract model behaves similar to

the comprehensive model presented in Chapter 3 (this investigation forms our fourth goal but before that we have the third goal which was devoted to checkpoints efficiency analysis).

The third goal of this study was to investigate the relative efficiency of G1-S and G2-M checkpoints in detecting damaged cells as there is biological evidence that G2-M checkpoint is more efficient in detecting damaged cells in the presence of DNA damage. We developed a Checkpoint Efficiency Evaluation (CEE) model enabling us to count the number of damaged cells passing cell cycle checkpoints as healthy (normal) cells. We also performed further investigation on efficiency of checkpoints by calculating the number of healthy cells got arrested incorrectly as damaged cells at checkpoints. The simulation results of CEE applied to our comprehensive model showed that cell cycle is about 96% efficient in arresting damaged cells with G2-M checkpoint being more efficient than G1-S and both checkpoint systems are near perfect (98.6%) in passing healthy cells (under ±5% parameter perturbation). The results were in good agreement with biological findings showing the usefulness of our comprehensive model in gaining deeper insights into mammalian cell cycle control system. The work associated with this goal was presented in Chapter 5.

The last goal of this thesis centred around the idea of model abstraction using the most significant parameters identified in Chapter 4. As mammalian cell cycle is a complex system with reactions with different time-scales, in order to develop an abstract model, we used a hybrid modelling approach that combined discrete and continuous interactions and elements (proteins). Therefore, we adopted an intuitive graphical modelling approach called Petri Nets (PNs) to present the most significant identified elements of mammalian cell cycle system. This modelling approach also enabled us to present the system in different levels of abstraction (High, Stage, and Low-levels). At high-level of abstraction, Cyc_Cdks, as the key players of cell cycle machinery, were modelled as continuous elements (places). At stage-level, the interactions between Cyc_Cdks and cell cycle stages (i.e., Late_G1, S, G2, etc.) were introduced. And finally, the interactions between Cyc_Cdks and their regulators (i.e., Ubiquitin ligases, phosphatases, CKIs, etc.) were provided at low-level of abstraction. We called our model Multi-Layer Hybrid Petri Net (MLHPN). The simulation results of MLHPN were qualitatively similar to its parent model (the comprehensive mathematical model presented in Chapter 3) with some minor differences that were expected when downsizing a model with 61 equations to just 4. To investigate whether the MLHPN model can be used to validate some biological findings on mammalian cell cycle control systems, we conducted the CEE analysis on the MLHPN to evaluate and compare the efficiency of checkpoints in detecting damaged cells and found out that the MLHPN results are consistent with those of the comprehensive model. In other words, the MLHPN was able to correctly show that G2-M checkpoint is more efficient than G1-S in capturing damaged cells as well as not arresting healthy cells.

7.2 Research Highlights

The highlights of our research are briefly outlined as follows:

- Developed the most comprehensive ODE-based mammalian cell cycle model
- Presented a holistic complex systems modelling approach involving interacting sub-systems and modules
- Abstracted known cell cycle pathways into sub-systems and added new essential modules and elements.
- Demonstrated the value and role of the newly added components
- Introduced a Global parameter sensitivity approach using Self-Organising Maps with Correlation Coefficient Analysis (SOMCCA model)
- Identified the most significant sub-systems, modules and parameters in cell cycle
- Introduced a statistical/simulation-based approach to assess efficiency of DNA damage checkpoints and quantified the efficiency of checkpoints in arresting damaged cells and not sacrificing healthy cells (CEE model)
- Revealed a relatively higher G2-M checkpoint efficiency compared to G1-S checkpoint
- Performed a model abstraction using a PN-based modelling approach (MLHPN model)
- Showed that the MLHPN model is capable of mimicking the systems dynamics of the comprehensive mathematical model and validating biological findings regarding relative efficiency of G1-S and G2-M checkpoints in correctly detecting damaged/healthy cells

7.3 Recommendations for Future Research

The current study recommends the following directions for future research:

- One area that could be investigated more is exploring the impact of Growth Factor deprivation at different stages of cell cycle as biological findings show that Growth Factor deprivation can prevent cell division and promote cell Apoptosis (Kearney & Martin, 2013; Mason & Rathmell, 2011; Vander Heiden et al., 2001). Further investigation could involve the

relationship between the stage the Growth Factor deprivation occurs and the effect it may have on cell cycle progression.

- Following the point noted in the previous bullet-point, the Apoptosis pathway can be added to the model to further explore the effect of Growth Factor on cell Apoptosis.

- In Chapter 3, we mentioned that since Iwamoto et al. (2011) model is not cyclic, some updates need to be made to make the model cyclic. Therefore, we identified a missing protein called PP1 and added that to our model and also made changes to some existing parameters to make the model cyclic. Although our comprehensive model was cyclic, the cyclic behaviour was dampened. This could be due to the assumed values for the parameters and there might be a better set of parameters that need to be estimated to fix the dampening behaviour. Thus, future work could address this issue.

- In our comprehensive mathematical model, DNA damage repair mechanism has been modelled with a constant rate. A future work could focus on adding DNA damage repair signalling to investigate the repair process more thoroughly as there are a lot of biological findings on DNA damage repair mechanisms (Branzei & Foiani, 2008; Giglia-Mari et al., 2010; Hoeijmakers, 2009).

7.4 Conclusions

Mammalian cell cycle is one of the most complex biological systems; and because of its complexity, it is not only challenging but also expensive to explore the underlying mechanisms of this system just by *in vitro* technologies. Therefore, computational modelling approaches, such as mathematical models, Boolean networks, Petri Nets (PNs), etc., provide a good avenue to study and investigate the behaviour of biological systems. Furthermore, computational models are able to shed lights on biological processes and interactions through variety of predictions that can be verified by experiments later which shows the value of computational modelling in biological discovery. In this research, we showed that our comprehensive mathematical model (comprising four essential sub-systems: Growth Factor signalling, G1-S & G2-M checkpoints, and DNA damage pathway) can be used to explore underlying mechanisms of G1-S and G2-M checkpoints in the presence of DNA damage and Growth Factor signals. Using analysis of GSA through our developed model called SOMCCA, we characterised and identified the most significant parameters, sub-systems, and modules on system response (G1-S and G2-M transitions). Moreover, to validate our model regarding biological evidence on the relative efficiency of checkpoints (G2-M being more efficient in detecting damaged cell than G1-S), we developed a model called Checkpoint Efficiency Evaluation (CEE). The results showed that

our comprehensive model is in good agreement with biological findings. Lastly, we investigated the possibility of PN-based modelling approach for model abstraction from our comprehensive mathematical model to an abstract minimal model that can qualitatively present the behaviour of the parent model. We successfully performed the abstraction using the parameters identified as the most significant in the comprehensive model. The developed abstract model was called MLHPN. More importantly, we investigated the ability of the MLHPN model in revealing the efficiency of checkpoints using the CEE analysis. The CEE analysis results on the MLHPN were consistent with the corresponding biological evidence.

While the current study tried to cover the most essential pathways of mammalian cell cycle including Growth Factor signalling, G1-S and G2-M checkpoints, and DNA damage signalling, there is still a variety of pathways, such as Apoptosis, TGF-Beta signalling pathway, etc., that can be incorporated into cell cycle system to shed more lights on behaviour of this complex system in response to different internal and external signals. We believe that the models developed in this research together with corresponding insightful analyses provide a good understanding of different aspects of mammalian cell cycle system separately and as an integrated system that will also be beneficial in exploring targeted therapy in future cancer treatments.

Appendix A

Equations of the Comprehensive Mathematical Model

This section contains Ordinary Differential Equation (ODEs) of different sub-systems/modules of the comprehensive mathematical model presented in Chapter 3. In the formulae, dot sign indicates multiplication; i and a prefixes denote inactive and active, respectively. We provide all equations here while Chapter 3 contains only equations that have the newly added proteins in them. Initial values and definition of all parameters are presented in Appendices B and C. The software used for simulation and analysis is Matlab.

A.1 Growth Factor Signalling Sub-system

$$\frac{d[icMyc]}{dt} = k_1 \cdot [acMyc] - k_2 \cdot GF \cdot [icMyc] \quad \text{(A-1)}$$

$$\frac{d[acMyc]}{dt} = k_2 \cdot GF \cdot [icMyc] - k_1 \cdot [acMyc] \quad \text{(A-2)}$$

Within brackets is shown the concentration of respective proteins. Active and inactive c-Myc are shown as [acMyc] and [icMyc], respectively.

A.2 DNA Damage Signalling Sub-system

A.2.1 Chk-Related Module

The detailed dynamics of this module is formulated as follows (the formulae for Cdc25 phosphatases and Cyc_Cdks are presented in subsequent sections):

$$\frac{d[ATM]}{dt} = k_5 \cdot DSB(t) - k_6 \cdot [ATM] \quad \text{(A-3)}$$

$$\frac{d[iChk2]}{dt} = k_3 \cdot [aChk2] - k_4 \cdot [iChk2] \cdot [ATM] \quad \text{(A-4)}$$

$$\frac{d[aChk2]}{dt} = k_4 \cdot [iChk2] \cdot [ATM] - k_3 \cdot [aChk2] \quad \text{(A-5)}$$

where $DSB(t) = DDS \cdot exp(-k_7 \cdot t)$, $t\ is\ time$, and DDS is the DNA Damage Strength. $DSB(t)$ is Double-Strand Break signal that can trigger the DNA damage response in both Chk-Related and p53-Related modules and it varies as repair progresses as shown by the formula. It is important to note

that the repair process is also embedded in the model by parameter k_7 (see Appendices B and C for initial values and definition of all parameters).

A.2.2 p53-Related Module

The temporal dynamics of this module can be expressed as follows (since p21, 14-3-3σ and Gadd45α have interactions with elements in G1-S and G2-M sub-systems, the corresponding dynamics may include some elements from those systems):

$$\frac{d[p53]}{dt} = k_8 + k_9 \cdot [ATM] - k_{10} \cdot [p53] - DEG(t) \cdot [Mdm2] \cdot [p53] \quad \text{(A-6)}$$

$$\frac{d[Mdm2]}{dt} = k_{14} + \frac{(k_{15} \cdot [IF]^{50})}{{k_{16}}^{50} \cdot [IF]^{50}} - k_{17} \cdot [Mdm2] \quad \text{(A-7)}$$

$$\frac{d[IF]}{dt} = \frac{k_{18} \cdot [p53] \cdot DSB(t)}{1 + k_{19} \cdot [p53] \cdot [Mdm2]} - k_{20} \cdot [IF] \quad \text{(A-8)}$$

$$\begin{aligned} \frac{d[p21]}{dt} = {} & k_{21} + k_{22} \cdot [p53] + k_{23} \cdot [p21\_CycD\_Cdk4] + k_{25} \cdot [p21\_aCycE\_Cdk2] + \\ & k_{27} \cdot [p21\_aCycA\_Cdk2] + k_{29} \cdot [p21\_aCycB\_Cdk1\_Nuc] - (k_{24} \cdot \\ & [CycD\_Cdk4] + k_{26} \cdot [aCycE\_Cdk2] + k_{28} \cdot [aCycA\_Cdk2] + \ k_{30} \cdot \\ & [aCycB\_Cdk1\_Nuc] + k_{31}) \cdot [p21] \end{aligned} \quad \text{(A-9)}$$

$$\frac{d[14\_3\_3\sigma]}{dt} = k_{32} + k_{33} \cdot [p53] - k_{34} \cdot [14\_3\_3\sigma] - k_{35} \cdot [14\_3\_3\sigma] \cdot [iCdc25C\_Ps216] \quad \text{(A-10)}$$

$$\frac{d[\text{Gadd45}\alpha]}{dt} = k_{36} + k_{37} \cdot [p53] - k_{38} \cdot [\text{Gadd45}\alpha] \quad \text{(A-11)}$$

where $DEG(t) = k_{11} - k_{12} \cdot (DSB(t) - DDS \cdot \exp(-k_{13} \cdot DDS \cdot t))$. $DEG(t)$ is a time-dependent function that represents the degradation rate of p53 and it also depends on $DSB(t)$ and the level of DNA damage (DDS).

A.3 G1-S Checkpoint Signalling Sub-system

A.3.1 Cdk4-Related Module

The dynamics of Cdk4-Related module can be written as follows:

$$\begin{aligned} \frac{d[CycD]}{dt} = {} & k_{39} + k_{40} \cdot [acMyc] + k_{41} \cdot [CycD\_Cdk4] - (\ k_{44} + k_{42} \cdot [Cdk4] + \\ & k_{43} \cdot [aSCF] + \ k_{147} \ \cdot [aAPC\_Cdc20]) \cdot [CycD] \end{aligned} \quad \text{(A-12)}$$

$$\begin{aligned} \frac{d[Cdk4]}{dt} = {} & k_{45} \cdot [CycD\_Cdk4] + k_{46} \cdot [p27\_CycD\_Cdk4] + k_{41} \cdot [CycD\_Cdk4] - \\ & k_{42} \cdot [CycD] \cdot [Cdk4] \end{aligned} \quad \text{(A-13)}$$

$$\frac{d[CycD\_Cdk4]}{dt} = k_{42} \cdot [CycD] \cdot [Cdk4] + k_{23} \cdot [p21\_CycD\_Cdk4] + k_{47} \cdot [p27\_CycD\_Cdk4] - (k_{41} + k_{45} + k_{24} \cdot [p21] + k_{48} \cdot [p27]) \cdot [CycD\_Cdk4] \quad \text{(A-14)}$$

$$\frac{d[p27]}{dt} = k_{49} + k_{47} \cdot [p27\_CycD\_Cdk4] + k_{50} \cdot [p27\_CycE\_Cdk2] + k_{51} \cdot [p27\_aCycA\_Cdk2] - (k_{48} \cdot [CycD\_Cdk4] + k_{52} \cdot [aCycE\_Cdk2] + k_{53} \cdot [aCycE\_Cdk2] + k_{54} \cdot [aCycA\_Cdk2] + k_{55} \cdot [aCycA\_Cdk2]) \cdot [p27] \quad \text{(A-15)}$$

$$\frac{d[p27\_CycD\_Cdk4]}{dt} = k_{48} \cdot [CycD\_Cdk4] \cdot [p27] - (k_{46} + k_{47}) \cdot [p27\_CycD\_Cdk4] \quad \text{(A-16)}$$

$$\frac{d[p21\_CycD\_Cdk4]}{dt} = k_{24} \cdot [p21] \cdot [CycD\_Cdk4] - k_{23} \cdot [p21\_CycD\_Cdk4] \quad \text{(A-17)}$$

A.3.2 E2F-pRb Module

The equations of elements of this module are as follows:

$$\frac{d[E2F\_pRb]}{dt} = k_{56} \cdot [E2F] \cdot [pRb] - (k_{57} \cdot [CycD\_Cdk4] + k_{58} \cdot [p27\_CycD\_Cdk4] + k_{59} \cdot [p21\_CycD\_Cdk4]) \cdot [E2F\_pRb] \quad \text{(A-18)}$$

$$\frac{d[iPP1]}{dt} = k_{62} \cdot [aPP1] - k_{63} \cdot [iPP1].[aCycB\_Cdk1\_Nuc] \quad \text{(A-19)}$$

$$\frac{d[aPP1]}{dt} = k_{63} \cdot [iPP1].[aCycB\_Cdk1\_Nuc] - k_{62} \cdot [aPP1] \quad \text{(A-20)}$$

$$\frac{d[pRbPPP]}{dt} = (k_{60} \cdot [aCycE\_Cdk2] + k_{61} \cdot [aCycA_{Cdk2}]) \cdot [E2F\_pRbPP] - k_{64} \cdot [pRbPPP] \quad \text{(A-21)}$$

$$\frac{d[pRb]}{dt} = k_{65} + k_{64} \cdot [aPP1].[pRbPPP] - (k_{56} \cdot [E2F] + k_{66}) \cdot [pRb] \quad \text{(A-22)}$$

$$\frac{d[E2F]}{dt} = k_{67} + k_{68} \cdot [\mathrm{E2F}] + (k_{60} \cdot [aCycE\_Cdk2] + k_{61} \cdot [aCycA\_Cdk2]) \cdot [E2F\_pRbPP] - (k_{56} \cdot [pRb] + k_{146} \cdot [aCycA\_Cdk2] + k_{69}) \cdot [E2F] \quad \text{(A-23)}$$

A.3.3 Cdk2-Related Module

The mathematical equations of this module can be expressed as follows:

$$\frac{d[CycE]}{dt} = k_{70} \cdot [E2F] + k_{72} \cdot [iCycE\_Cdk2] - (k_{73} + k_{71} \cdot [Cdk2] + k_{74} \cdot [aSCF]) \cdot [CycE] \quad \text{(A-24)}$$

$$\frac{d[CycA]}{dt} = k_{75} \cdot [E2F] + k_{76} \cdot [aBMyb] + k_{77} \cdot [NFY] + k_{78} \cdot [iCycA\_Cdk2] - (k_{79} + k_{80} \cdot [Cdk2] + k_{81} \cdot [aAPC\_Cdc20] + k_{82} \cdot [aAPC\_Cdh1]) \cdot [CycA] \quad \text{(A-25)}$$

$$\frac{d[Cdk2]}{dt} = k_{72} \cdot [iCycE\_Cdk2] + k_{83} \cdot [iCycE\_Cdk2] + k_{84} \cdot [aCycE\_Cdk2] \cdot [aCycE\_Cdk2] + k_{78} \cdot [iCycA\_Cdk2] + (k_{85} \cdot [iCycA\_Cdk2] + k_{86} \cdot [aCycA\_Cdk2]) \cdot ([aAPC\_Cdc20] + [aAPC\_Cdh1]) - (k_{71} \cdot [CycE] + k_{80} \cdot [CycA]) \cdot [Cdk2], \quad \text{(A-26)}$$

$$\frac{d[iCycE\_Cdk2]}{dt} = k_{71} \cdot [CycE] \cdot [Cdk2] + k_{87} \cdot [aCycE\_Cdk2] - (k_{72} + k_{83} + k_{88} \cdot [aCdc25A]) \cdot [iCycE\_Cdk2] \quad \text{(A-27)}$$

$$\frac{d[aCycE\_Cdk2]}{dt} = k_{88} \cdot [iCycE\_Cdk2] \cdot [aCdc25A] + k_{50} \cdot [p27\_aCycE\_Cdk2] + k_{25} \cdot [p21\_aCycE\_Cdk2] - (k_{87} + k_{84} \cdot [aCycE\_Cdk2] + k_{52} \cdot [p27] + k_{26} \cdot [p21]) \cdot [aCycE\_Cdk2] \quad \text{(A-28)}$$

$$\frac{d[iCycA\_Cdk2]}{dt} = k_{80} \cdot [Cdk2] \cdot [CycA] + k_{89} \cdot [aCycA\_Cdk2] - (k_{78} + k_{85} \cdot ([aAPC\_Cdc20] + [aAPC\_Cdh1]) + k_{90} \cdot [aCdc25A]) \cdot [iCycA\_Cdk2] \quad \text{(A-29)}$$

$$\frac{d[aCycA\_Cdk2]}{dt} = k_{90} \cdot [iCycA\_Cdk2] \cdot [aCdc25A] + k_{51} \cdot [p27\_aCycE\_Cdk2] + k_{27} \cdot [p21\_aCycA\_Cdk2] - (k_{89} + k_{55} \cdot [p27] + k_{28} \cdot [p21] + k_{86} \cdot ([aAPC\_Cdc20] + [aAPC\_Cdh1])) \cdot [aCycA\_Cdk2] \quad \text{(A-30)}$$

$$\frac{d[p27\_aCycE\_Cdk2]}{dt} = k_{52} \cdot [p27] \cdot [aCycE\_Cdk2] - k_{50} \cdot [p27\_aCycE\_Cdk2] \quad \text{(A-31)}$$

$$\frac{d[p21\_aCycE\_Cdk2]}{dt} = k_{26} \cdot [p21] \cdot [aCycE\_Cdk2] - k_{25} \cdot [p21\_aCycE\_Cdk2] \quad \text{(A-32)}$$

$$\frac{d[p27\_aCycA\_Cdk2]}{dt} = k_{55} \cdot [p27] \cdot [aCycA\_Cdk2] - k_{51} \cdot [p27\_aCycA\_Cdk2] \quad \text{(A-33)}$$

$$\frac{d[p21\_aCycA\_Cdk2]}{dt} = k_{28} \cdot [p21] \cdot [aCycA\_Cdk2] - k_{27} \cdot [p21\_aCycA\_Cdk2] \quad \text{(A-34)}$$

$$\frac{d[iSCF]}{dt} = k_{91} \cdot [aSCF] \cdot [aAPC\_Cdh1] - k_{92} \cdot [aCycE\_Cdk2] \cdot [iSCF] \quad \text{(A-35)}$$

$$\frac{d[aSCF]}{dt} = k_{92} \cdot [aCycE\_Cdk2] \cdot [iSCF] - k_{91} \cdot [aSCF] \cdot [aAPC\_Cdh1] \quad \text{(A-36)}$$

$$\frac{d[iBMyb]}{dt} = k_{93} \cdot [E2F] - k_{94} \cdot [iBMyb] \cdot [aCycA\_Cdk2] \quad \text{(A-37)}$$

$$\frac{d[aBMyb]}{dt} = k_{94} \cdot [iBMyb] \cdot [aCycA\_Cdk2] - k_{95} \cdot [aBMyb] \quad \text{(A-38)}$$

$$\frac{d[NFY]}{dt} = k_{96} \cdot [aCycA\_Cdk2] - k_{97} \cdot [NFY] \quad \text{(A-39)}$$

A.3.4 Tyrosine Phosphatase Module

The dynamics of this module can be formulated as follows:

$$\frac{d[iCdc25A]}{dt} = k_{98} \cdot [E2F] + k_{99} \cdot [aCdc25A] - (k_{100} + k_{101} \cdot ([aCycE\_Cdk2] + [aCycA\_Cdk2]) + k_{102} \cdot [aChk1]) \cdot [iCdc25A] \quad \text{(A-40)}$$

$$\frac{d[aCdc25A]}{dt} = k_{101} \cdot ([aCycE\_Cdk2] + [aCycA\_Cdk2]) \cdot [iCdc25A] - (k_{103} + k_{99} + k_{104} \cdot [aChk1]) \cdot [aCdc25A] \quad \text{(A-41)}$$

A.4 G2-M Checkpoint Signalling Sub-system

A.4.1 Tyrosine Kinase Module

The temporal dynamics of this module can be written as follows:

$$\frac{d[iWee1]}{dt} = [aWee1] \cdot (k_{105} \cdot [aPlk1]) - (k_{106} + k_{107} \cdot [aSCF]) \cdot [iWee1] \quad \text{(A-42)}$$

$$\frac{d[aWee1]}{dt} = k_{108} + k_{106} \cdot [iWee1] - k_{105} \cdot [aPlk1] \cdot [aWee1] \quad \text{(A-43)}$$

A.4.2 Tyrosine Phosphatase Module

The dynamics of Tyrosine Phosphatase module can be written as follows:

$$\frac{d[iCdc25C]}{dt} = k_{109} + k_{110} \cdot [aCdc25C] - (k_{111} \cdot [aChk1] + k_{112} \cdot ([aCycB\_Cdk1\_Cyto] + [aCycB\_Cdk1\_Nuc]) + k_{113} \cdot [aPlk1]) \cdot [iCdc25C] \quad \text{(A-44)}$$

$$\frac{d[aCdc25C]}{dt} = k_{112} \cdot [iCdc25C] \cdot ([aCycB\_Cdk1\_Cyto] + [aCycB\_Cdk1\_Nuc]) + k_{113} \cdot [iCdc25C] \cdot [aPlk1] + k_{114} \cdot [aCdc25CP\_S216] - (k_{110} + k_{115} + k_{116} \cdot [aChk1]) \cdot [aCdc25C] \quad \text{(A-45)}$$

$$\frac{d[iCdc25CP\_S216]}{dt} = k_{111} \cdot [iCdc25C] \cdot [aChk1] + k_{117} \cdot [aCdc25CP\_S216] - (k_{118} \cdot ([aCycB\_Cdk1\_Cyto] + [aCycB\_Cdk1\_Nuc]) + k_{119} \cdot [aPlk1] + k_{35} \cdot [14\_3\_3\sigma]) \cdot [iCdc25CP\_S216] \quad \text{(A-46)}$$

$$\frac{d[aCdc25CP\_S216]}{dt} = k_{116} \cdot [aCdc25C] \cdot [aChk1] + k_{118} \cdot [iCdc25CP\_S216] \cdot ([aCycB\_Cdk1\_Cyto] + [aCycB\_Cdk1\_Nuc]) + k_{119} \cdot [iCdc25CP\_S216] \cdot [aPlk1] - (k_{114} + k_{117}) \cdot [aCdc25CP\_S216] \quad \text{(A-47)}$$

$$\frac{d[14\_3\_3\sigma\_iCdc25CP\_S216]}{dt} = k_{35} \cdot [iCdc25CP\_S216] \cdot [14\_3\_3\sigma] - k_{120} \cdot [14\_3\_3\sigma\_iCdc25CP\_S216] \quad \text{(A-48)}$$

A.4.3 Plk1-Related Module

The dynamics of Plk1-Related module can be written as follows:

$$\frac{d[iPlk1]}{dt} = k_{121} \cdot [aPlk1] \cdot [aAPC\_Cdh1] - k_{122} \cdot [iPlk] \cdot [aCycB\_Cdk1\_Cyto] \quad \text{(A-49)}$$

$$\frac{d[aPlk1]}{dt} = k_{122} \cdot [iPlk] \cdot [aCycB\_Cdk1\_Cyto] - k_{121} \cdot [aPlk1] \cdot [aAPC\_Cdh1] \quad \text{(A-50)}$$

A.4.4 Cdk1-Related Module

The Cdk1-Related module has the following temporal dynamics:

$$\frac{d[CycB]}{dt} = k_{123} \cdot [NFY] + [iCycB\_Cdk1\_Cyto] \cdot (k_{124} + k_{125} \cdot [Gadd45]) - (k_{126} + k_{127} \cdot [Cdk1] + (k_{128} \cdot [aAPC\_Cdc20] + k_{129} \cdot [aAPC\_Cdh1])) \cdot [CycB] \quad \text{(A-51)}$$

$$\frac{d[Cdk1]}{dt} = k_{130} \cdot [iCycB\_Cdk1\_Cyto] \cdot ([aAPC\_Cdc20] + [aAPC\_Cdh1]) + [aCycB\_Cdk1\_Cyto] \cdot (k_{131} \cdot [aAPC\_Cdc20] + k_{132} \cdot [aAPC\_Cdh1]) + [iCycB\_Cdk1\_Cyto] \cdot (k_{124} + k_{125} \cdot [Gadd45]) - k_{127} \cdot [CycB \cdot Cdk1] \quad \text{(A-52)}$$

$$\frac{d[iCycB\_Cdk1\_Cyto]}{dt} = k_{127} \cdot [CycB] \cdot [Cdk1] + k_{133} \cdot [aCycB\_Cdk1\_Cyto] - (k_{124} + k_{125} \cdot [Gadd45] + k_{134} \cdot ([aCdc25C] + [aCdc25CP\_S216]) + k_{130} \cdot ([aAPC\_Cdc20] + [aAPC\_Cdh1])) \cdot [iCycB\_Cdk1\_Cyto] \quad \text{(A-53)}$$

$$\frac{d[aCycB\_Cdk1\_Cyto]}{dt} = k_{135} \cdot [aCycB\_Cdk1\_Nuc] + k_{134} \cdot [iCycB\_Cdk1\_Cyto] \cdot ([aCdc25C] + [aCdc25CP\_S216]) - (k_{133} + k_{131} \cdot [aAPC\_Cdc20] + k_{132} \cdot [aAPC\_Cdh1] - k_{136} \cdot [aPlk1]) \cdot [aCycB\_Cdk1\_Nuc] \quad \text{(A-54)}$$

$$\frac{d[iCycB\_Cdk1\_Nuc]}{dt} = k_{137} \cdot [aCycB\_Cdk1\_Nuc] * [aWee1] - k_{138} \cdot [iCycB\_Cdk1\_Nuc] \cdot [aCdc25C] - k_{139} \cdot ([aAPC\_Cdc20] + [aAPC\_Cdh1]) \cdot [iCycB\_Cdk1\_Nuc] \quad \text{(A-55)}$$

$$\frac{d[aCycB\_Cdk1\_Nuc]}{dt} = k_{136} \cdot [aCycB\_Cdk1\_Cyto] \cdot [aPlk1] + k_{138} \cdot [iCycB\_Cdk1\_Nuc] \cdot [aCdc25C] + k_{29} \cdot [p21\_aCycB\_Cdk1\_Nuc] - (k_{135} + k_{137} \cdot [aWee1] + k_{140} \cdot [aAPC\_Cdc20] + k_{141} \cdot [aAPC\_Cdh1] + k_{30} \cdot p21) \cdot [aCycB\_Cdk1\_Nuc] \quad \text{(A-56)}$$

$$\frac{d[p21\_aCycB\_Cdk1\_Nuc]}{dt} = k_{30} \cdot [aCycB\_Cdk1\_Nuc] \cdot [p21] - k_{29} \cdot [p21\_aCycB\_Cdk1\_Nuc] \quad \text{(A-57)}$$

A.4.5 APC-Related Module

The mathematical equations of this module are as follows:

$$\frac{d[iAPC\_Cdc20]}{dt} = k_{142} \cdot [aAPC\_Cdc20] \cdot [aAPC\_Cdh1] - (k_{143} \cdot [aCycB\_Cdk1\_Nuc] + k_{148} \cdot [aPlk1]) \cdot [iAPC\_Cdc20] \quad \text{(A-58)}$$

$$\frac{d[aAPC\_Cdc20]}{dt} = (k_{143} \cdot [aCycB\_Cdk1\_Nuc] + k_{148} \cdot [aPlk1]) \cdot [iAPC\_Cdc20] - k_{142} \cdot [aAPC\_Cdh1] \cdot [aAPC\_Cdc20] \quad \text{(A-59)}$$

$$\frac{d[iAPC\_Cdh1]}{dt} = k_{144} \cdot [aAPC\_Cdh1] \cdot ([aCycB\_Cdk1\_Nuc] + [aCycA\_Cdk2] + [aCycE\_Cdk2]) - k_{145} \cdot [iAPC\_Cdh1] \quad \text{(A-60)}$$

$$\frac{d[aAPC\_Cdh1]}{dt} = k_{145} \cdot [iAPC\_Cdh1] - k_{144} \cdot ([aCycB\_Cdk1\_Nuc] + [aCycA\_Cdk2] + [aCycE\_Cdk2]) \cdot [aAPC\_Cdh1] \quad \text{(A-61)}$$

Appendix B

Initial Values of Concentration of Chemical Species of the Comprehensive Mathematical Model

This section contains initial values of concentration of chemical species of the comprehensive mathematical model presented in Chapter 3. The initial values are presented in Table B. 1 (they have been mainly taken from the mathematical model of Iwamoto et al. (2011)).

Table B. 1 Initial values of concentration (mg/ml) of chemical species used in the comprehensive mathematical model presented in Chapter 3.

Chemical Specie	Initial Value
Cyclin D	0.03
Cdk4	5
CycD_Cdk4	0.01
p21	0
p21_CycD_Cdk4	0
p27	1
p27_CycD_Cdk4	0.001
E2F_pRb	1.95
E2F_pRbPP	0.001
pRbPP	0.01
pRbPPP	0.01
pRb	0.05
E2F	0
iBMyb	0
aBMyb	0
Cyclin E	0.001
iCycE_Cdk2	0.001
Cdk2	15

iCdc25A	0.001
aCdc25A	1e-04
aCycE_Cdk2	0.001
p27_aCycE_Cdk2	0.1
p21_aCycE_Cdk2	0
Cyclin A	4e-05
iCycA_Cdk2	4e-04
aCycA_Cdk2	1e-04
p27_aCycA_Cdk2	1e-04
p21_aCycA_Cdk2	0
NFY	0
iPP1	0.1
aPP1	0.9
iCdc25C	1e-06
aCdc25C	1e-06
iCdc25CP_S216	0.03
aCdc25CP_S216	0
14-3-3σ	2
14-3-3σ_iCdc25CP_S216	0.03
Cyclin B	0
Cdk1	10
iCycB_Cdk1_Cyto	1e-04
aCycB_Cdk1_Cyto	1e-04
iCycB_Cdk1_Nuc	0
aCycB_Cdk1_Nuc	0
p21_aCycB_Cdk1_Nuc	0
iWee1	0
aWee1	0.001

iAPC_Cdc20	0.9
aAPC_Cdc20	0.1
iAPC_Cdh1	0.1
aAPC_Cdh1	0.9
p53	0.0265
ATM	0
Mdm2	2.35e-04
Im	0
iChk2	0.99
aChk2	0.01
iSCF	0.9
aSCF	0.1
Gaddα45	1e-04
acMyc	0.1
icMyc	0.9
aPlk1	0.1
iPlk1	0.9

Appendix C

Parameters of the Comprehensive Mathematical Model

This section contains parameters of the comprehensive mathematical model presented in Chapter 3. The kinetic parameters and the corresponding biochemical meaning are shown in Table C. 1. The parameters have been mainly taken from the mathematical model of Iwamoto et al. (2011).

Table C. 1 Kinetic parameters and their biochemical meaning used in the comprehensive mathematical model presented in Chapter 3. The unit is concentration change per hour.

Kinetic Parameter	Biochemical meaning	Value
k_1	rate of acMyc inactivation	0.001
k_2	rate of icMyc activation	0.01
k_3	rate of aChk2 inactivation	1
k_4	rate of iChk2 activation through ATM	1
k_5	rate of ATM activation	0.2
k_6	rate of ATM inactivation	0.01
k_7	rate of DNA damage repair	1e-08
k_8	rate of p53 basal synthesis	1e-04
k_9	rate of p53 synthesis through ATM	0.07
k_{10}	rate of p53 degradation	0.001
k_{11}	rate of p53 degradation through Mdm2	0.0556
k_{12}	rate of suppression of p53 degradation through DSB(t)	0.772
k_{13}	rate of suppression of Mdm2-mediated degradation of p53	0.02
k_{14}	rate of Mdm2 basal synthesis	9.4e-04

k_{15}	synthesis rate of Mdm2 through IF	10
k_{16}	Hill function constant	9.5
k_{17}	rate of Mdm2 degradation	0.02
k_{18}	rate of p53 activity through binding to DNA after damage	6
k_{19}	rate of Mdm2 and p53 association	0.004
k_{20}	rate of IF degradation	0.005
k_{21}	rate of p21 basal synthesis	5e-05
k_{22}	rate of p21 synthesis through p53	0.001
k_{23}	rate of p21_CycD_Cdk4 dissociation	0.005
k_{24}	rate of p21 and CycD_Cdk4 association	5e-04
k_{25}	rate of p21_aCycE_Cdk2 dissociation	1.75e-04
k_{26}	rate of p21 and aCycE_Cdk2 association	0.0225
k_{27}	rate of p21_aCycA_Cdk2 dissociation	1.75e-04
k_{28}	rate of p21 and aCycA_Cdk2 association	0.0025
k_{29}	rate of p21_aCycB_Cdk1_Nuc dissociation	1.75e-04
k_{30}	rate of p21 and aCycB_Cdk1_Nuc association	0.0225
k_{31}	rate of p21 degradation	0.005
k_{32}	rate of 14-3-3σ basal synthesis	1
k_{33}	rate of 14-3-3σ synthesis through p53	0.01
k_{34}	rate of 14-3-3σ degradation	1
k_{35}	rate of 14-3-3σ and iCdc25CP_S216 association	100
k_{36}	rate of Gaddα45 basal synthesis	1e-05

k_{37}	rate of Gaddα45 synthesis through p53	1e-04
k_{38}	rate of Gaddα45 degradation	1e-06
k_{39}	rate of Cyclin D basal synthesis	1e-05
k_{40}	rate of Cyclin D synthesis through acMyc	0.003
k_{41}	rate of CycD_Cdk4 dissociation	0.0025
k_{42}	rate of Cyclin D and Cdk4 association	0.08
k_{43}	rate of Cyclin D degradation through aSCF	0.2
k_{44}	rate of Cyclin D degradation	5e-05
k_{45}	rate of CycD_Cdk4 degradation to Cdk4	8e-05
k_{46}	rate of p27_CycD_Cdk4 degradation to Cdk4	0.001
k_{47}	rate of p27_CycD_Cdk4 dissociation	5e-04
k_{48}	rate of p27 and CycD_Cdk4 association	0.009
k_{49}	rate of p27 basal synthesis	0.0015
k_{50}	rate of p27_aCycE_Cdk2 dissociation	1.75e-04
k_{51}	rate of p27_aCycA_Cdk2 dissociation	1.75e-04
k_{52}	rate of p27 and aCycE_Cdk2 association	0.0225
k_{53}	degradation rate of p27 through aCycE_Cdk2	0.05
k_{54}	degradation rate of p27 through aCycA_Cdk2	0.0015
k_{55}	rate of p27 and aCycA_Cdk2 association	0.0025
k_{56}	rate of pRb and E2F association	5e-02
k_{57}	rate of E2F_pRb phosphorylation through CycD_Cdk4	0.0025
k_{58}	rate of E2F_pRb phosphorylation through p27_CycD_Cdk4	0.0025

k_{59}	rate of E2F_pRb phosphorylation through p21_CycD_Cdk4	0.0025
k_{60}	rate of E2F_pRbPP dissociation to E2F & pRbPPP through aCycE_Cdk2	0.04
k_{61}	rate of E2F_pRbPP dissociation to E2F & pRbPPP through aCycA_Cdk2	0.0025
k_{62}	rate of inactivation of PP1	1e-03
k_{63}	rate of activation of PP1 through aCycB_Cdk1_Nuc	5e-02
k_{64}	rate of dephosphorylation of pRbPPP to pRb through PP1	5e-03
k_{65}	rate of pRb basal synthesis	5e-05
k_{66}	rate of pRb degradation	5e-05
k_{67}	rate of E2F basal synthesis	5e-04
k_{68}	rate of E2F synthesis through E2F	5e-08
k_{69}	rate of E2F degradation	5e-04
k_{70}	rate of Cyclin E synthesis through E2F	0.1
k_{71}	rate of Cyclin E and Cdk2 association	0.0025
k_{72}	rate of aCycE_Cdk2 dissociation	2.5e-05
k_{73}	rate of Cyclin E degradation	0.0025
k_{74}	rate of Cyclin E degradation through aSCF	0.01
k_{75}	rate of Cyclin A synthesis through E2F	8e-05
k_{76}	rate of Cyclin A synthesis through aBMyb	2e-04
k_{77}	rate of Cyclin A synthesis through NFY	1e-06
k_{78}	rate of iCycA_Cdk2 dissociation	2e-04
k_{79}	rate of Cyclin A degradation	5e-04
k_{80}	rate of Cyclin A and Cdk2 association	5e-04

k_{81}	rate of Cyclin A degradation through aAPC_Cdc20	0.005
k_{82}	rate of Cyclin A degradation through aAPC_Cdh1	0.005
k_{83}	rate of iCycE_Cdk2 degradation to Cdk2	0.005
k_{84}	rate of aCycE_Cdk2 degradation to Cdk2	0.05
k_{85}	rate of iCycA_Cdk2 degradation to Cdk2 through aAPC_Cdc20 & aAPC_Cdh1	0.005
k_{86}	rate of aCycA_Cdk2 degradation to Cdk2 through aAPC_Cdc20 & aAPC_Cdh1	0.0075
k_{87}	rate of aCycE_Cdk2 inactivation to form iCycE_Cdk2	0.00175
k_{88}	rate of iCycE_Cdk2 dephosphorylation and activation through aCdc25A	0.006
k_{89}	rate of aCycA_Cdk2 inactivation to form iCycA_Cdk2	5e-05
k_{90}	rate of iCycA_Cdk2 dephosphorylation and activation through aCdc25A	9e-04
k_{91}	rate of aSCF inactivation through aAPC_Cdh1	0.015
k_{92}	rate of iSCF activation through aCycE_Cdk2	0.01
k_{93}	rate of iBMyb production through E2F	0.05
k_{94}	rate of iBMyb activation through aCycA_Cdk2	0.05
k_{95}	rate of aBMyb degradation	0.002
k_{96}	rate of NFY production mediated by aCycA_Cdk2	0.001
k_{97}	rate of NFY degradation	0.005
k_{98}	rate of iCdc25A synthesis through E2F	0.04
k_{99}	rate of aCdc25A inactivation	0.005
k_{100}	rate of iCdc25A degradation	0.005

k_{101}	rate of iCdc25A degradation through aCycE_Cdk2 & aCycA_Cdk2	0.05
k_{102}	rate of iCdc25A degradation through aChk1	0.001
k_{103}	rate of aCdc25A degradation	5e-04
k_{104}	rate of aCdc25A degradation through aChk1	0.001
k_{105}	rate of aWee1 phosphorylation and inactivation through aPlk1	0.1
k_{106}	rate of iWee1 activation	1
k_{107}	rate of iWee1 degradation through aSCF	1
k_{108}	rate of aWee1 basal synthesis	2e-04
k_{109}	rate of iCdc25C basal synthesis	1e-05
k_{110}	rate of aCdc25C inactivation	0.01
k_{111}	rate of iCdc25C phosphorylation on Serine216 through aChk1	0.001
k_{112}	rate of iCdc25C activation through aCycB_Cdk1_Cyto & aCycB_Cdk1_Nuc	1
k_{113}	rate of iCdc25C activation through aPlk1	0.1
k_{114}	rate of aCdc25CP_S216 dephosphorylation to form aCdc25C	0.01
k_{115}	rate of aCdc25C degradation	1e-04
k_{116}	rate of aCdc25C phosphorylation on Serine216 through aChk1	0.001
k_{117}	rate of aCdc25CP_S216 inactivation	0.01
k_{118}	rate of iCdc25CP_S216 phosphorylation and activation through aCycB_Cdk1_Cyto & aCycB_Cdk1_Nuc	1
k_{119}	rate of iCdc25CP_S216 phosphorylation and activation through aPlk1	0.1
k_{120}	rate of 14-3-3σ_iCdc25CP_S216 degradation	1
k_{121}	rate of aPlk1 inactivation through aAPC_Cdh1	0.1

k_{122}	rate of iPlk1 activation through aCycB_Cdk1_Cyto	0.015
k_{123}	rate of Cyclin B synthesis through NFY	0.02
k_{124}	rate of iCycB_Cdk1_Cyto dissociation	1e-05
k_{125}	rate of iCycB_Cdk1_Cyto dissociation mediated by Gaddα45	2e-04
k_{126}	rate of Cyclin B degradation	0.005
k_{127}	rate of Cyclin B and Cdk1 association	0.00125
k_{128}	rate of Cyclin B degradation through aAPC_Cdc20	0.001
k_{129}	rate of Cyclin B degradation through aAPC_Cdh1	0.3
k_{130}	rate of iCycB_Cdk1_Cyto degradation to form Cdk1 through aAPC_Cdc20 & aAPC_Cdh1	0.005
k_{131}	rate of aCycB_Cdk1_Cyto degradation to form Cdk1 through aAPC_Cdc20	0.005
k_{132}	rate of aCycB_Cdk1_Cyto degradation to form Cdk1 through aAPC_Cdh1	0.05
k_{133}	rate of aCycB_Cdk1_Cyto inactivation	1e-04
k_{134}	rate of iCycB_Cdk1_Cyto activation through aCdc25C & aCdc25CP_S216	0.05
k_{135}	rate of translocation of aCycB_Cdk1 from Nucleus to Cytoplasm	5e-05
k_{136}	rate of translocation of aCycB_Cdk1 from Cytoplasm to Nucleus mediated by aPlk1	0.01
k_{137}	rate of aCycB_Cdk1_Nuc phosphorylation and inactivation through aWee1	5e-04
k_{138}	rate of iCycB_Cdk1_Nuc dephosphorylation and activation through aCdc25C	0.01
k_{139}	rate of iCycB_Cdk1_Nuc degradation through aAPC_Cdc20 &	0.005

	aAPC_Cdh1	
k_{140}	rate of aCycB_Cdk1_Nuc degradation through aAPC_Cdc20	0.005
k_{141}	rate of aCycB_Cdk1_Nuc degradation through aAPC_Cdh1	0.03
k_{142}	rate of aAPC_Cdc20 inactivation through aAPC_Cdh1	0.05
k_{143}	rate of iAPC_Cdc20 activation through aCycB_Cdk1_Nuc	0.01
k_{144}	rate of aAPC_Cdh1 inactivation through aCycE_Cdk2 & aCycA_Cdk2 & aCycB_Cdk1_Nuc	0.1
k_{145}	rate of iAPC_Cdh1 activation	0.005
k_{146}	EF2 degradation rate through aCycA_Cdk2	0.01
k_{147}	rate of Cyclin D degradation through aAPC_Cdc20	10
k_{148}	rate of iAPC_Cdc20 activation through aPlk1	1e-04
GF	Growth Factor	1
DDS	DNA Damage Strength	0.012

Appendix D

Simulation of the Comprehensive Mathematical Model Over More Than One Cycle

We assessed the dynamics of the comprehensive mathematical model presented in Chapter 3 over more than one cell proliferation cycles and the results are shown in Figure D.1. The model produces cyclic behaviour reasonably well. There is still some dampening in the behaviour and indicates that further investigation is required in future to modify the model to further improve cyclic behaviour.

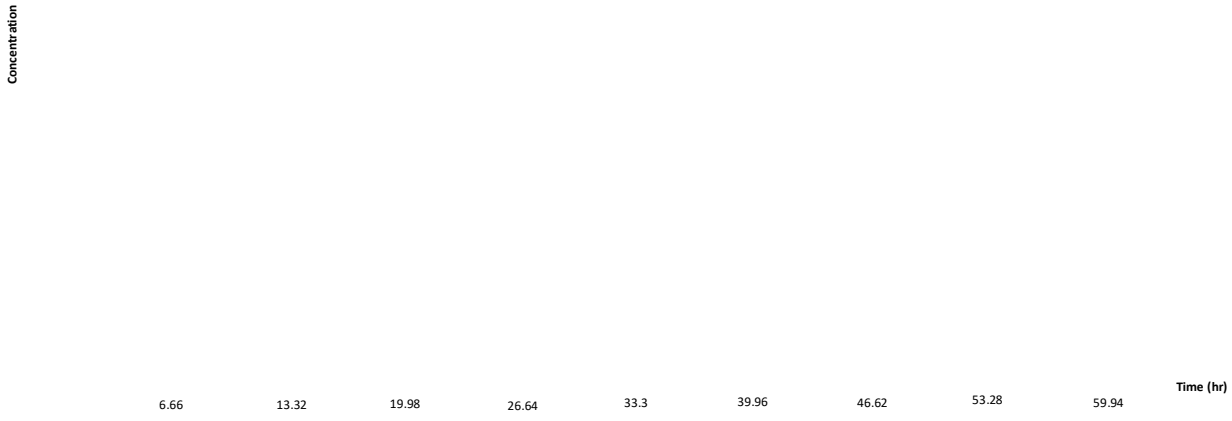

Figure D.1 Cyclic behaviour of the comprehensive mathematical model presented in Chapter 3; [x-axis indicates time (simulation time units as well as hours); y-axis indicates protein concentration (mg/ml)].

Appendix E

Results of GSA on Iwamoto et al. Model

The most sensitive parameters from Global Sensitivity Analysis (GSA) on Iwamoto et al. (2011) model for G1-S under no DDS is presented below (sorted based on the level of significance).

- $k1$: synthesis of Cyclin D (through GF)
- $k34$: rate of synthesis of p27
- $k24$: rate of association of p27 and CycE_Cdk2
- $k5$: synthesis of Cyclin E by E2F
- $k80$: synthesis of Cdc25A through E2F
- $k82$: Activation of Cdc25A through CycE_Cdk2 and CycA_Cdk2
- $k20$: association of p27 and Cyc_Cdk4
- $k22$: Activation of CycE_Cdk2 through Cdc25A

Results of GSA on Iwamoto et al. (2011) model for G2-M under no DDS show that all the above parameters as well as the parameters presented below are significant.

- $k9$: synthesis of Cyclin A by B-Myb
- $K89$: synthesis of NFY through CycA_Cdk2
- $k91$: synthesis of Cyclin B by NFY
- $k93$: association of Cyclin B and Cdk1
- $k105$: synthesis of B-Myb by E2F
- $k110$: activation of Cdc25C through CycB_Cdk1 (Nuc and Cyt)

Therefore, the results of GSA on Iwamoto et al. (2011) model show consistency between the significant parameters identified in our model (presented in Chapter 4) and theirs. The only difference is about c-Myc and PP1 which are absent in Iwamoto et al. model (in fact, these are the most effective elements in the model).

Appendix F

Kinetic Parameters of the MLHPN Model

Kinetic parameters and corresponding biochemical meaning of the MLHPN model (presented in Chapter 6) are shown in Table F. 1. The software used for simulation and analysis is Matlab.

Table F. 1 Kinetic parameters of the MLHPN model and their biochemical meaning.

Kinetic Parameter	Biochemical meaning	Value
k_1	basal production rate of CycD_Cdk4	0.01
k_2	production rate of CycD_Cdk4 through aG0_G1_TF	1
k_3	The rate showing the effect of aDDS_Ctrls on activity of CycD_Cdk4	0.1
k_4	The rate showing the effect of ap27 on activity of CycD_Cdk4	0.001
k_5	basal degradation rate of CycD_Cdk4	0.065
k_6	degradation rate of CycD_Cdk4 through aSCF	0.05
k_7	degradation rate of CycD_Cdk4 through aAPC_Cdc20A	0.8
k_8	degradation rate of CycD_Cdk4 through aAPC_Cdc20B	0.8
k_9	basal production rate of CycE_Cdk2	0.1
k_{10}	production rate of CycE_Cdk2 through aG1_S_TF	5
k_{11}	production rate of CycE_Cdk2 through the effect of aCdc25A	0.001
k_{12}	basal degradation rate of CycE_Cdk2	0.05
k_{13}	degradation rate of CycE_Cdk2 through aSCF	0.6
k_{14}	The rate showing the effect of aDDS_Ctrls on activity of CycE_Cdk2	0.1
k_{15}	The rate showing the effect of ap27 on activity of CycE_Cdk2	0.01
k_{16}	basal production rate of CycA_Cdk2	0.2
k_{17}	production rate of CycA_Cdk2 through aG1_S_TF	0.2
k_{18}	production rate of CycA_Cdk2 through aG2_M_TF	7.5
k_{19}	production rate of CycA_Cdk2 through the effect of aCdc25A	0.001
k_{20}	basal degradation rate of CycA_Cdk2	0.1

k_{21}	degradation rate of CycA_Cdk2 through aAPC_Cdc20A	2
k_{22}	degradation rate of CycA_Cdk2 through aAPC_Cdh1	0.8
k_{23}	The rate showing the effect of ap27 on activity of CycA_Cdk2	0.01
k_{24}	The rate showing the effect of aDDS_Ctrls on activity of CycA_Cdk2	0.1
k_{25}	basal production rate of CycB_Cdk1	0.1
k_{26}	production rate of CycB_Cdk1 through aG2_M_TF	1
k_{27}	production rate of CycB_Cdk1 through the effect of aCdc25C	0.001
k_{28}	basal degradation rate of CycB_Cdk1	0.05
k_{29}	degradation rate of CycB_Cdk1 through aAPC_Cdc20B	2
k_{30}	degradation rate of CycB_Cdk1 through aAPC_Cdh1	0.8
k_{31}	The rate showing the effect of aDDS_Ctrls on activity of CycB_Cdk1	0.1

Appendix G

Initial Values of Places of the MLHPN Model

Definition of places, place type and corresponding initial values for the MLHPN model (presented in Chapter 6) are given in Table G. 1.

Table G. 1 Places of the MLHPN model and corresponding initial values.

Place	Type	Definition	Initial Value
CycD_Cdk4	Continuous	This place represents the CycD_Cdk4 complex	0
CycE_Cdk2	Continuous	This place represents the CycE_Cdk2 complex	0
CycA_Cdk2	Continuous	This place represents the CycA_Cdk2 complex	0
CycB_Cdk1	Continuous	This place represents the CycB_Cdk1 complex	0
DNA_Damage	Macro	This Macro place comprises the components associated with DNA damage sub-system	N/A
p27	Macro	This Macro place represents the elements related to Cyclin Dependent Kinase Inhibitor p27	N/A
UBQ_D	Macro	This macro place comprises the elements associated with degradation of CycD_Cdk4	N/A
UBQ_E	Macro	This macro place encompasses the elements related to degradation of CycE_Cdk2	N/A
UBQ_A	Macro	This macro place comprises the elements associated with degradation of CycA_Cdk2	N/A
UBQ_B	Macro	This macro place includes the elements related to degradation of CycB_Cdk1	N/A
Cdc25A	Macro	This Macro place represents the elements related to Tyrosine Phosphatase Cdc25A	N/A
Cdc25C	Macro	This Macro place comprises the elements associated with Tyrosine Phosphatase Cdc25C	N/A
GF	Discrete	Growth Factor	1
iG0_G1_TF	Discrete	Inactive G0_G1 transcription factor (mainly corresponds to transcription factor c-Myc)	1
aG0_G1_TF	Discrete	Active G0_G1 transcription factor (mainly corresponds to	0

		transcription factor c-Myc)	
iG1_S_TF	Discrete	Inactive G1_S transcription factor (mainly corresponds to transcription factor E2F)	1
aG1_S_TF	Discrete	Active G1_S transcription factor (mainly corresponds to transcription factor E2F)	0
aG2_M_TF	Discrete	Inactive G2_M transcription factor (mainly corresponds to transcription factor NFY)	0
iG2_M_TF	Discrete	Active G2_M transcription factor (mainly corresponds to transcription factor NFY)	1
ip27	Discrete	Inactive p27	0
ap27	Discrete	Active p27	1
iCdc25A	Discrete	Inactive Cdc25A	0
aCdc25A	Discrete	Active Cdc25A	1
iCdc25C	Discrete	Inactive Cdc25C	0
aCdc25C	Discrete	Active Cdc25C	1
iSCF	Discrete	Inactive SCF	0
aSCF	Discrete	Active SCF	1
iAPC_Cdh1	Discrete	Inactive APC_Cdh1	0
aAPC_Cdh1	Discrete	Active APC_Cdh1	1
iAPC_Cdc20A	Discrete	Inactive APC_Cdc20A	0
aAPC_ Cdc20A	Discrete	Active APC_ Cdc20A	1
iAPC_ Cdc20B	Discrete	Inactive APC_ Cdc20B	0
aAPC_ Cdc20B	Discrete	Active APC_ Cdc20B	1
Early_G1	Discrete	The discrete place representing early G1 phase	1
Mid_G1	Discrete	The discrete place representing mid G1 phase	0
Late_G1	Discrete	The discrete place representing late G1 phase	0
S	Discrete	The discrete place representing S phase	0
G2	Discrete	The discrete place representing G2 phase	0
Prophase	Discrete	The discrete place representing Prophase phase	0
Metaphase	Discrete	The discrete place representing Metaphase phase	0

Anaphase	Discrete	The discrete place representing Anaphase phase	0
Telophase	Discrete	The discrete place representing Telophase phase	0
DDS	Discrete	The discrete place representing DNA damage	0
iDDS_Ctrls	Discrete	DNA damage signalling controllers in its inactive form	1
aDDS_Ctrls	Discrete	DNA damage signalling controllers in its active form	0

Appendix H

Transitions of the MLHPN Model

Transitions of the MLHPN model (presented in Chapter 6) and type of transitions together with their definitions are presented in Tables H. 1.

Table H. 1 Transitions of the MLHPN model and their corresponding definition.

Transition	Transition type	Definition	Firing Rule
T1	Continuous	The transition associated with production of CycD_Cdk4	(aG0_G1_TF) *OR* (ap27) *OR* (aDDS_Ctrls)
T2	Continuous	The transition associated with degradation of CycD_Cdk4	(aSCF) *OR* (aAPC_Cdc20A) *OR* (aAPC_Cdc20B)
T3	Continuous	The transition associated with degradation of CycE_Cdk2	(aSCF)
T4	Continuous	The transition associated with degradation of CycA_Cdk2	(aAPC_Cdc20A) *OR* (aAPC_Cdh1)
T5	Continuous	The transition associated with degradation of CycB_Cdk1	(aAPC_Cdc20B) *OR* (aAPC_Cdh1)
T6	Continuous	The transition associated with production of CycE_Cdk2	(aG1_S_TF) *OR* aCdc25A *OR* *NOT*(ap27) *OR* *NOT*(aDDS_Ctrls)
T7	Continuous	The transition associated with production of CycA_Cdk2	(aG1_S_TF) *OR* (aG2_M_TF) *OR* aCdc25A *OR* *NOT*(ap27) *OR* *NOT*(aDDS_Ctrls)
T8	Continuous	The transition associated with production of CycB_Cdk1	(aG2_M_TF) *OR* aCdc25C *OR* *NOT*(aDDS_Ctrls)
t1_1	Discrete	The transition presenting the activation of G0_G1_TF	GF
t1_2	Discrete	The transition presenting the inactivation of G0_G1_TF	*NOT*(GF)
t3_1	Discrete	The transition presenting the activation of p27	Early_G1
t3_2	Discrete	The transition presenting the inactivation of p27	Late_G1

t3_3	Discrete	The transition presenting the activation of SCF	S
t3_4	Discrete	The transition presenting the inactivation of SCF	Mid_G1
t4_1	Discrete	The transition presenting the activation of APC_Cdh1	Telophase
t4_2	Discrete	The transition presenting the inactivation of APC_Cdh1	Late_G1
t4_3	Discrete	The transition presenting the activation of APC_Cdc20A	CycB_Cdk1 > 3.9
t4_4	Discrete	The transition presenting the inactivation of APC_Cdc20A	Mid_G1
t5_1	Discrete	The transition presenting the activation of APC_Cdc20B	Prophase
t5_2	Discrete	The transition presenting the inactivation of APC_Cdc20B	Mid_G1
t6_1	Discrete	The transition presenting the activation of G1_S_TF	(Late_G1) *AND* (CycD_Cdk4 > 4.25) *AND* (CycE_Cdk2 > 0.4)
t6_2	Discrete	The transition presenting the inactivation of G1_S _TF	CycA_Cdk2 > 2.3
t6_3	Discrete	The transition presenting the activation of Cdc25A	(Late_G1) *AND* (CycE_Cdk2 > 0.4) *AND* (CycA_Cdk2 > 0.22)
t6_4	Discrete	The transition presenting the inactivation of Cdc25A	Mid_G1
t7_1	Discrete	The transition presenting the activation of G2_M_TF	CycA_Cdk2 > 2.1
t7_2	Discrete	The transition presenting the inactivation of G2_M_TF	Telophase
t8_1	Discrete	The transition presenting the activation of Cdc25C	Prophase
t8_2	Discrete	The transition presenting the inactivation of Cdc25C	Mid_G1
t9_1	Discrete	The transition presenting the activation of DDS_Ctrls	DDS
t9_2	Discrete	The transition presenting the	*NOT*(DDS)

		inactivation of DDS_Ctrls	
G0_G1_Activation	Macro	The transition that encompasses the elements associated with cell cycle start and Growth Factor sub-system	Not Applicable
G1_S_Activation	Macro	The transition that encompasses the elements associated with G1_S checkpoint sub-system	Not Applicable
G2_M_Activation	Macro	The transition that encompasses the elements associated with G2_M checkpoint sub-system	Not Applicable
Sensing_GF	Discrete	The transition associated with changing the cell cycle stage from Early_G1 to Mid_G1	GF
R_Point	Discrete	The transition associated with changing the cell cycle stage from Mid_G1 to Late_G1	CycD_Cdk4 > 4.25
G1_S	Discrete	The transition associated with changing the cell cycle stage from Late_G1 to S	CycE_Cdk2 > 8.5
S_G2	Discrete	The discrete delayed transition associated with changing the cell cycle stage from S to G2	Delay = 7 time units
G2_M	Discrete	The transition associated with changing the cell cycle stage from G2 to M	CycB_Cdk1 > 5.6
Pro_Meta	Discrete	The discrete delayed transition associated with changing the cell cycle stage from Prophase to Metaphase	Delay = 0.75 time units
Meta_Ana	Discrete	The discrete delayed transition associated with changing the cell cycle stage from Metaphase to Anaphase	Delay = 1.5 time units
Ana_Telo	Discrete	The discrete delayed transition associated with changing the cell cycle stage from Anaphase	Delay = 0.5 time units

		to Telophase	
M_G1	Discrete	The transition associated with changing the cell cycle stage from M to G1	CycB_Cdk1 < 0.15

References

Abbas, T., & Dutta, A. (2009). p21 in cancer: intricate networks and multiple activities. *Nature Reviews Cancer, 9*(6), 400-414.

Abraham, R. T. (2001). Cell cycle checkpoint signaling through the ATM and ATR kinases. *Genes & development, 15*(17), 2177-2196.

Abroudi, A., Samarasinghe, S., & Kulasiri, D. (2015). *A Review of Computational Models of Mammalian Cell Cycle*. Paper presented at the meeting of the 21st International Congress on Modelling and Simulation (MODSIM), Australia.

Abroudi, A., Samarasinghe, S., & Kulasiri, D. (2017). A comprehensive complex systems approach to the study and analysis of mammalian cell cycle control system in the presence of DNA damage stress. *Journal of theoretical biology, 429*, 204-228.

Aderem, A. (2005). Systems biology: its practice and challenges. *Cell, 121*(4), 511-513.

Adhikary, S., & Eilers, M. (2005). Transcriptional regulation and transformation by Myc proteins. *Nature Reviews Molecular Cell Biology, 6*(8), 635-645.

Agarwal, M. L., Agarwal, A., Taylor, W. R., & Stark, G. R. (1995). p53 controls both the G2/M and the G1 cell cycle checkpoints and mediates reversible growth arrest in human fibroblasts. *Proceedings of the National Academy of Sciences, 92*(18), 8493-8497.

Aguda, B., & Tang, Y. (1999). The kinetic origins of the restriction point in the mammalian cell cycle. *Cell proliferation, 32*(5), 321-335.

Aguda, B. D. (1999a). A quantitative analysis of the kinetics of the G2 DNA damage checkpoint system. *PNAS, 96*(20), 11352-11357.

Aguda, B. D. (1999b). A quantitative analysis of the kinetics of the G2 DNA damage checkpoint system. *Proceedings of the National Academy of Sciences, 96*(20), 11352-11357.

Alao, J. P. (2007). The regulation of cyclin D1 degradation: roles in cancer development and the potential for therapeutic invention. *Molecular cancer, 6*(1), 24.

Alarcon, T., Byrne, H., & Maini, P. (2004). A mathematical model of the effects of hypoxia on the cell-cycle of normal and cancer cells. *Journal of theoretical biology, 229*(3), 395-411.

Albert, R., & Wang, R. S. (2009). Discrete dynamic modeling of cellular signaling networks. *Methods in enzymology, 467*, 281-306.

Alberts, B., Johnson, A., Lewis, J., Morgan, D., Raff, M., Roberts, K., & Walter, P. (2014). *Molecular Biology of the Cell, Sixth Edition*: Taylor & Francis Group.

Alfieri, R., Barberis, M., Chiaradonna, F., Gaglio, D., Milanesi, L., Vanoni, M., . . . Alberghina, L. (2009). Towards a systems biology approach to mammalian cell cycle: modeling the entrance into S phase of quiescent fibroblasts after serum stimulation [journal article]. *BMC Bioinformatics, 10*(12), S16. doi:10.1186/1471-2105-10-s12-s16

Alfieri, R., Bartocci, E., Merelli, E., & Milanesi, L. (2011). Modeling the cell cycle: From deterministic models to hybrid systems. *Biosystems, 105*(1), 34-40.

Alon, U. (2006). *An Introduction to Systems Biology: Design Principles of Biological Circuits*: Taylor & Francis.

Altinok, A., Gonze, D., Lévi, F., & Goldbeter, A. (2011). An automaton model for the cell cycle. *Interface focus, 1*(1), 36-47.

Ang, X. L., & Harper, J. W. (2004). Interwoven ubiquitination oscillators and control of cell cycle transitions. *Science Signaling, 2004*(242), pe31.

Bai, S., Goodrich, D., Thron, C. D., Tecarro, E., & Obeyesekere, M. (2003). Theoretical and experimental evidence for hysteresis in cell proliferation. *Cell Cycle, 2*(1), 46-51.

Baldan, P., Cocco, N., Marin, A., & Simeoni, M. (2010). Petri nets for modelling metabolic pathways: a survey. *Natural Computing, 9*(4), 955-989.

Baluchamy, S., Rajabi, H. N., Thimmapaya, R., Navaraj, A., & Thimmapaya, B. (2003). Repression of c-Myc and inhibition of G1 exit in cells conditionally overexpressing p300 that is not dependent on its histone acetyltransferase activity. *Proceedings of the National Academy of Sciences, 100*(16), 9524-9529.

Banin, S., Moyal, L., Shieh, S.-Y., Taya, Y., Anderson, C., Chessa, L., . . . Shiloh, Y. (1998). Enhanced phosphorylation of p53 by ATM in response to DNA damage. *Science, 281*(5383), 1674-1677.

Bar-Or, R. L., Maya, R., Segel, L. A., Alon, U., Levine, A. J., & Oren, M. (2000). Generation of oscillations by the p53-Mdm2 feedback loop: a theoretical and experimental study. *Proceedings of the National Academy of Sciences, 97*(21), 11250-11255.

Bartek, J., Falck, J., & Lukas, J. (2001). CHK2 kinase—a busy messenger. *Nature Reviews Molecular Cell Biology, 2*(12), 877-886.

Bartek, J., & Lukas, J. (2001). Mammalian G1-and S-phase checkpoints in response to DNA damage. *Current opinion in cell biology, 13*(6), 738-747.

Bartek, J., & Lukas, J. (2003). Chk1 and Chk2 kinases in checkpoint control and cancer. *Cancer cell, 3*(5), 421-429.

Basse, B., Baguley, B. C., Marshall, E. S., Joseph, W. R., van Brunt, B., Wake, G., & Wall, D. J. (2003). A mathematical model for analysis of the cell cycle in cell lines derived from human tumors. *Journal of mathematical biology, 47*(4), 295-312.

Batchelor, E., Mock, C. S., Bhan, I., Loewer, A., & Lahav, G. (2008). Recurrent initiation: a mechanism for triggering p53 pulses in response to DNA damage. *Molecular cell, 30*(3), 277-289.

Battogtokh, D., & Tyson, J. J. (2006). Periodic forcing of a mathematical model of the eukaryotic cell cycle. *Physical Review E, 73*(1), 011910.

Beishline, K., & Azizkhan-Clifford, J. (2014). Interplay between the cell cycle and double-strand break response in mammalian cells. In E. Noguchi & M. Gadaleta (Eds.), *Cell Cycle Control: Methods in Molecular Biology (Methods and Protocols)* (pp. 41-59). New York: Humana Press.

Benesty, J., Chen, J., Huang, Y., & Cohen, I. (2009). Pearson correlation coefficient. In *Noise reduction in speech processing* (pp. 1-4): Springer, Berlin, Heidelberg.

Berndt, N. (2002). Roles and regulation of serine/threonine-specific protein phosphatases in the cell cycle. *Progress in cell cycle research, 5*, 497-510.

Berns, K., Martins, C., Dannenberg, J.-H., Berns, A., Riele, H. t., & Bernards, R. (2000). p27kip1-independent cell cycle regulation by MYC. *Oncogene, 19*(42), 4822-4827.

Berridge, M. J. (2014). Module 9: Cell Cycle and Proliferation. *Cell Signalling Biology, 6*.

Besson, A., Dowdy, S. F., & Roberts, J. M. (2008). CDK inhibitors: cell cycle regulators and beyond. *Developmental cell, 14*(2), 159-169.

Blain, S. (2008). Switching cyclin D-Cdk4 kinase activity on and off. *Cell Cycle, 7*(7), 892-898.

Blätke, M. A., Heiner, M., & Marwan, W. (2011). *Petri Nets in Systems Biology*: Technical Report, Otto-von-Guericke University Magdeburg, Centre for Systems Biology.

Blomberg, I., & Hoffmann, I. (1999). Ectopic expression of Cdc25A accelerates the G1/S transition and leads to premature activation of cyclin E-and cyclin A-dependent kinases. *Molecular and cellular biology, 19*(9), 6183-6194.

Bollen, M., & Beullens, M. (2002). Signaling by protein phosphatases in the nucleus. *Trends in cell biology, 12*(3), 138-145.

Boutros, R., Dozier, C., & Ducommun, B. (2006). The when and wheres of CDC25 phosphatases. *Current opinion in cell biology, 18*(2), 185-191.

Boutros, R., Lobjois, V., & Ducommun, B. (2007). CDC25 phosphatases in cancer cells: key players? Good targets? *Nature Reviews Cancer, 7*(7), 495-507.

Branzei, D., & Foiani, M. (2008). Regulation of DNA repair throughout the cell cycle. *Nature reviews Molecular cell biology, 9*(4), 297-308.

Brown, E. J., & Baltimore, D. (2003). Essential and dispensable roles of ATR in cell cycle arrest and genome maintenance. *Genes & development, 17*(5), 615-628.

Bucher, N., & Britten, C. (2008). G2 checkpoint abrogation and checkpoint kinase-1 targeting in the treatment of cancer. *British journal of cancer, 98*(3), 523.

Cann, K. L., & Hicks, G. G. (2007). Regulation of the cellular DNA double-strand break response. *Biochemistry and cell biology, 85*(6), 663-674.

Cardozo, T., & Pagano, M. (2004). The SCF ubiquitin ligase: insights into a molecular machine. *Nature reviews Molecular cell biology, 5*(9), 739-751.

Carvajal, D., Tovar, C., Yang, H., Vu, B. T., Heimbrook, D. C., & Vassilev, L. T. (2005). Activation of p53 by MDM2 antagonists can protect proliferating cells from mitotic inhibitors. *Cancer research, 65*(5), 1918-1924.

Cazzalini, O., Scovassi, A. I., Savio, M., Stivala, L. A., & Prosperi, E. (2010). Multiple roles of the cell cycle inhibitor p21CDKN1A in the DNA damage response. *Mutation Research/Reviews in Mutation Research, 704*(1-3), 12-20.

Chae, H.-D., Kim, J.-B., & Shin, D.-Y. (2011). NF-Y binds to both G1-and G2-specific cyclin promoters; a possible role in linking CDK2/Cyclin A to CDK1/Cyclin B. *BMB reports, 44*(8), 553-557.

Chae, H.-D., Yun, J., Bang, Y.-J., & Shin, D. Y. (2004). Cdk2-dependent phosphorylation of the NF-Y transcription factor is essential for the expression of the cell cycle-regulatory genes and cell cycle G1/S and G2/M transitions. *Oncogene, 23*(23), 4084-4088.

Chae, H. D., & Shin, D. Y. (2011). NF-Y binds to both G1-and G2-specific cyclin promoters; a possible role in linking CDK2/Cyclin A to CDK1/Cyclin B. *Biochemistry and Molecurar Biology Reports, 44*(8), 553-557.

Chan, T. A., Hwang, P. M., Hermeking, H., Kinzler, K. W., & Vogelstein, B. (2000). Cooperative effects of genes controlling the G2/M checkpoint. *Genes & Development, 14*(13), 1584-1588.

Chaouiya, C. (2007). Petri net modelling of biological networks. *Briefings in bioinformatics, 8*(4), 210-219.

Chassagnole, C., Jackson, R., Hussain, N., Bashir, L., Derow, C., Savin, J., & Fell, D. (2006). Using a mammalian cell cycle simulation to interpret differential kinase inhibition in anti-tumour pharmaceutical development. *Biosystems, 83*(2), 91-97.

Chaturvedi, P., Eng, W. K., Zhu, Y., Mattern, M. R., Mishra, R., Hurle, M. R., . . . Faucette, L. F. (1999). Mammalian Chk2 is a downstream effector of the ATM-dependent DNA damage checkpoint pathway. *Oncogene, 18*(28), 4047-4054.

Chauhan, A., Lorenzen, S., Herzel, H., & Bernard, S. (2011). Regulation of mammalian cell cycle progression in the regenerating liver. *Journal of theoretical biology, 283*(1), 103-112.

Chehab, N. H., Malikzay, A., Stavridi, E. S., & Halazonetis, T. D. (1999). Phosphorylation of Ser-20 mediates stabilization of human p53 in response to DNA damage. *Proceedings of the National Academy of Sciences, 96*(24), 13777-13782.

Chen, K., & Rajewsky, N. (2007). The evolution of gene regulation by transcription factors and microRNAs. *Nature Reviews Genetics, 8*(2), 93-103.

Chen, M.-S., Ryan, C. E., & Piwnica-Worms, H. (2003). Chk1 kinase negatively regulates mitotic function of Cdc25A phosphatase through 14-3-3 binding. *Molecular and cellular biology, 23*(21), 7488-7497.

Chen, T., Stephens, P. A., Middleton, F. K., & Curtin, N. J. (2012). Targeting the S and G2 checkpoint to treat cancer. *Drug discovery today, 17*(5-6), 194-202.

Chiorino, G., & Lupi, M. (2002). Variability in the timing of G1/S transition. *Mathematical biosciences, 177*, 85-101.

Chu, I. M., Hengst, L., & Slingerland, J. M. (2008). The Cdk inhibitor p27 in human cancer: prognostic potential and relevance to anticancer therapy. *Nature Reviews Cancer, 8*(4), 253-267.

Conradie, R., Bruggeman, F. J., Ciliberto, A., Csikász-Nagy, A., Novák, B., Westerhoff, H. V., & Snoep, J. L. (2010). Restriction point control of the mammalian cell cycle via the cyclin E/Cdk2: p27 complex. *FEBS journal, 277*(2), 357-367.

Cooper, G. M. (2000). *The Cell: A Molecular Approach*: ASM Press.

Csikász-Nagy, A. (2009). Computational systems biology of the cell cycle. *Briefings in bioinformatics, 10*(4), 424-434.

Csikász-Nagy, A., Battogtokh, D., Chen, K. C., Novák, B., & Tyson, J. J. (2006). Analysis of a generic model of eukaryotic cell-cycle regulation. *Biophysical journal, 90*(12), 4361-4379.

Dang, C. V. (1999). c-Myc target genes involved in cell growth, apoptosis, and metabolism. *Molecular and cellular biology, 19*(1), 1-11.

de Alboran, I. M., O'Hagan, R. C., Gärtner, F., Malynn, B., Davidson, L., Rickert, R., . . . Alt, F. W. (2001). Analysis of C-MYC function in normal cells via conditional gene-targeted mutation. *Immunity, 14*(1), 45-55.

De Souza, C. P., Ellem, K. A., & Gabrielli, B. G. (2000). Centrosomal and cytoplasmic Cdc2/cyclin B1 activation precedes nuclear mitotic events. *Experimental cell research, 257*(1), 11-21.

Deckbar, D., Jeggo, P. A., & Löbrich, M. (2011). Understanding the limitations of radiation-induced cell cycle checkpoints. *Critical reviews in biochemistry and molecular biology, 46*(4), 271-283.

Deineko, I., Kel, A., Kel-Margoulis, O., Wingender, E., & Ratner, V. (2003). Simulation of the dynamics of gene networks regulating the cell cycle in mammalian cells. *Russian Journal of Genetics, 39*(9), 1085-1091.

Di Leonardo, A., Linke, S. P., Clarkin, K., & Wahl, G. M. (1994). DNA damage triggers a prolonged p53-dependent G1 arrest and long-term induction of Cip1 in normal human fibroblasts. *Genes & development, 8*(21), 2540-2551.

Donnet, S., & Robert, C. (2012). Stochastic Modelling for Systems Biology. *CHANCE, 25*(4), 55-56.

Donzelli, M., & Draetta, G. F. (2003). Regulating mammalian checkpoints through Cdc25 inactivation. *EMBO reports, 4*(7), 671-677.

Eckerdt, F., & Strebhardt, K. (2006). Polo-Like Kinase 1: Target and Regulator of Anaphase-Promoting Complex/Cyclosome–Dependent Proteolysis. *Cancer research, 66*(14), 6895-6898.

Elmore, S. (2007). Apoptosis: a review of programmed cell death. *Toxicologic pathology, 35*(4), 495-516.

Fauré, A., Naldi, A., Chaouiya, C., & Thieffry, D. (2006). Dynamical analysis of a generic Boolean model for the control of the mammalian cell cycle. *Bioinformatics, 22*(14), e124-e131.

Ferrell, James E., Tsai, Tony Y.-C., & Yang, Q. (2011). Modeling the Cell Cycle: Why Do Certain Circuits Oscillate? *Cell, 144*(6), 874-885.

Fry, R. C., Begley, T. J., & Samson, L. D. (2005). Genome-wide responses to DNA-damaging agents. *Annu. Rev. Microbiol., 59*, 357-377.

Fujita, S., Matsui, M., Matsuno, H., & Miyano, S. (2004). Modeling and simulation of fission yeast cell cycle on hybrid functional Petri net. *IEICE transactions on fundamentals of electronics, communications and computer sciences, 87*(11), 2919-2928.

Fung, T. K., & Poon, R. Y. C. (2005). A roller coaster ride with the mitotic cyclins. *Seminars in Cell & Developmental Biology, 16*(3), 335-342.

Fuβ, H., Dubitzky, W., Downes, C. S., & Kurth, M. J. (2005). Mathematical models of cell cycle regulation. *Briefings in bioinformatics, 6*(2), 163-177.

Gardner, T. S., Dolnik, M., & Collins, J. J. (1998). A theory for controlling cell cycle dynamics using a reversibly binding inhibitor. *Proceedings of the National Academy of Sciences, 95*(24), 14190-14195.

Gauthier, J. H., & Pohl, P. I. (2011). A general framework for modeling growth and division of mammalian cells. *BMC systems biology, 5*(1), 3.

Gérard, C., & Goldbeter, A. (2009). Temporal self-organization of the cyclin/Cdk network driving the mammalian cell cycle. *Proceedings of the National Academy of Sciences, 106*(51), 21643-21648.

Gérard, C., & Goldbeter, A. (2010). A skeleton model for the network of cyclin-dependent kinases driving the mammalian cell cycle. *Interface Focus 1*, 24-35.

Gérard, C., & Goldbeter, A. (2012). From quiescence to proliferation: Cdk oscillations drive the mammalian cell cycle. *Front Physiol, 3*(413), 1-18.

Gérard, C., & Goldbeter, A. (2014). The balance between cell cycle arrest and cell proliferation: control by the extracellular matrix and by contact inhibition. *Interface Focus, 4*(3), 20130075.

Gérard, C., & Goldbeter, A. (2015). Dynamics of the mammalian cell cycle in physiological and pathological conditions. *Wiley Interdisciplinary Reviews: Systems Biology and Medicine*.

Gérard, C., Gonze, D., & Goldbeter, A. (2012). Effect of positive feedback loops on the robustness of oscillations in the network of cyclin-dependent kinases driving the mammalian cell cycle. *FEBS Journal, 279*(18), 3411-3431.

Geva-Zatorsky, N., Rosenfeld, N., Itzkovitz, S., Milo, R., Sigal, A., Dekel, E., . . . Lahav, G. (2006). Oscillations and variability in the p53 system. *Molecular systems biology, 2*(1).

Giglia-Mari, G., Zotter, A., & Vermeulen, W. (2010). DNA Damage Response. *Cold Spring Harbor Perspectives in Biology*.

Gilbert, D., & Heiner, M. (2006). From Petri Nets to Differential Equations – An Integrative Approach for Biochemical Network Analysis. In S. Donatelli & P. S. Thiagarajan (Eds.), *Petri Nets and Other Models of Concurrency* (pp. 181-200). Heidelberg, Berlin: Springer.

Golan, A., Yudkovsky, Y., & Hershko, A. (2002). The cyclin-ubiquitin ligase activity of cyclosome/APC is jointly activated by protein kinases Cdk1-cyclin B and Plk. *Journal of Biological Chemistry, 277*(18), 15552-15557.

Goldbeter, A. (1991). A minimal cascade model for the mitotic oscillator involving cyclin and cdc2 kinase. *Proceedings of the National Academy of Sciences, 88*(20), 9107-9111.

Gonze, D., & Goldbeter, A. (2001). A model for a network of phosphorylation–dephosphorylation cycles displaying the dynamics of dominoes and clocks. *Journal of theoretical biology, 210*(2), 167-186.

Goulev, Y., & Charvin, G. (2011). Ultrasensitivity and positive feedback to promote sharp mitotic entry. *Molecular cell, 41*(3), 243-244.

Grunwald, S., Speer, A., Ackermann, J., & Koch, I. (2008). Petri net modelling of gene regulation of the Duchenne muscular dystrophy. *Biosystems, 92*(2), 189-205.

Haberichter, T., Mädge, B., Christopher, R. A., Yoshioka, N., Dhiman, A., Miller, R., . . . Dowdy, S. F. (2007). A systems biology dynamical model of mammalian G1 cell cycle progression. *Molecular systems biology, 3*(1), 84.

Hamada, H., Tashima, Y., Kisaka, Y., Iwamoto, K., Hanai, T., Eguchi, Y., & Okamoto, M. (2009). Sophisticated framework between cell cycle arrest and apoptosis induction based on p53 dynamics. *PloS one, 4*(3), e4795.

Hamer, P. C. D. W., Mir, S. E., Noske, D., Van Noorden, C. J., & Würdinger, T. (2011). WEE1 kinase targeting combined with DNA-damaging cancer therapy catalyzes mitotic catastrophe. *Clinical cancer research, 17*(13), 4200-4207.

Hao, B., Zheng, N., Schulman, B. A., Wu, G., Miller, J. J., Pagano, M., & Pavletich, N. P. (2005). Structural basis of the Cks1-dependent recognition of p27Kip1 by the SCFSkp2 ubiquitin ligase. *Molecular cell, 20*(1), 9-19.

Hardy, S., & Robillard, P. N. (2004). Modeling and simulation of molecular biology systems using petri nets: modeling goals of various approaches. *Journal of Bioinformatics and Computational Biology, 2*(04), 619-637.

Harper, J. W., & Elledge, S. J. (1998). The role of Cdk7 in CAK function, a retro-retrospective. *Genes & development, 12*(3), 285-289.

Hartwell, L. H., & Kastan, M. B. (1994). Cell cycle control and cancer. *Science, 266*(5192), 1821-1828.

Hartwell, L. H., & Weinert, T. A. (1989). Checkpoints: controls that ensure the order of cell cycle events. *Science, 246*(4930), 629-634.

Hatzimanikatis, V., Lee, K., & Bailey, J. (1999). A mathematical description of regulation of the G1-S transition of the mammalian cell cycle. *Biotechnology and bioengineering, 65*(6), 631-637.

Hatzimanikatis, V., Lee, K. H., Renner, W. A., & Bailey, J. E. (1995). A mathematical model for the G1/S transition of the mammalian cell cycle. *Biotechnology letters, 17*(7), 669-674.

He, E., Kapuy, O., Oliveira, R. A., Uhlmann, F., Tyson, J. J., & Novák, B. (2011). System-level feedbacks make the anaphase switch irreversible. *Proceedings of the National Academy of Sciences, 108*(24), 10016-10021.

Heiner, M., Donaldson, R., & Gilbert, D. (2010). Petri nets for systems biology. *Symbolic Systems Biology: Theory and Methods. Jones and Bartlett Publishers, Inc., USA (in Press, 2010)*.

Heiner, M., Herajy, M., Liu, F., Rohr, C., & Schwarick, M. (2012). Snoopy–a unifying Petri net tool. In *Application and Theory of Petri Nets* (pp. 398-407): Springer.

Heiner, M., Richter, R., Schwarick, M., & Rohr, C. (2008). Snoopy-a tool to design and execute graph-based formalisms. *Petri Net Newsletter, 74*, 8-22.

Heldt, F. S., Barr, A. R., Cooper, S., Bakal, C., & Novák, B. (2018). A comprehensive model for the proliferation–quiescence decision in response to endogenous DNA damage in human cells. *Proceedings of the National Academy of Sciences, 115*(10), 2532-2537.

Helin, K. (1998). Regulation of cell proliferation by the E2F transcription factors. *Current opinion in genetics & development, 8*(1), 28-35.

Herajy, M., & Heiner, M. (2012). Hybrid representation and simulation of stiff biochemical networks. *Nonlinear Analysis: Hybrid Systems, 6*(4), 942-959.
Herajy, M., Schwarick, M., & Heiner, M. (2013). Hybrid Petri Nets for Modelling the Eukaryotic Cell Cycle. In M. Koutny, W. M. P. Van Der Aalst & A. Yakovlev (Eds.), *Transactions on Petri Nets and Other Models of Concurrency VIII* (pp. 123-141). Heidelberg, Berlin: Springer.
Hermeking, H., & Benzinger, A. (2006). 14-3-3 proteins in cell cycle regulation. *Seminars in Cancer Biology, 16*(3), 183-192.
Hoeijmakers, J. H. (2009). DNA damage, aging, and cancer. *New England Journal of Medicine, 361*(15), 1475-1485.
Hu, B., Mitra, J., van den Heuvel, S., & Enders, G. H. (2001). S and G2 phase roles for Cdk2 revealed by inducible expression of a dominant-negative mutant in human cells. *Molecular and cellular biology, 21*(8), 2755-2766.
Huang, S., & Ingber, D. E. (2000). Shape-dependent control of cell growth, differentiation, and apoptosis: switching between attractors in cell regulatory networks. *Experimental cell research, 261*(1), 91-103.
Ideker, T., Galitski, T., & Hood, L. (2001). A new approach to decoding life: systems biology. *Annual review of genomics and human genetics, 2*(1), 343-372.
Iritani, B. M., & Eisenman, R. N. (1999). c-Myc enhances protein synthesis and cell size during B lymphocyte development. *Proceedings of the National Academy of Sciences, 96*(23), 13180-13185.
Iwamoto, K., Hamada, H., Eguchi, Y., & Okamoto, M. (2011). Mathematical modeling of cell cycle regulation in response to DNA damage: exploring mechanisms of cell-fate determination. *Biosystems, 103*(3), 384-391.
Iwamoto, K., Tashima, Y., Hamada, H., Eguchi, Y., & Okamoto, M. (2008). Mathematical modeling and sensitivity analysis of G1/S phase in the cell cycle including the DNA-damage signal transduction pathway. *Biosystems, 94*(1), 109-117.
Jackson, R. C., Di Veroli, G. Y., Koh, S.-B., Goldlust, I., Richards, F. M., & Jodrell, D. I. (2017). Modelling of the cancer cell cycle as a tool for rational drug development: A systems pharmacology approach to cyclotherapy. *PLoS computational biology, 13*(5), e1005529.
Ji, J. Y., & Dyson, N. J. (2010). Interplay Between Cyclin-Dependent Kinases and E2F-Dependent Transcription. In G. Enders (Ed.), *Cell Cycle Deregulation in Cancer* (pp. 23-41). New York: Springer.
Jin, S., Tong, T., Fan, W., Fan, F., Antinore, M. J., Zhu, X., . . . Rajasekaran, B. (2002). GADD45-induced cell cycle G2-M arrest associates with altered subcellular distribution of cyclin B1 and is independent of p38 kinase activity. *Oncogene, 21*(57), 8696-8704.
Joaquin, M., & Watson, R. (2003). Cell cycle regulation by the B-Myb transcription factor. *Cellular and Molecular Life Sciences CMLS, 60*(11), 2389-2401.
Kamura, T., Hara, T., Matsumoto, M., Ishida, N., Okumura, F., Hatakeyama, S., . . . Nakayama, K. I. (2004). Cytoplasmic ubiquitin ligase KPC regulates proteolysis of p27Kip1 at G1 phase. *Nature cell biology, 6*(12), 1229-1235.
Kapuy, O., He, E., Uhlmann, F., & Novák, B. (2009). Mitotic exit in mammalian cells. *Molecular systems biology, 5*(1), 324.
Kar, S., Baumann, W. T., Paul, M. R., & Tyson, J. J. (2009). Exploring the roles of noise in the eukaryotic cell cycle. *Proceedings of the National Academy of Sciences, 106*(16), 6471-6476.
Karimian, A., Ahmadi, Y., & Yousefi, B. (2016). Multiple functions of p21 in cell cycle, apoptosis and transcriptional regulation after DNA damage. *DNA repair, 42*, 63-71.
Karlsson-Rosenthal, C., & Millar, J. (2006). Cdc25: mechanisms of checkpoint inhibition and recovery. *Trends in cell biology, 16*(6), 285-292.
Kastan, M. B., & Bartek, J. (2004). Cell-cycle checkpoints and cancer. *Nature, 432*(7015), 316-323.
Kastan, M. B., & Lim, D.-s. (2000). The many substrates and functions of ATM. *Nature Reviews Molecular Cell Biology, 1*(3), 179-186.
Kearney, C. J., & Martin, S. J. (2013). Competition for growth factors: a lot more death with a little less Aktion. *Cell Death And Differentiation, 20*, 1291-1292.

Kiehl, T. R., Mattheyses, R. M., & Simmons, M. K. (2004). Hybrid simulation of cellular behavior. *Bioinformatics, 20*(3), 316-322.
Kitano, H. (2002a). Computational systems biology. *Nature, 420*(6912), 206-210.
Kitano, H. (2002b). Systems biology: a brief overview. *Science, 295*(5560), 1662-1664.
Kitano, H. (2007). Towards a theory of biological robustness. *Molecular Systems Biology, 3*(1).
Kiyokawa, H., & Ray, D. (2008). In vivo roles of CDC25 phosphatases: biological insight into the anti-cancer therapeutic targets. *Anti-Cancer Agents in Medicinal Chemistry (Formerly Current Medicinal Chemistry-Anti-Cancer Agents), 8*(8), 832-836.
Klipp, E., Herwig, R., Kowald, A., Wierling, C., & Lehrach, H. (2008). *Systems biology in practice: concepts, implementation and application*: John Wiley & Sons.
Klipp, E., Liebermeister, W., Wierling, C., Kowald, A., & Herwig, R. (2016). *Systems biology: a textbook*: John Wiley & Sons.
Koch, A., & Schaechter, M. (1962). A model for statistics of the cell division process. *Journal of General Microbiology, 29*(3), 435-454.
Koch, I., Reisig, W., & Schreiber, F. (2010). *Modeling in systems biology: the Petri net approach* (Vol. 16). New York: Springer.
Kohn, K. W. (1998). Functional capabilities of molecular network components controlling the mammalian G1/S cell cycle phase transition. *Oncogene, 16*(8), 1065-1075.
Kohn, K. W., & Pommier, Y. (2005). Molecular interaction map of the p53 and Mdm2 logic elements, which control the Off–On switch of p53 in response to DNA damage. *Biochemical and biophysical research communications, 331*(3), 816-827.
Kristjansdottir, K., & Rudolph, J. (2004). Cdc25 phosphatases and cancer. *Chemistry & biology, 11*(8), 1043-1051.
Kumagai, A., & Dunphy, W. G. (1999). Binding of 14-3-3 proteins and nuclear export control the intracellular localization of the mitotic inducer Cdc25. *Genes & development, 13*(9), 1067-1072.
Latchman, D. S. (1997). Transcription factors: an overview. *The international journal of biochemistry & cell biology, 29*(12), 1305-1312.
Lecca, P., & Priami, C. (2007). Cell cycle control in eukaryotes: A biospi model. *Electronic Notes in Theoretical Computer Science, 180*(3), 51-63.
Lee, D. Y., Zimmer, R., Lee, S. Y., & Park, S. (2006). Colored Petri net modeling and simulation of signal transduction pathways. *Metabolic Engineering, 8*(2), 112-122.
Levine, M., & Tjian, R. (2003). Transcription regulation and animal diversity. *Nature, 424*(6945), 147-151.
Li, M., & Zhang, P. (2009). The function of APC/CCdh1 in cell cycle and beyond. *Cell division, 4*(1), 2.
Lindon, C., & Pines, J. (2004). Ordered proteolysis in anaphase inactivates Plk1 to contribute to proper mitotic exit in human cells. *The Journal of cell biology, 164*(2), 233-241.
Lindqvist, A., Rodríguez-Bravo, V., & Medema, R. H. (2009). The decision to enter mitosis: feedback and redundancy in the mitotic entry network. *The Journal of cell biology, 185*(2), 193-202.
Ling, H., Kulasiri, D., & Samarasinghe, S. (2010). Robustness of G1/S checkpoint pathways in cell cycle regulation based on probability of DNA-damaged cells passing as healthy cells. *Biosystems, 101*(3), 213-221.
Liu, F., & Heiner, M. (2010). Colored Petri nets to model and simulate biological systems. *Recent advances in Petri Nets and concurrency, 827*, 71-85.
Liu, F., & Heiner, M. (2013). Modeling membrane systems using colored stochastic Petri nets. *Natural Computing, 12*(4), 617-629.
Liu, F., Heiner, M., & Yang, M. (2014). Modeling and analyzing biological systems using colored hierarchical Petri nets illustrated by C. elegans vulval development. *Journal of Biological Systems, 22*(03), 463-493.
Liu, W.-F., Yu, S.-S., Chen, G.-J., & Li, Y.-Z. (2006). DNA Damage Checkpoint, Damage Repair, and Genome Stability. *Acta Genetica Sinica, 33*(5), 381-390.
Liu, Z., Pu, Y., Li, F., Shaffer, C. A., Hoops, S., Tyson, J. J., & Cao, Y. (2012). Hybrid modeling and simulation of stochastic effects on progression through the eukaryotic cell cycle. *The Journal of Chemical Physics, 136*, 034105.

Ludlow, J., Glendening, C., Livingston, D., & DeCarprio, J. (1993). Specific enzymatic dephosphorylation of the retinoblastoma protein. *Molecular and Cellular Biology, 13*(1), 367-372.

Mailand, N., Podtelejnikov, A. V., Groth, A., Mann, M., Bartek, J., & Lukas, J. (2002). Regulation of G2/M events by Cdc25A through phosphorylation-dependent modulation of its stability. *The EMBO journal, 21*(21), 5911-5920.

Malumbres, M., & Barbacid, M. (2005). Mammalian cyclin-dependent kinases. *Trends in biochemical sciences, 30*(11), 630-641.

Malumbres, M., & Barbacid, M. (2009). Cell cycle, CDKs and cancer: a changing paradigm. *Nature Reviews Cancer, 9*(3), 153-166.

Mason, E. F., & Rathmell, J. C. (2011). Cell metabolism: an essential link between cell growth and apoptosis. *Biochimica et Biophysica Acta (BBA)-Molecular Cell Research, 1813*(4), 645-654.

Massagué, J. (2004). G1 cell-cycle control and cancer. *Nature, 432*(7015), 298-306.

Mateo, F., Vidal-Laliena, M., Canela, N., Busino, L., Martinez-Balbas, M. A., Pagano, M., . . . Bachs, O. (2009). Degradation of cyclin A is regulated by acetylation. *Oncogene, 28*(29), 2654-2666.

Matsui, M., Fujita, S., Suzuki, S., Matsuno, H., & Miyano, S. (2004). Simulated cell division processes of the Xenopus cell cycle pathway by Genomic Object Net. *Journal of Integrative Bioinformatics (JIB), 1*(1), 27-37.

Matsuno, H., Tanaka, Y., Aoshima, H., Doi, A., Matsui, M., & Miyano, S. (2003). Biopathways representation and simulation on hybrid functional Petri net. *In silico biology, 3*(3), 389-404.

Meek, D. W. (2004). The p53 response to DNA damage. *DNA repair, 3*(8), 1049-1056.

Molinari, M., Mercurio, C., Dominguez, J., Goubin, F., & Draetta, G. F. (2000). Human Cdc25 A inactivation in response to S phase inhibition and its role in preventing premature mitosis. *EMBO reports, 1*(1), 71-79.

Mombach, J. C., Bugs, C. A., & Chaouiya, C. (2014). Modelling the onset of senescence at the G1/S cell cycle checkpoint. *BMC genomics, 15*(7), S7.

Morgan, D. O. (1997). Cyclin-dependent kinases: engines, clocks, and microprocessors. *Annual review of cell and developmental biology, 13*(1), 261-291.

Morgan, D. O. (2007). *The cell cycle: principles of control*. London, UK: New Science Press.

Münzer, D. G. G., Kostoglou, M., Georgiadis, M. C., Pistikopoulos, E. N., & Mantalaris, A. (2015). Cyclin and DNA distributed cell cycle model for GS-NS0 cells. *PLoS Comput Biol, 11*(2), e1004062.

Mura, I., & Csikász-Nagy, A. (2008). Stochastic Petri Net extension of a yeast cell cycle model. *Journal of theoretical biology, 254*(4), 850-860.

Murata, T. (1989). Petri nets: Properties, analysis and applications. *Proceedings of the IEEE, 77*(4), 541-580.

Murray, A. W. (2004). Recycling the cell cycle: cyclins revisited. *Cell, 116*(2), 221-234.

Musgrove, E. A., Caldon, C. E., Barraclough, J., Stone, A., & Sutherland, R. L. (2011). Cyclin D as a therapeutic target in cancer. *Nature Reviews Cancer, 11*(8), 558-572.

Nagasaki, M., Fujita, S., Matsuno, H., & Miyano, S. (2002). Genomic Object Net: II. Modelling biopathways by hybrid functional Petri net with extension. *Applied Bioinformatics, 2*(3), 185-188.

Nagasaki, M., Matsuno, H., & Miyano, S. (2002). Genomic Object Net: I. A platform for modelling and simulating biopathways. *Applied Bioinformatics, 2*(3), 181-184.

Nagasaki, M., Saito, A., Doi, A., Matsuno, H., & Miyano, S. (2009). *Foundations of systems biology: using Cell Illustrator and pathway databases* (Vol. 13). New York: Springer Science & Business Media.

Nakayama, K. I., & Nakayama, K. (2005). Regulation of the cell cycle by SCF-type ubiquitin ligases. *Seminars in Cell & Developmental Biology, 16*(3), 323-333.

Nakayama, K. I., & Nakayama, K. (2006). Ubiquitin ligases: cell-cycle control and cancer. *Nature Reviews Cancer, 6*(5), 369-381.

Naldi, A., Hernandez, C., Abou-Jaoudé, W., Monteiro, P. T., Chaouiya, C., & Thieffry, D. (2018). Logical modelling and analysis of cellular regulatory networks with GINsim 3.0. *bioRxiv*.

Nelson, D. A., Krucher, N. A., & Ludlow, J. W. (1997). High molecular weight protein phosphatase type 1 dephosphorylates the retinoblastoma protein. *Journal of Biological Chemistry, 272*(7), 4528-4535.
Nelson, D. L., Lehninger, A. L., & Cox, M. M. (2008). *Lehninger principles of biochemistry*: Macmillan.
Noble, D. (2008). *The Music of Life: Biology Beyond Genes*. New York: OUP Oxford.
Noel, V., Vakulenko, S., & Radulescu, O. (2013). A hybrid mammalian cell cycle model. *EPTCS, 125*, 68-83.
Norel, R., & Agur, Z. (1991). A model for the adjustment of the mitotic clock by cyclin and MPF levels. *Science, 251*(4997), 1076-1078.
Novak, B., Csikasz-Nagy, A., Gyorffy, B., Nasmyth, K., & Tyson, J. J. (1998). Model scenarios for evolution of the eukaryotic cell cycle. *Philosophical Transactions of the Royal Society of London. Series B: Biological Sciences, 353*(1378), 2063-2076.
Novák, B., Sible, J. C., & Tyson, J. J. (2001). Checkpoints in the cell cycle. *e LS*.
Novak, B., & Tyson, J. J. (1993). Numerical analysis of a comprehensive model of M-phase control in Xenopus oocyte extracts and intact embryos. *Journal of cell science, 106*(4), 1153-1168.
Novak, B., & Tyson, J. J. (2004). A model for restriction point control of the mammalian cell cycle. *Journal of theoretical biology, 230*(4), 563-579.
Novak, B., Tyson, J. J., Gyorffy, B., & Csikasz-Nagy, A. (2007). Irreversible cell-cycle transitions are due to systems-level feedback. *Nature cell biology, 9*(7), 724-728.
Nurse, P. (1990). Universal control mechanism regulating onset of M-phase. *Nature, 344*(6266), 503-508.
Nurse, P. (2000). A long twentieth century of the cell cycle and beyond. *Cell, 100*(1), 71-78.
Nyberg, K. A., Michelson, R. J., Putnam, C. W., & Weinert, T. A. (2002). Toward maintaining the genome: DNA damage and replication checkpoints. *Annual review of genetics, 36*(1), 617-656.
Obeyesekere, M., Knudsen, E., Wang, J., & Zimmerman, S. (1997). A mathematical model of the regulation of the G1 phase of Rb+/+ and Rb—/—mouse embryonic fibroblasts and an osteosarcoma cell line. *Cell proliferation, 30*(3-4), 171-194.
Obeyesekere, M. N., Herbert, J. R., & Zimmerman, S. O. (1995). A model of the G1 phase of the cell cycle incorporating cyclin E/cdk2 complex and retinoblastoma protein. *Oncogene, 11*(6), 1199-1205.
Obeyesekere, M. N., Tecarro, E., & Lozano, G. (2004). Model predictions of MDM2 mediated cell regulation. *Cell Cycle, 3*(5), 653-659.
Obeyesekere, M. N., Zimmerman, S. O., Tecarro, E. S., & Auchmuty, G. (1999). A model of cell cycle behavior dominated by kinetics of a pathway stimulated by growth factors. *Bulletin of mathematical biology, 61*(5), 917-934.
Ohtsubo, M., Theodoras, A. M., Schumacher, J., Roberts, J. M., & Pagano, M. (1995). Human cyclin E, a nuclear protein essential for the G1-to-S phase transition. *Molecular and cellular biology, 15*(5), 2612-2624.
Palsson, B., & Palsson, B. Ø. (2015). *Systems biology*. Cambridge, UK: Cambridge university press.
Pandey, N., & Vinod, P. (2018). Mathematical modelling of reversible transition between quiescence and proliferation. *PloS one, 13*(6), e0198420.
Pardee, A. B. (1989). G1 events and regulation of cell proliferation. *Science, 246*(4930), 603-608.
Pardee, A. B. (2002). Regulation, restriction, and reminiscences. *Journal of Biological Chemistry, 277*(30), 26709-26716.
Park, M.-T., & Lee, S.-J. (2003). Cell cycle and cancer. *Journal of biochemistry and molecular biology, 36*(1), 60-65.
Peleg, M., Rubin, D., & Altman, R. B. (2005). Using Petri net tools to study properties and dynamics of biological systems. *Journal of the American Medical Informatics Association, 12*(2), 181-199.
Perry, J., & Kornbluth, S. (2007). Cdc25 and Wee1: analogous opposites? *Cell division, 2*(1), 12.
Peters, J.-M. (2002). The anaphase-promoting complex: proteolysis in mitosis and beyond. *Molecular cell, 9*(5), 931-943.
Pfeuty, B. (2012). Strategic cell-cycle regulatory features that provide mammalian cells with tunable G1 length and reversible G1 arrest. *PLoS One, 7*(4), e35291.

Pfeuty, B., David-Pfeuty, T., & Kaneko, K. (2008). Underlying principles of cell fate determination during G. *Cell cycle, 7*(20), 3246-3257.
Pfeuty, B., & Kaneko, K. (2007). Minimal requirements for robust cell size control in eukaryotic cells. *Physical biology, 4*(3), 194.
Pinney, J. W., Westhead, D. R., & McConkey, G. A. (2003). Petri Net representations in systems biology. *Biochemical Society Transactions, 31*(6), 1513-1515.
Qiao, X., Zhang, L., Gamper, A. M., Fujita, T., & Wan, Y. (2010). APC/C-Cdh1: from cell cycle to cellular differentiation and genomic integrity. *Cell Cycle, 9*(19), 3904.
Qu, Z., MacLellan, W. R., & Weiss, J. N. (2003). Dynamics of the cell cycle: checkpoints, sizers, and timers. *Biophysical journal, 85*(6), 3600-3611.
Qu, Z., Weiss, J. N., & MacLellan, W. R. (2003). Regulation of the mammalian cell cycle: a model of the G1-to-S transition. *American Journal of Physiology-Cell Physiology, 284*(2), C349-C364.
Qu, Z., Weiss, J. N., & MacLellan, W. R. (2004). Coordination of cell growth and cell division: a mathematical modeling study. *Journal of Cell Science, 117*(18), 4199-4207.
Rohr, C., Marwan, W., & Heiner, M. (2010). Snoopy—a unifying Petri net framework to investigate biomolecular networks. *Bioinformatics, 26*(7), 974-975.
Rouse, J., & Jackson, S. P. (2002). Interfaces between the detection, signaling, and repair of DNA damage. *Science, 297*(5581), 547-551.
Ruddon, R. W. (2007). *Cancer biology*: Oxford University Press.
Ryan, K. M., Phillips, A. C., & Vousden, K. H. (2001). Regulation and function of the p53 tumor suppressor protein. *Current opinion in cell biology, 13*(3), 332-337.
Sahin, Ö., Fröhlich, H., Löbke, C., Korf, U., Burmester, S., Majety, M., . . . Thieffry, D. (2009). Modeling ERBB receptor-regulated G1/S transition to find novel targets for de novo trastuzumab resistance. *BMC systems biology, 3*(1), 1.
Samarasinghe, S. (2006). *Neural networks for applied sciences and engineering: from fundamentals to complex pattern recognition*: CRC Press.
Sancar, A., Lindsey-Boltz, L. A., Ünsal-Kaçmaz, K., & Linn, S. (2004). Molecular mechanisms of mammalian DNA repair and the DNA damage checkpoints. *Annual review of biochemistry, 73*(1), 39-85.
Satyanarayana, A., & Kaldis, P. (2009). Mammalian cell-cycle regulation: several Cdks, numerous cyclins and diverse compensatory mechanisms. *Oncogene, 28*(33), 2925-2939.
Sauro, H. M. (2012). *Enzyme kinetics for systems biology*: Future Skill Software.
Schmidt, E. V. (1999). The role of c-myc in cellular growth control. *Oncogene, 18*, 2988-2996.
Seeley, R. R., Stephens, T. D., & Tate, P. (2007). Anatomy and physiology. *New York, NY: McGraw Hill*.
Sexl, V., Diehl, J. A., Sherr, C. J., Ashmun, R., Beach, D., & Roussel, M. F. (1999). A rate limiting function of cdc25A for S phase entry inversely correlates with tyrosine dephosphorylation of Cdk2. *Oncogene, 18*(3), 573-582.
Sha, W., Moore, J., Chen, K., Lassaletta, A. D., Yi, C.-S., Tyson, J. J., & Sible, J. C. (2003). Hysteresis drives cell-cycle transitions in Xenopus laevis egg extracts. *PNAS, 100*(3), 975-980.
Sheaff, R. J., Groudine, M., Gordon, M., Roberts, J. M., & Clurman, B. E. (1997). Cyclin E-CDK2 is a regulator of p27Kip1. *Genes & development, 11*(11), 1464-1478.
Sherr, C. J., & McCormick, F. (2002). The RB and p53 pathways in cancer. *Cancer cell, 2*(2), 103-112.
Sherr, C. J., & Roberts, J. M. (1999). CDK inhibitors: positive and negative regulators of G1-phase progression. *Genes & development, 13*(12), 1501-1512.
Shields, R. (1977). Transition probability and the origin of variation in the cell cycle. *Nature, 267*, 704-707.
Shiloh, Y., & Ziv, Y. (2013). The ATM protein kinase: regulating the cellular response to genotoxic stress, and more. *Nature Reviews Molecular Cell Biology, 14*(4), 197-210.
Silva, M. (2013). Half a century after Carl Adam Petri's Ph. D. thesis: A perspective on the field. *Annual Reviews in Control, 37*(2), 191-219.
Singhania, R., Sramkoski, R. M., Jacobberger, J. W., & Tyson, J. J. (2011). A hybrid model of mammalian cell cycle regulation. *PLoS computational biology, 7*(2), e1001077.
Siu, W. Y., Yam, C. H., & Poon, R. Y. (1999). G1 versus G2 cell cycle arrest after adriamycin-induced damage in mouse Swiss3T3 cells. *FEBS letters, 461*(3), 299-305.

Smith, A., Simanski, S., Fallahi, M., & Ayad, N. G. (2007). Redundant ubiquitin ligase activities regulate wee1 degradation and mitotic entry. *Cell Cycle, 6*(22), 2795-2799.

Smith, J., & Martin, L. (1973). Do cells cycle? *Proceedings of the National Academy of Sciences, 70*(4), 1263-1267.

Smith, J., Mun Tho, L., Xu, N., & A. Gillespie, D. (2010). The ATM–Chk2 and ATR–Chk1 Pathways in DNA Damage Signaling and Cancer. *Advances in Cancer Research, 108*, 73-112.

Stein, G. S., & Pardee, A. B. (2004). *Cell cycle and growth control: biomolecular regulation and cancer*. Hoboken NJ: John Wiley & Sons.

Steuer, R. (2004). Effects of stochasticity in models of the cell cycle: from quantized cycle times to noise-induced oscillations. *Journal of theoretical biology, 228*(3), 293-301.

Su, C.-C., Lin, J.-G., Chen, G.-W., Lin, W.-C., & Chung, J.-G. (2006). Down-regulation of Cdc25c, CDK1 and Cyclin B1 and Up-regulation of Wee1 by Curcumin Promotes Human Colon Cancer Colo 205 Cell Entry into G2/M-phase of Cell Cycle. *Cancer Genomics - Proteomics, 3*(1), 55-61.

Swat, M., Kel, A., & Herzel, H. (2004). Bifurcation analysis of the regulatory modules of the mammalian G1/S transition. *Bioinformatics, 20*(10), 1506-1511.

Tashima, Y., Hamada, H., Okamoto, M., & Hanai, T. (2008). Prediction of key factor controlling G1/S phase in the mammalian cell cycle using system analysis. *Journal of bioscience and bioengineering, 106*(4), 368-374.

Tashima, Y., kisaka, Y., Hanai, T., Hamada, H., Eguchi, Y., & Okamoto, M. (2007). Mathematical modeling of G2/M phase in the cell cycle with involving the p53/Mdm2 oscillation system. In R. Magjarevic & J. H. Nagel (Eds.), *World Congress on Medical Physics and Biomedical Engineering 2006* (Vol. 14, pp. 197-200). Heidelberg, Berlin Springer.

Thron, C. (1991). Mathematical analysis of a model of the mitotic clock. *Science, 254*(5028), 122-123.

Thron, C. (1997). Bistable biochemical switching and the control of the events of the cell cycle. *Nonlinear Analysis: Theory, Methods & Applications, 30*(3), 1825-1834.

Timofeev, O., Cizmecioglu, O., Settele, F., Kempf, T., & Hoffmann, I. (2010). Cdc25 phosphatases are required for timely assembly of CDK1-cyclin B at the G2/M transition. *Journal of Biological Chemistry, 285*(22), 16978-16990.

Trimarchi, J. M., & Lees, J. A. (2002). Sibling rivalry in the E2F family. *Nature Reviews Molecular Cell Biology, 3*(1), 11-20.

Trinkle-Mulcahy, L., Andrews, P. D., Wickramasinghe, S., Sleeman, J., Prescott, A., Lam, Y. W., . . . Lamond, A. I. (2003). Time-lapse imaging reveals dynamic relocalization of PP1γ throughout the mammalian cell cycle. *Molecular biology of the cell, 14*(1), 107-117.

Trunnell, N. B., Poon, A. C., Kim, S. Y., & Ferrell Jr, J. E. (2011). Ultrasensitivity in the regulation of Cdc25C by Cdk1. *Molecular cell, 41*(3), 263-274.

Tyers, M. (2004). Cell cycle goes global. *Current opinion in cell biology, 16*(6), 602-613.

Tyson, J. J. (1991). Modeling the cell division cycle: cdc2 and cyclin interactions. *Proceedings of the National Academy of Sciences, 88*(16), 7328-7332.

Tyson, J. J., Chen, K., & Novak, B. (2001). Network dynamics and cell physiology. *Nature Reviews Molecular Cell Biology, 2*(12), 908-916.

Tyson, J. J., Chen, K. C., & Novak, B. (2003). Sniffers, buzzers, toggles and blinkers: dynamics of regulatory and signaling pathways in the cell. *Current opinion in cell biology, 15*(2), 221-231.

Tyson, J. J., & Novak, B. (2001). Regulation of the eukaryotic cell cycle: molecular antagonism, hysteresis, and irreversible transitions. *Journal of Theoretical Biology, 210*(2), 249-263.

Van De Weerdt, B. C., & Medema, R. H. (2006). Review Polo-Like Kinases. *Cell Cycle, 5*(8), 853-864.

van Vugt, M. A., & Medema, R. H. (2005). Getting in and out of mitosis with Polo-like kinase-1. *Oncogene, 24*(17), 2844-2859.

Vander Heiden, M. G., Plas, D. R., Rathmell, J. C., Fox, C. J., Harris, M. H., & Thompson, C. B. (2001). Growth factors can influence cell growth and survival through effects on glucose metabolism. *Molecular and cellular biology, 21*(17), 5899-5912.

Vassilev, L. T., Vu, B. T., Graves, B., Carvajal, D., Podlaski, F., Filipovic, Z., . . . Klein, C. (2004). In vivo activation of the p53 pathway by small-molecule antagonists of MDM2. *Science, 303*(5659), 844-848.

Vermeulen, K., Van Bockstaele, D. R., & Berneman, Z. N. (2003). The cell cycle: a review of regulation, deregulation and therapeutic targets in cancer. *Cell proliferation, 36*(3), 131-149.

Vibert, J., & Thomas-Vaslin, V. (2017). Modelling T cell proliferation: Dynamics heterogeneity depending on cell differentiation, age, and genetic background. *PLoS computational biology, 13*(3), e1005417.

Vodermaier, H. C. (2004). APC/C and SCF: controlling each other and the cell cycle. *Current Biology, 14*(18), R787-R796.

Walworth, N. C. (2000). Cell-cycle checkpoint kinases: checking in on the cell cycle. *Current opinion in cell biology, 12*(6), 697-704.

Wasserman, L. (2013). *All of statistics: a concise course in statistical inference*: Springer Science & Business Media.

Watanabe, N., Arai, H., Nishihara, Y., Taniguchi, M., Watanabe, N., Hunter, T., & Osada, H. (2004). M-phase kinases induce phospho-dependent ubiquitination of somatic Wee1 by SCFβ-TrCP. *Proceedings of the National Academy of Sciences of the United States of America, 101*(13), 4419-4424.

Weiers, R. M. (2010). *Introduction to business statistics*. Mason, OH, USA: Cengage Learning.

Weis, M. C., Avva, J., Jacobberger, J. W., & Sreenath, S. N. (2014). A Data-Driven, Mathematical Model of Mammalian Cell Cycle Regulation. *PloS one, 9*(5), e97130.

Windhager, L., & Zimmer, R. (2008). *Intuitive Modeling of Dynamic Systems with Petri Nets and Fuzzy Logic*. Paper presented at the meeting of the German Conference on Bioinformatics, Germany.

Xu, B., Kim, S.-T., Lim, D.-S., & Kastan, M. B. (2002). Two molecularly distinct G2/M checkpoints are induced by ionizing irradiation. *Molecular and cellular biology, 22*(4), 1049-1059.

Yang, L., Han, Z., Robb MacLellan, W., Weiss, J. N., & Qu, Z. (2006). Linking cell division to cell growth in a spatiotemporal model of the cell cycle. *Journal of theoretical biology, 241*(1), 120-133.

Yang, L., MacLellan, W. R., Han, Z., Weiss, J. N., & Qu, Z. (2004). Multisite phosphorylation and network dynamics of cyclin-dependent kinase signaling in the eukaryotic cell cycle. *Biophysical journal, 86*(6), 3432-3443.

Yang, L., Meng, Y., Bao, C., Liu, W., Ma, C., Li, A., . . . Jia, Y. (2013). Robustness and backbone motif of a cancer network regulated by miR-17-92 cluster during the G1/S transition. *PloS one, 8*(3), e57009.

Yao, G., Lee, T. J., Mori, S., Nevins, J. R., & You, L. (2008). A bistable Rb–E2F switch underlies the restriction point. *Nature cell biology, 10*(4), 476-482.

Yoon, M.-K., Mitrea, D. M., Ou, L., & Kriwacki, R. W., &. (2012). *Cell cycle regulation by the intrinsically disordered proteins p21 and p27*: Portland Press Limited.

Yuan, X., Srividhya, J., De Luca, T., Ju-hyong, E. L., & Pomerening, J. R. (2014). Uncovering the role of APC-Cdh1 in generating the dynamics of S-phase onset. *Molecular biology of the cell, 25*(4), 441-456.

Yun, J., Chae, H.-D., Choi, T.-S., Kim, E.-H., Bang, Y.-J., Chung, J., . . . Shin, D. Y. (2003). Cdk2-dependent phosphorylation of the NF-Y transcription factor and its involvement in the p53-p21 signaling pathway. *Journal of Biological Chemistry, 278*(38), 36966-36972.

Zámborszky, J., Hong, C. I., & Nagy, A. C. (2007). Computational analysis of mammalian cell division gated by a circadian clock: quantized cell cycles and cell size control. *Journal of biological rhythms, 22*(6), 542-553.

Zhan, Q. (2005). Gadd45a, a p53-and BRCA1-regulated stress protein, in cellular response to DNA damage. *Mutation Research/Fundamental and Molecular Mechanisms of Mutagenesis, 569*(1), 133-143.

Zhang, K., Zhang, L., & Mou, S. (2017). An application of invertibility of Boolean control networks to the control of the mammalian cell cycle. *IEEE/ACM Transactions on Computational Biology and Bioinformatics (TCBB), 14*(1), 225-229.

Zhang, L., Cheng, Y., & Liew, K. (2013). A mathematical analysis of DNA damage induced G2 phase transition. *Applied Mathematics and Computation, 225*, 765-774.

Zhang, L., Cheng, Y., & Liew, K. (2014a). Mathematical modeling of p53 pulses in G2 phase with DNA damage. *Applied Mathematics and Computation, 232*, 1000-1010.

Zhang, L., Cheng, Y., & Liew, K. (2014b). A mathematical study of the robustness of G2/M regulatory network in response to DNA damage with parameters sensitivity. *Applied Mathematics and Computation, 232*, 365-374.

Zhang, Y., & Xiong, Y. (2001). A p53 amino-terminal nuclear export signal inhibited by DNA damage-induced phosphorylation. *Science, 292*(5523), 1910-1915.

Zhao, H., & Piwnica-Worms, H. (2001). ATR-mediated checkpoint pathways regulate phosphorylation and activation of human Chk1. *Molecular and cellular biology, 21*(13), 4129-4139.

Zhou, B.-B. S., & Elledge, S. J. (2000). The DNA damage response: putting checkpoints in perspective. *Nature, 408*(6811), 433-439.

Zhu, W., Giangrande, P. H., & Nevins, J. R. (2004). E2Fs link the control of G1/S and G2/M transcription. *The EMBO journal, 23*(23), 4615-4626.

Zitouni, S., Nabais, C., Jana, S. C., Guerrero, A., & Bettencourt-Dias, M. (2014). Polo-like kinases: structural variations lead to multiple functions. *Nature Reviews Molecular Cell Biology, 15*(7), 433-452.